Investigations of D-glycero-D-ido-octulose (D-g-D-i-oct) metabolism and transketolases in the resurrection plant *Craterostigma plantagineum*

Qingwei Zhang

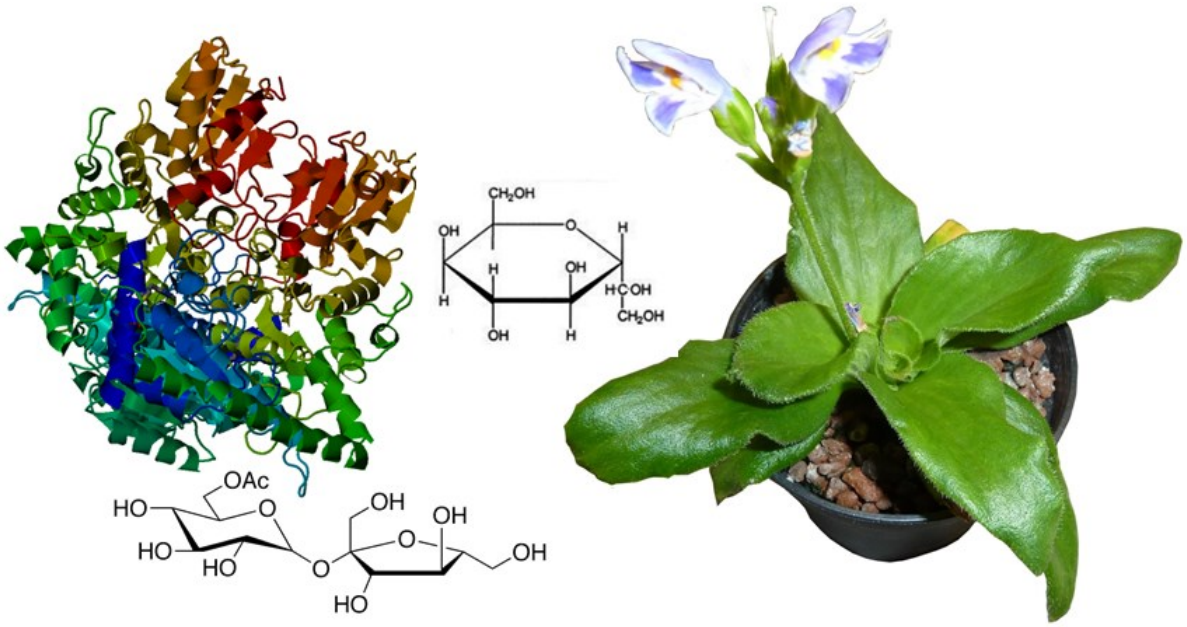

Investigations of D-glycero-D-ido-octulose (D-g-D-i-oct) metabolism and transketolases in the resurrection plant *Craterostigma plantagineum*

Dissertation

zur

Erlangung des Doktorgrades (Dr. rer. nat.)

der

Mathematisch-Naturwissenschaftlichen Fakultät

der

Rheinischen Friedrich-Wilhelms-Universität Bonn

vorgelegt von

Qingwei Zhang

aus

Henan, Volksrepublik China

Bonn, 2015

Angefertigt mit Genehmigung der Mathematisch-Naturwissenschaftlichen Fakultät der Rheinischen Friedrich-Wilhelms-Universität Bonn

Erstgutachter: Prof. Dr. Dorothea Bartels

Zweitgutachter: Prof. Dr. Lukas Schreiber

Tag der Promotion: 17.12.2015

Erscheinungsjahr: 2016

Abstract

Eight-carbon monosaccharides ($C_8H_{16}O_8$) occur naturally in a number of higher plants (e.g. avocado and sedum species), but they did not get much attention in research compared to common sugars (e.g. glucose, fructose and sucrose). D-glycero-D-ido-octulose (D-g-D-i-oct), an eight carbon monosaccharide has been reported as a rare but abundant monosaccharide in leaves of the resurrection plant *Craterostigma plantagineum*. When *C. plantagineum* plants encounter dehydration, D-g-D-i-oct is converted to sucrose that plays a fundamental role in regulating osmotic potential and protecting membranes as well as macro-molecules in resurrection plants. Previous studies suggested that the metabolism of D-g-D-i-oct involves transketolase and the exchange reaction of an alternative Calvin cycle may be responsible for the synthesis of D-g-D-i-oct phosphate. However, the metabolic pathways and the properties of the octulose molecule have not been well investigated. Three different isoforms of transketolase of *C. plantagineum* and their functions are not clearly characterized. Thus, some questions need to be answered: whether the exchange reaction exists in *C. plantagineum* and whether the three different isoforms of transketolase in *C. plantagineum* have the same function, as well as how the three different isoforms are regulated in *C. plantagineum*?

In this study I focused on the carbohydrate status in relation to desiccation tolerance, developmental stage and selected environmental factors to explore the function of D-g-D-i-oct in *C. plantagineum*. The transketolases in *C. plantagineum* were extracted and the recombinant transketolase 3, 7 and 10 were purified. All proteins were tested in the enzymatic assays to determine the reaction products. In addition, the inhibitor of transketolase oxythiamine, was used in the rehydration of leaves of *C. plantagineum* to determine the activity of transketolase and in the enzymatic assays of recombinant transketolases. Besides, the relationship between D-g-D-i-oct and phosphate was studied.

From the results, it is concluded that desiccation tolerance is regulated by senescence and this reflects the strategy of resurrection plants to adapt to a complex environment. The differences in expression patterns of senescence-related genes and carbohydrate status of senescent and vigorous *C. plantagineum* plants indicate that resurrection plants or their organs will be prepared in different ways for possible dehydration stress in a developmental-stage specific manner. By

analyzing the levels of sucrose, it is found that sucrose synthesis is more inclined to be regulated by water stress than by senescence in *C. plantagineum*. Light is an important factor for D-g-D-i-oct synthesis. The D-g-D-i-oct level is strictly controlled in *C. plantagineum* and D-g-D-i-oct was consumed to defend reactive oxygen species (ROS) produced by paraquat. D-g-D-i-oct is also localized in the cytosol and could be exported from leaves. Relative to common sugars present in *C. plantagineum* leaves, the substantial accumulation of D-g-D-i-oct may propose that D-g-D-i-oct is not primarily a sensing molecule but has a "structural" role. The excellent hydroxyl scavenging ability of D-g-D-i-oct implies that D-g-D-i-oct may be important for ROS scavenging which could further explain the substantial accumulation.

Our study suggests that the three isoforms of *C. plantagineum* transketolase may exert different functions. The tkt3 plays a role in the photosynthesis and the pentose phosphate pathway. The tkt7 and tkt10 isoforms of transketolase, which show distinct specificity in function and evolution catalyze the formation of D-g-D-i-oct-8-phosphate using glucose-6-phosphate and fructose-6-phosphate as substrate. The activity of transketolase was inhibited by the analogue of thiamine diphosphate, oxythiamine. The transketolase of *E. coli* could perform the same reactions as tkt7and tkt10. This may indicate that the D-g-D-i-oct and its metabolism might commonly exist in organisms. Although the phosphatase that hydrolyzes D-g-D-i-oct phosphate to produce D-g-D-i-oct could not be identified and characterized so far, the influence of phosphate on D-g-D-i-oct metabolism indicates that the phosphatase exists and is activated by a lack of phosphate and attenuated by an excess of phosphate.

Content

Chapter 1 introduction

1.1 Introduction of Saccharides

1.1.1 The definition of saccharides

Carbohydrates, lipids, nucleic acids and proteins are the four main classes of biomolecules that are usually composed by the polymerization of monomer units. In biochemistry “saccharides” is more accurate than “carbohydrates” in terms of organic chemical definition. Saccharides are poly-hydroxyl aldehydes and ketones consisting of carbon, hydrogen, and oxygen. They play fundamental roles in the life of organisms including the usage and storage of energy, the transformation among different biomolecules, the formation of cellular structure, signaling in cells and the regulation of various physiological processes. According to the degrees of polymerization (DP), saccharides are classified as monosaccharides (DP1), disaccharides (DP2), oligosaccharides (DP ≤10) and polysaccharides (DP >10) (Peshev *et al.*, 2013).

1.1.2 The complexity of saccharides

Given the degrees of polymerization, the structural diversity and stereo-chemical diversity, there should be millions of saccharides theoretically. Additionally, as the basic unit of disaccharides, oligosaccharides and polysaccharides, monosaccharides exist always in bound state with linking to phosphate or nucleotide-diphosphate, and still have many important derivatives including sugar acid, sugar alcohol, deoxy sugar and amino sugar. In organisms, metabolism of saccharides may comprise of the hydrolysis and formation of disaccharides, oligosaccharides and polysaccharides, the synthesis and breakdown of monosaccharides, the conversion between monosaccharides and their derivatives. Thus sugar metabolism is very complex. For example, the ADP-α-D-glucose which is the precursor for the synthesis of starch (a major storage polysaccharide in most plants) may be derived from photosynthesis, the hydrolysis of translocated sucrose, the sugars released from oligosaccharides, the salvage of sugars from glycoproteins and glycolipids, the recycling of sugars released during primary and secondary cell wall restructuring, and the sugar generated during plant-microbe interactions (Bar-Peled and O'Neill, 2011).

1.1.3 The Diversity of saccharides in plants

Hundreds of millions of years of evolution has shaped plant metabolic phenotypes, during which some ancient metabolic networks change with environments while others are stably inherited (Milo and Last, 2012). Therefore, based on the main physiological processes (e.g. photosynthesis and respiration), various saccharide metabolic pathways have evolved in plants. In nature about 200 different monosaccharides exist and most of them are five-carbon or six-carbon sugars (Robyt, 1998). Most plants researched choose glucose, fructose, sucrose and starch as the core of their energy-operating system. However, considerable numbers of plants possess special saccharide metabolism including the accumulation of uncommon monosaccharides, disaccharides, oligosaccharides, polysaccharides and even sugar alchols etc. For example, trehalose is highly accumulated in *Selaginella lepidophylla* (Pampurova and Van Dijck, 2014); mannitol comprises a significant portion of the soluble carbohydrate in species of *Oleaeeae* (olive, privet), *Apiaceae* (celery, carrot, parsley) and *Rubiaceae* (coffee) (Stoop *et al.*, 1996).

1.1.4 The main metabolic pathways of saccharides in plants

Although the metabolism of saccharides in plants is of great complexity and plants have evolved various specific pathways in saccharide metabolism, most plants still share some common pathways in energy usage, cell structure formation, and transformation between different biomolecules etc.

1.1.4.1 Monosaccharide metabolism: photosynthesis, glycolysis and the pentose phosphate pathway

Photosynthesis that ultimately provides energy for life on earth achieves the synthesis of saccharides from carbon dioxide and water with the generation of oxygen in photosynthetic organisms (Taiz and Zeiger, 2010). In the process of photosynthesis in the majority of plant species, a range of monosaccharide-phosphates (including triose phosphate, tetrose phosphate phosphate, pentose phosphate, hexoses phosphate and heptose phosphate) participate in the metabolism and the harvested solar energy is stored in glucose, a six carbon monosaccharide. Glucose can be the component of sucrose and starch that act as the most common sugar transport form and energy storage substance in plants, respectively.

Glycolysis is the metabolic pathway that converts glucose into pyruvate, in which the free energy released in this process is used to form the high-energy compounds adenosine triphosphate (ATP) and reduced nicotinamide adenine dinucleotide (NADH). Abundant monosaccharides such as fructose and galactose can be converted to the intermediates of glycolysis to enter into it. As the parallel pathway of glycolysis, the pentose phosphate pathway (PPP) involves the oxidation of glucose to generate reduced nicotinamide adenine dinucleotide phosphate (NADPH) and pentoses (e.g. ribose).

There are close interconnections between photosynthesis, glycolysis and the PPP in plants. The enzymatic reactions of the PPP could subdivide itself into two biochemical branches, known as the oxidative and non-oxidative PPP (Krüger and von Schaewen, 2003). There is over-lapping between reactions of the non-oxidative PPP and Calvin cycle (photosynthesis) and Entner–Doudoroff pathways (glycolysis). By sharing intermediate metabolites (e.g. fructose 6-phosphate and glyceraldehyde 3-phosphate), the PPP can be connected with glycolysis. The light-independent reactions of carbon fixation in the Calvin cycle share enzymes and reactions with the pentose phosphate pathway [e.g. the transformation of ribose-5-phosphate into ribulose-5-phosphate catalyzed by ribose-5-phosphate isomerase (EC 5.3.1.6)] and glycolysis [e.g. the transformation between glyceraldehyde 3-phosphate and dihydroxy acetonephosphate catalyzed by triosephosphate isomerase (EC 5.3.1.1)] (Stincone *et al.*, 2015).

1.1.4.2 Synthesis and hydrolysis of sucrose

Sucrose plays a central role in plant growth and development. It is a major end product of photosynthesis and functions as a primary transport sugar and in some cases as a direct or indirect regulator of gene expression (Winter and Huber, 2000). Sucrose is synthesized in the cytosol. Uridine diphosphate glucose (UDP-glucose), fructose-6-phosphate, sucrose-6-phosphate, glucose and fructose participate in sucrose metabolism in plants. The principal sucrose-biosynthesis route involves sucrose-phosphate synthase (SPS; UDP–glucose:d-fructose-6-phosphate 2-α-d-glucosyltransferase, EC 2.4.1.14) and sucrose-phosphate phosphatase (SPP; sucrose-6^F-phosphate-phosphohydrolase, EC 3.1.3.24). The former catalyzes the synthesis of sucrose-6-phosphate and the latter yields free sucrose and inorganic phosphate (Huber and Huber, 1996). The hydrolysis of the sucrose-6-phosphate by SPP is irreversible to efficiently produce sucrose

even when the substrate is at low concentration. Sucrose synthase (SuS; UDP–glucose:d-fructose 2-α-d-glucosyltransferase, EC 2.4.1.13) catalyzes a readily reversible reaction and could be involved in both the synthesis and cleavage of sucrose (Salerno and Curatti, 2003). However, SuS is usually assigned a role in sucrose cleavage under most physiological conditions in sucrose-using tissues, supplying sugar nucleotides, precursors in the formation of structural and storage polysaccharide (Winter and Huber, 2000). The hydrolysis of sucrose into hexoses is an irreversible reaction catalyzed by invertases (EC 3.2.1.26), which exist in several isoforms and play an important role when there is a demand for carbon and energy. In plant tissues, there are two classes of invertase activity: neutral and alkaline invertases and acid invertase. The neutral and alkaline invertases are localized in the cytosol and their pH optima are between 6.5 and 8.0. The acid invertase are extracellular or vacuolar and their pH optimum is about 5.0 (Sturm, 1999; Winter and Huber, 2000).

1.1.4.3 Synthesis and hydrolysis of starch

Starch is a polysaccharide composed exclusively of D-glucose and is one of the most abundant organic compounds found on the earth. Starch is accumulated mainly in leaves and also in stems, seeds, roots and tubers of many higher plants. It serves to store the chemical energy obtained from the light energy in photosynthesis (Robyt, 1998). Chloroplast is the site of starch synthesis in leaves. Starch metabolism involves phosphoglucomutase (PGM), phosphoglucose isomerase (PGI), ADPglucose pyrophosphorylase (AGPase), starch synthase (SS); branching enzyme (BE), debranching enzyme (DBE); triose-phosphate/phosphate translocator (TPT), UDPglucose pyrophosphorylase (UGPase), sucrose-phosphate synthase (SPS); sucrose phosphate phosphatase (SPP), glucan water dikinase (GWD), phosphoglucan, water dikinase (PWD), phosphoglucan phosphatases SEX4 and LSF2, α-amylase (AMY), β-amylase (BAM), disproportionating enzyme (DPE) and α -glucan phosphorylase (PHS) (Kötting *et al.*, 2010).

Starch has two major components, the basically linear α -polyglucan amylose and the branched α -polyglucan amylopectin. The α -1,4-glucosidic link chains of both amylose and amylopectin are elongated by the addition of the glucose moieties from ADPglucose, which is synthesized by (AGPase) from glucose-1-P, to the non-reducing end of the α-glucan acceptor molecule. The elongation reactions for the α-1,4-chains of amylose and amylopectin are distinctively catalyzed

by a starch granule-bound form of starch synthase (GBSS) and SS, respectively. Amylose is synthesized by AGPase and GBSS while amylopectin is synthesized by the coordinated actions of AGPase, SS, SBE, and DBE (Ohdan *et al.*, 2005).

Starch breakdown is facilitated by glucan phosphorylation mediated by the sequential actions of (GWD) and PWD, which phosphorylate different glucosyl residues at the C6 and C3 positions, respectively. Glucan degradation is mediated by a suite of enzymes, the most important of which are BAM (liberating maltose) and DBE (hydrolyzing the α-1,6-branch points of the glucans comprising starch). Additionally, AMY and DPE play roles in the liberation and metabolism of malto-oligosaccharides in the stroma; PHS hydrolyzes the linear glucans into glucose-1-phosphate (Stitt and Zeeman, 2012).

1.4.4.4 Cellulose and hemicelluloses

Cell walls of higher plants consist of cellulose, hemicelluloses, and lignin. The three substances are physically entangled and held together by secondary forces such as hydrogen bonding and van der Waals forces. Lignin, as non-carbohydrate component can be separated from plant cell walls by treating the plant material with chlorous acid at 70-75 °C. The resulting material is known as holocellulose. Hemicelluloses can be extracted from the holocellulose with alkaline solutions of 2-18% (w/v) sodium hydroxide while the isolation of cellulose from the holocellulose needs more steps (Robyt, 1998).

Cellulose has been said to be the most abundant organic compound on the Earth. It is a homopolysaccharide composed of D-glucose units linked to each other via β-1,4-glucosidic bonds. The repeating unit in cellulose is anhydrocellobiose (Mäki-Arvela *et al.*, 2011). Cellulose synthesis takes place in the plasma membrane. The plasma membrane is tightly appressed to the cell wall so that most of the cellulose synthase is in or below the plane of the membrane, which minimizes friction as the enzyme moves through the plasma membrane in response to elongation of the growing glucan chains by addition of glucan moieties from cytoplasmic UDP-glucose. The cellulose synthase complex is thought to contain as many as 36 CESA proteins (a member of a family of related proteins that compose cellulose synthase), only a subset of which are illustrated. That three types of CESA proteins are required to form a functional complex suggested that

different types of CESA proteins perform specific functions, such as interacting with the cortical microtubules (Somerville, 2006).

Hemicelluloses are a heterogeneous group of polysaccharides that vary from plant to plant and from one plant part to another. There are four basic types of hemicellulose polysaccharides: D-xyloglucans, composed of D-xylopyranose attached to a cellulose chain; D-xylans, composed of D-xylose; D-mannans, composed of D-mannose; and D-galactans, composed of D-galactose. These polysaccharides are similar to cellulose in having their main chains linked via β-1,4-glucosidic bonds. Most of the hemicelluloses are, however, heteropolysaccharides with one to three monosaccharides units linked to the main monosaccharide chains (Robyt, 1998). The biosynthesis of hemicelluloses mainly involve with the biosynthesis of mannans, xylans, arabinans, and galactans, which all use nucleotide sugars as substrate and are catalyzed by a series of polysaccharide synthases and glycosyl transferases. The biosynthesis of hemicelluloses has been reviewed by Pauly *et al.* (2013).

1.2 “Sugars” in plants: common sugars and rare sugars

Despite of many saccharides in nature, only a small number of them are observed and thoroughly studied in the majority of plant species and so far constitute what are referred to as ‘sugars’ in plants. More restrictively, they are referred to as monosaccharides and disaccharides which have a low molecular weight and exist in easily observable amounts in plants (Flitsch and Ulijn, 2003). For example in *Arabidopsis thaliana* ‘sugars’ often represent the sugars glucose, fructose and sucrose.

Therefore in the scope of ‘sugars’ in plant, some are closely related to basic carbon metabolism (e.g. photosynthesis, carbon transporting and energy storage) and widely found in plants, while others are produced only in specific metabolic pathways and are limited to a few species. Sugar metabolism could hereby be divided into ‘general sugar metabolism’ and ‘unusual sugar metabolism’ (or ‘special sugar metabolism’). Correspondingly, we could simply sort sugars into ‘common sugars’ and ‘rare sugars’, though the boundary between common sugars and rare sugars might change with more novel findings.

1.2.1 Physiological functions of common sugars

In plants, common sugars play important roles as both nutrients and signal molecules. Both glucose and sucrose are recognized as pivotal integrating regulatory molecules that control gene expression related to plant metabolism, stress resistance, growth and development (Pego *et al.*, 2000; Rolland *et al.*, 2006). Plant growth is a highly energy-demanding process that needs complex molecular networks to adapt continuously to a changing environment. However, plants have to experience various biotic and abiotic stresses that often lead to an adaption response resulting in the inhibition of growth and development to preserve vital resources. Sugars serve as key components reflecting the plant's energy status. Therefore, the ability to continuously sense sugar levels and control the energy status is very important for survival. All eukaryotes harbor two important regulatory networks to respond to changes in nutrient and energy status. In plants these are the Snf1-related kinase 1 (SnRK1) which is the homologue of the animal AMP-activated protein kinase (AMPK) and yeast sucrose non-fermenting 1 (SNF1) kinase, and the plant target of rapamycin (TOR) kinase. These are central regulators that link growth and development to carbon nutrient and energy status. TOR promotes growth in response to high sugar levels, while SnRK1 is particularly active upon sugar deprivation. TOR and SnRK1 activities are modulated by the plant's sugar status that is sensed in signaling processes (Lastdrager *et al.*, 2014). For example, hexokinase (HXK), the first enzyme in glycolysis also functions as a glucose sensor, triggering changes in metabolic (e.g. repressing photosynthetic) gene expression, altering hormone sensitivity, and stimulating growth in response to glucose availability. Glucose 6-phosphate (G6P), the product of HXK enzymatic activity, was found to inhibit SnRK1 kinase activity *in vitro* (Smeekens *et al.*, 2010).

Soluble sugars such as disaccharides, raffinose family oligosaccharides and fructans are strongly related to stress-induced ROS accumulation in plants (Keunen *et al.*, 2013). In plants, stress-induced ROS accumulation is counteracted by two different processes: (1) prevention or avoidance of ROS formation and (2) actual ROS scavenging by both enzymatic and non-enzymatic metabolic antioxidants (Mittler, 2002). Soluble sugars can not only be involved in ROS producing metabolic pathways [such as production of energy (ATP) in mitochondria], but also enhance NADPH-producing metabolism such as the oxidative pentose phosphate pathway, thereby contributing to ROS scavenging (Couée *et al.*, 2006; Bolouri-Moghaddam *et al.*, 2010).

However, it is becoming increasingly clear that sugars, especially those interacting with membranes (Bolouri-Moghaddam *et al.*, 2010), can also act as true ROS scavengers in plants (Van den Ende & Valluru, 2009; Peshev *et al.*, 2013).

1.2.2 Special sugar metabolism

Usual sugar metabolism has been described above, while special sugar metabolism has not been studied fully and lots of gaps need to be filled. However, typical examples show the strategy of plants to synthesize special sugars in energy metabolism, signaling and response to biotic or abiotic stresses, including the synthesis of disacharides (e.g. maltose and trehalose) and raffinose family oligosaccharides (e.g. staychose), sugar alcohols (e.g. mannitol) and some rare sugars (e.g. octulose).

1.2.2.1 Typical examples of special sugar metabolism

Trehalose is detected in a wide range of organisms, including bacteria, fungi, invertebrates and plants and in resurrection plants, such as *Myrothamnus flabellifolius* or *Selaginella lepidophylla* the content of trehalose could reach up to 10 mg per g fresh weight (Fernandez *et al.*, 2010). Trehalose is synthesized in higher plants by the trehalose phosphate synthase (TPS)–trehalose phosphate phosphatase (TPP) pathway, in which TPS catalyzes the binding of a glucose-6-phosphate to a UDP-glucose to produce trehalose-6-phosphate (T6P) and T6P is cleaved into trehalose by TPP. Trehalose breaks down to form two glucose residues (Paul *et al.*, 2008).

Sugar alcohols are present in many food crops: from apples, to seaweeds, and to mushrooms. Red raspberry, as an example of rubus fruit, has been reported to contain glucose, fructose, sucrose, sorbitol, mannitol, and myo-inositol (Lee, 2015). Mannitol, a six carbon sugar alcohol, is widely distributed in nature (Stoop *et al.*, 1996). In vascular plants, mannitol is synthesized from mannose-6-phosphate through the action of an NADPH mannose-6-phosphate reductase (M-6-PR) that catalyzes the conversion of mannose-6-phosphate to mannitol-1-phosphate; then mannitol-1-phosphate is dephosphorylated by a phosphatase (Rumpho *et al.*, 1983). Sorbitol is found mostly in Rosaceae (Loescher, 1987). There is a NADPH dependent aldose 6-phosphate reductase (EC 1.1.1.200) that catalyzes the synthesis of sorbitol-6-phosphate, and the NAD

dependent dehydrogenase or the NAD dependent sorbitol oxidase converts sorbitol to fructose or glucose.

The raffinose family oligosaccharides (RFOs) are ubiquitous in plants, with certain plant species using RFOs as the main transport compounds (dos Santos et al. 2013). RFO-producing plants include cucurbits, mints, legumes, olives, grapes, pines and grains (Elsayed *et al.*, 2013). Raffinose is found in all plants while stachyose and other higher degree of polymerization RFOs such as verbascose and ajugose accumulate in the vacuole of only certain plant species (Janeček *et al.*, 2011). RFOs are synthesized from sucrose by the subsequent addition of activated galactinol moieties (Gal). Galactinol is synthesized from uridine diphosphate UDP-Gal and "myo-inositol" by galactinol synthase (GolS; EC 2.4.1.123; (Peterbauer *et al.*, 2001). Raffinose is synthesized by raffinose synthase (RS; EC 2.4.1.82) which transfers a Gal residue from galactinol to sucrose. Other oligosaccharides of this pathway (stachyose, manninotriose and melibiose) are sequentially formed by the action of specific galactosyltransferases using galactinol as a galactosyl moiety donor (Zhou *et al.*, 2012).

Free sedoheptulose can be found in a range of families including Apiaceae, Aquifoliaceae, Euphorbiaceae, Lamiaceae, Primulaceae, and Saxifragaceae; and accumulates to a high extent in some members of the Crassulaceae family such as *Sedum spectabile* (Ceusters *et al.*, 2013) .Despite of the universal presence of its mono- and bisphosphate esters in the plant kingdom, the role of free sedoheptulose in plants remains a matter of speculation. Ceusters *et al.* (2013) found that sedoheptulose accumulated under elevated CO_2 and proposed that sedoheptulose should be produced from the oxidative pentose phosphate pathway intermediate sedoheptulose-7-phosphate, by a sedoheptulose-7-phosphate phosphatase that is attenuated by ADP and inorganic phosphate.

1.2.2.2 Physiological functions of rare sugars

The disaccharide trehalose is involved in stress response in many organisms. However, in plants, its precise role remains unclear, although some data indicate that trehalose has a protective role during abiotic stresses. By contrast, some trehalose metabolism mutants exhibit growth aberrations, revealing potential negative effects on plant physiology. Contradictory effects also appear under biotic stress conditions. Specifically, trehalose is essential for the infectivity of

several pathogens but at the same time elicits plant defense. Here, we argue that trehalose should not be regarded only as a protective sugar but rather like a double-faced molecule and that further investigation is required to elucidate its exact role in stress tolerance in plants (Fernandez *et al.*, 2010).

It is demonstrated for the first time that manninotriose is a novel and important player in the RFO metabolism of red deadnettle. It is proposed that manninotriose represents a temporary storage carbohydrate in early-spring deadnettle, at the same time perhaps functioning as a membrane protector and/or as an antioxidant in the vicinity of membranes, as recently suggested for other RFOs and fructans. This novel finding urges further research on this peculiar carbohydrate on a broader range of RFO accumulators (dos Santos *et al.*, 2013).

Recent findings concerning the biochemistry and physiology of higher plants indicate that species that metabolize mannitol have several advantages over those that exclusively translocate sugars. One advantage is increased tolerance to salt- and osmotic-stress as a result of mannitol's function as a 'compatible solute'. Another advantage is a possible role in plant responses to pathogen attack, thus mannitol metabolism may play roles in plant responses to both biotic and abiotic stresses (Stoop *et al.*, 1996).

Sugar signals may also contribute to immune responses against pathogens and probably function as priming molecules leading to pathogen-associated molecular patterns (PAMP)-triggered immunity and effector-triggered immunity in plants (Moghaddam and Van den Ende, 2012).

D-allose, could induce resistance to *Xanthomonas oryzae pv.oryzae* in susceptible rice leaves with defence responses: reactive oxygen species, lesion mimic formation, and PR-protein gene expression. These responses were suppressed by ascorbic acid or diphenylene iodonium (Kano *et al.*, 2013).

The accumulation of free sedoheptulose is proposed to act as a mechanism contributing to both carbon and phosphorus homeostasis by serving as an alternative carbon store under elevated CO_2 or a compromised sink capacity to avoid sucrose accumulation, depletion of inorganic phosphate, and suppression of photosynthesis (Ceusters *et al.*, 2013).

RFOs are characterised as compatible solutes involved in stress tolerance mechanisms. Although evidence suggests that they act as antioxidants, they are part of carbon partitioning strategies and may serve as signals in response to stress. The key enzyme and regulatory point in RFO biosynthesis is galactinol synthase (GolS), and an increase of GolS in expression and activity is often associated with abiotic stress. It has been shown that different GolS isoforms are expressed in response to abiotic stress, suggesting that the timing and accumulation of RFOs are controlled for each abiotic stress. However, the accumulation of RFOs in response to stress is not universal and other functional roles have been suggested for RFOs, such as being part of a carbon storage mechanism. Transgenic Arabidopsis plants with increased galactinol and raffinose concentrations had better reactive oxygen species (ROS) scavenging capacities, The RFO pathway also interacts with other carbohydrate pathways, such as that of O-methyl inositol (OMI), which shows that the functional relevance of RFOs must not be seen in isolation to overall carbon re-allocation during stress responses (Elsayed *et al.*, 2013).

1.3 Sugar transport

Transport is an important part in sugar metabolism. The transported compounds enter the phloem primarily in mature leaves but also exchange with surrounding tissues along the transport route (Turgeon and Wolf, 2009). Among the sugars synthesized in a plant, only a few are transported in the phloem over a long-distance. In all cases, sucrose is the main form of carbon found in the phloem. In addition to sucrose, polyols (mainly sorbitol and mannitol) and oligosaccharides of the raffinose family can also be found. In some species, both polyols and raffinose are found in the phloem. (Lemoine *et al.*, 2013) Source-to-sink transport of sugar is one of the major determinants of plant growth and relies on the efficient and controlled distribution of sucrose (and some other sugars such as raffinose and polyols) across plant organs through the phloem. However, sugar transport through the phloem can be affected by many abiotic stressors (water and salt stress, mineral deficiency, CO_2, light, temperature, air, and soil pollutants) and biotic (mutualistic and pathogenic microbes, viruses, aphids, and parasitic plants) factors that alter source/sink relationships.

1.4 Resurrection plants and the model plant *C. plantagineum* Hochst.

1.4.1 Resurrection plants

Water is the key component of life, and organisms exhibit a suite of adaptations for surviving and thriving within a water-limited environment. Terrestrial organisms are constantly losing water to the surrounding environment because they are in disequilibria with the atmosphere (i.e., the surrounding air is extremely "dry" relative to the organism). The vast majority of organisms cannot survive equilibrium with dry air and will die upon complete drying. However, a number of species can survive complete drying and "resurrect from the dead". They could be called "anhydrobiotes, or desiccation-tolerant organisms". Anhydrobiotes have been observed among the three domains of life—Archaea, Bacteria, and Eukarya. A central aspect of the land plant life cycle is the production of a reproductive structure(s) capable of surviving desiccation, most notably orthodox seeds but also spores and pollen. Desiccation-tolerant reproductive structures are found within the bryophytes, pteridophytes, gymnosperms, and angiosperms. Approximately 320 species of vascular plants (less than 0.15% of the total) possess vegetative desiccation tolerance. They reside within 9 pteridophyte families (Adiantaceae, Aspleniaceae, Davalliaceae, Grammitidaceae, Hymenophyllaceae, Isoëtaceae, Polypodiaceae, Schizaeaceae, and Selaginellaceae) and 10 angiosperm families (Acanthaceae, Cactaceae, Cyperaceae, Gesneriaceae, Labiatae, Liliaceae, Myrothamnaceae, Poaceae, Scrophulariaceae and Velloziaceae). Desiccation-tolerant plants or resurrection plants have been reported since about one century ago. Experiencing systematical studies, some resurrection plants, such as *Craterostigma plantagineum* Hochst and *Xerophyta viscosa* Baker, have been developed as model experimental systems (Wood and Jenks, 2007).

1.4.2 The model plant *C. plantagineum* among resurrection plants

C. plantagineum shows desiccation tolerance in vegetative tissues and in undifferentiated callus cultures. This makes it possible to analyze molecular mechanisms in the absence of developmental complications. Callus from *C. plantagineum* is not intrinsically desiccation tolerant, but it acquires tolerance after being cultured on medium containing the plant hormone ABA. Callus from *C. plantagineum* can be genetically transformed by *Agrobacterium*

tumefaciens and is suited for transient expression analysis using protoplasts or a ballistic approach (Bartels and Salamini, 2001).

1.5 Special sugar metabolism in *C. plantagineum*

1.5.1 The occurrence of eight-carbon monosaccharides

Eight-carbon monosaccharides occur naturally in a number of higher plants. Early in 1960, Charlson and Richtmyer (1960) reported that they isolated D-Glycero-D-manno-octulose from the Avocado and Sedum Species. D-glycero-L-galacto-octulose has been identified in only a few species, including *Persea gratissima*, *Sedum spectabile*, and *Primula oficinalis* (Haustveit *et al.*, 1975a). D-glycero-L-galacto-octulose and L-glycero-L-galacro-octulose could be accumulated when leaves of Kenland red clover (*Trifolium pratense*) were allowed to imbibe solutions of D-gulose or D-xylose and L-mannose or L-arabinose, respectively.(Haustveit *et al.*, 1975a) Similarly, the biosynthesis of D-glycero-D-altro-octulose in Kenland red clover leaves could be achieved when leaves were allowed to imbibe D-rlbose or D-allose (Haustveit *et al.*, 1975b). D-glycero-D-ido -2-octulose, a kind of eight carbon monosaccharide, has been reported as a rare but abundant monosaccharide in leaves of the resurrection plant *C. plantagineum*. D-glycero-D-ido -2-octulose would be converted to sucrose when *C. plantagineum* encounters dehydration (Bianchi *et al.*, 1991).

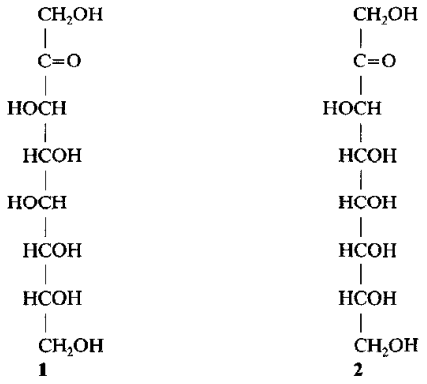

Fig. 1.1. The structures of D-glycero-D-ido-octulose (D-g-D-ido-oct, **1**) and D-glycero-D-altro-octulose (D-g-D-alt-oct, **2**)

1.5.2 The synthesis of eight-carbon sugar phosphates

Using isotope technology, Williams *et al.* (1978) proposed a different version of the pentose phosphate pathway (L-type pentose phosphate pathway) in rat liver in which arabinose 5-phosphate, sedoheptulose 1,7-bisphosphate and the mono-and bisphosphates of D-glycero-D-ido-octulose are included as the intermediates. In addition, Paoletti *et al.* (1979) used rabbit muscle aldolase to synthesize D-glycero-D-altro-octulose 1,8-bisphosphate or D-glycero-D-ido-octulose 1,8-bisphosphate by condensation of dihydroxyacetone phosphate with ribose-5-phosphate or arabinose-5-phosphate. 3-Deoxy-D-manno-octulosonate 8-phosphate synthase (KDOPS) (kdsA) was found to catalyze the stereospecific condensation of D-arabinose 5 -phosphate and PEP (phosphoenolpyruvate) to form 3-deoxy-D-manno-octulosonate 8-phosphate (KDO-8-phosphate) and phosphate. The kdsA genes from the hyperthermophilic bacterium *Aquifex aeolicus* and *Arabidopsis thaliana* were cloned, and functionally characterized (Duewel *et al.*, 1999; Wu *et al.*, 2004). In the study of the process of methylthiolincosamide biosynthesis, Sasaki *et al.* (2012) identified that D-glycero-D-altro-octulose is formed via a transaldol reaction catalyzed by a putative transaldolase (LmbR) using D-fructose 6-phosphate or D-sedoheptulose 7-phosphate as the C3 donor and D-ribose5-phosphate as the C5 acceptor. Subsequent 1,2-isomerization catalyzed by LmbN which displays moderate sequence identity with a sedoheptulose-7-phosphate isomerase (31% identity and 47% similarity to the *Escherichia coli* protein), converts the resulting 2-keto C8-sugar (octulose 8-phosphate) to D-erythro-D-gluco-octose 8-phosphate. 3,7-Anhydro-1-deoxy-D-glycero-D-gulo-2-octulose was isolated from the roots of *Brassica rapa* ssp. Campestri and was found to show significant ROS reduction and protective effect on glutamate-induced cell death in neuronal HT-22 nerve cells (derived from the mouse hippocampus) (Wu *et al.*, 2013).

D-glycero-D-ido-octulose mono- and bisphosphates and D-glycero-D-altro-octulose mono- and bisphosphates were identified in spinach leaves and chloroplasts by Williams and MacLeod (2006). They proposed that D-glycero-D-ido-octulose-8-phosphate, D-glycero-D-altro-octulose-8-phosphate and D-glycero-D-altro-octulose-1, 8-diphosphate may also be reactants in a modified Calvin–Benson–Bassham pathway reaction scheme (Fig. 1.2). (Flanigan *et al.*, 2006) and D-glycero-D-ido-octulose phosphates could be formed by the exchange reaction using fructose-6-phosphate and glucose-6-phosphate as substrate.

1.5.3 D-g-D-i-oct and sucrose in *C. plantagineum*

D-glycero-D-ido-2-octulose was found in the resurrection plant *C. plantagineum* in hydrated conditions and there is a conversion between D-glycero-D-ido-2-octulose and sucrose during dehydration and rehydration (Bianchi *et al.*, 1991). Norwood *et al.* (2000) reported that octulose is a product of photosynthesis and accumulates in the leaves of *C. plantagineum* during the light period and is mobilized at night. Raffinose series oligosaccharides (e.g. stachyose) are also the product of photosynthesis in leaves and are translocated into the phloem. Besides, it is proposed that stachyose which is stored in the roots of *C. plantagineum* is the carbohydrate reserve for the synthesis of sucrose during dehydration. Several researches revealed that sucrose plays an important role in regulating osmotic potential and protecting membrane and macro-molecules in resurrection plants (Dinakar and Bartels, 2013; Hoekstra *et al.*, 1997; Peters *et al.*, 2007; Vicré *et al.*, 2004). Given the importance of sucrose formation, two distinct classes of cDNAs (Cpsps1 and Cpsps2) encoding sucrose-phosphate synthase (SPS) were isolated from *C. plantagineum*. The transcripts of Cpsps1 and Cpsps2 decrease to very low levels in dehydrating leaves of *C. plantagineum*. Only the Cpsps1 transcript occurs in the roots and increases upon dehydration of the plant (Ingram *et al.*, 1997). In addition, the gene of sucrose synthase catalyzing the reversible conversion of UDP-sucrose into fructose and UDP-glucose was characterized. Sucrose-synthase transcript and protein levels are modulated by dehydration and rehydration. The class-I sucrose-synthase genes positively respond to dehydration stress and to *cis*-abscisic acid (Kleines *et al.*, 1999). Relative to common carbon metabolism in most high plants, the study regarding octulose did not get much attention. It is still a mystery why *C. plantagineum* chooses such a special pathway and it is intriguing to explore the relationship between octulose and desiccation tolerance.

1.5.4 The enzymes involved in the synthesis of D-g-D-i-oct

Sucrose that is accumulated to high amounts in dehydrated *C. plantagineum* leaves is converted to D-g-D-i-oct when plants are rehydrated (Bianchi *et al.*, 1991). Bernacchia *et al.* (1995) isolated three distinct classes of transketolase-encoding cDNA clones from *C. plantagineum* and proposed that transketolases may play a role in the conversion of sugars in the rehydration process. In a modified Calvin–Benson–Bassham pathway the reaction scheme proposed by Flanigan *et al.*

(2006) and Williams and MacLeod (2006), also suggested that D-glycero-D-ido-octulose 8-P in spinach leaves and chloroplasts may be formed by the reaction of transketolase. In the study of yeast by Clasquin *et al.* (2011), it was proposed that octulose-1,8-bisphosphate might be synthesized by the aldol addition of DHAP and ribose-5-phosphate, which is catalyzed by the ubiquitous glycolytic enzyme fructose bisphosphate aldolase (Clasquin *et al.*, 2011). This is consistent with the modified Calvin–Benson–Bassham pathway reaction scheme proposed by Flanigan *et al.* (2006) and Williams and MacLeod (2006). Thus it is necessary to verify whether D-g-D-i-oct is synthesized through transketolase.

Transketolase (TK, EC 2.2.1.1) occupies a pivotal place in metabolic regulation, providing a link between the glycolytic pathway and the pentose phosphate pathway. The enzyme has a controlling role in the supply of ribose units for nucleoside biosynthesis, and (in microorganisms) in the supply of erythrose-4-phosphate into the shikimate pathway for aromatic amino acid biosynthesis. Transkctolase was first identified by Racker *et al.* (1953) in the yeast *Saccharomyces cerevisiae* and subsequently located in other sources, including spinach (Villafranca and Axelrod, 1971). *In vivo* the enzyme catalyses the reversible transfer of a two carbon ketol unit from D-xylulose-5-phosphate to D-ribose-5-phosphate to generate D-sedoheptulose-7-phosphate and D-glyceraldchyde-3-phosphate. The activity of TK is dependent on divalent metal cations (usually Mg^{2+}) and thiamine pyrophosphate (TPP). There is a large family of TPP-dependent enzymes (e.g. pyruvate decarboxylase, dihydroxyacetone synthase, 1-deoxyxylulose-5-phosphate synthase) (Turner, 2000). They would be selectively inhibited by the phosphonate analogs of 2-oxo acids that mimick the enzyme-specific catalytic intermediates (Bunik *et al.*, 2013).

The work of (Willige *et al.*, 2009) showed that *C. plantagineum* transketolase 7 and transketolase 10 are localized in the cytosol while transketolase 3 is in chloroplasts. Transketolase extracts from rehydrated leaves of *C. plantagineum* could catalyze the formation of D-g-D-i-oct-8-phosphate using hydroxypyruvate and glucose-6-phosphate as substrate.

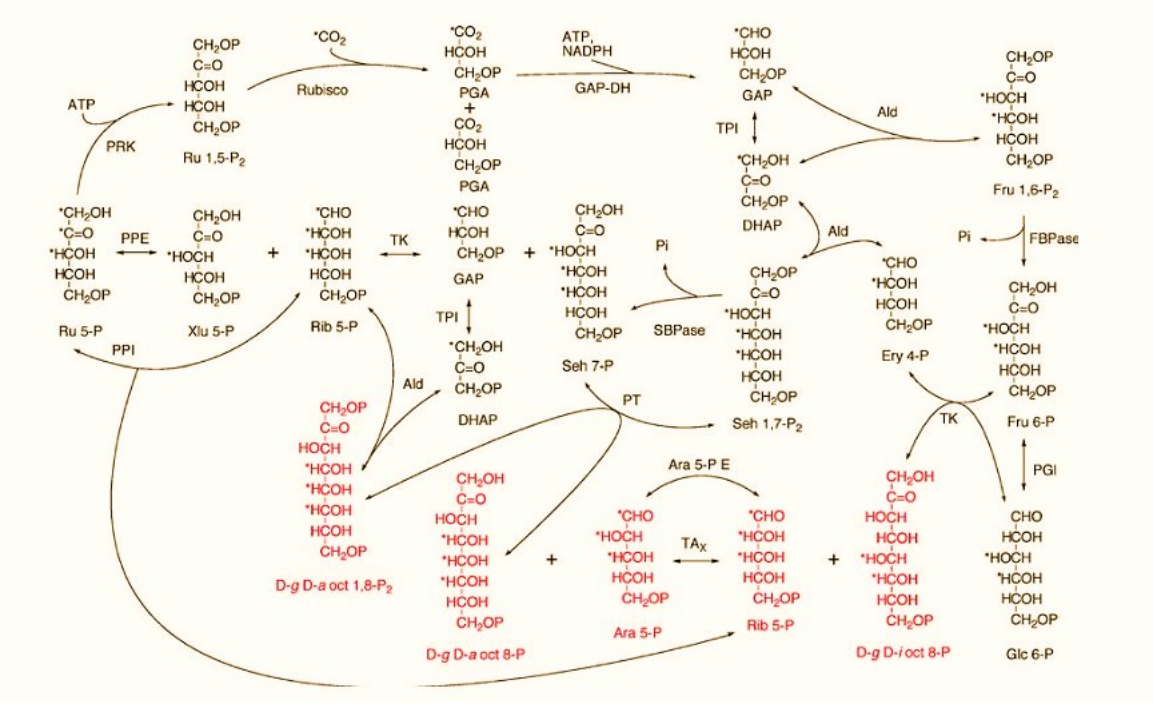

Fig. 1.2. An extension of the Calvin pathway including the octulose phosphate shunt represented in red [Cited from Flanigan *et al.* (2006)].

1.6 Sugar and sugar phosphate phosphatases

Sugars always accumulate as unmodified sugars in plants, while their phosphate compounds would participate in metabolism. Thus phosphatases must exist that lead to the production of abundant free sugars from their phosphates. The enzyme activities and genes for several specific plant phosphatases have been identified, such as phospho-glycolate phosphatase (Mamedov *et al.*, 2001), phosphor-serine phosphatase (Ho *et al.*, 1999), myo-inositol monophosphatase (Gillaspy *et al.*, 1995), sucrose-6-phosphate phosphatase (Lunn *et al.*, 2000), and trehalose-6-phosphate phosphatase (Vogel *et al.*, 1998), and L-galactose-1-phosphate phosphatase purified from young kiwifruit (*Actinidia deliciosa*) berries (Laing *et al.*, 2004). Besides, enzyme activity for other specific phosphatases has been identified but not yet cloned; e.g., sorbitol-6-phosphate phosphatase (Zhou *et al.*, 2003) and 2-carboxy-D-arabinitol-1-phosphate phosphatase (Kingstonsmith *et al.*, 1992) and sedoheptulose-7-phosphate phosphatase (Ceusters *et al.*, 2013). There is also a lot of information on specific acid phosphatases which would be expected to dephosphorylate specific sugar substrates (Duff *et al.*, 1994; Schenk *et al.*, 2000; Zhang *et al.*,

2014). Recent research reveals that two genes coding for haloacid dehalogenase (HAD)-like enzymes in brown algae were suggested to correspond to mannitol-1-phosphatase (M1Pase) activity (Groisillier *et al.*, 2014). They should be considered as members of a new family of phosphatases with substrate specificity within the HAD superfamily of proteins. In terms of eight-carbon sugar phosphatase, a phosphatase specific for the hydrolysis of 3-deoxy-D-manno-octulosonate (KDO)-8-phosphate was purified from crude extracts of *Escherichia coli* B (Ray and Benedict, 1980).

1.7 The questions explored in this study

This study focused on the occurrence of D-g-D-i-oct in *C. plantagineum* plants in different growth conditions. The relationship between sucrose and D-g-D-i-oct was taken into consideration. The incubation treatment of leaf tissues was conducted to observe the response of *C. plantagineum* to exogenous sugar, light and photosynthesis inhibitor. In addition, the localization of D-g-D-i-oct in cells was analyzed and the sugar transport from leaves to roots in *C. plantagineum* was estimated. Perhaps acting as antioxidant, the ability of D-g-D-i-oct in scavenging reactive oxygen species was tested. As a possible key enzyme in the synthesis of D-g-D-i-oct, three isoforms of *C. plantagineum* transketolase were cloned and expressed in *E. coli* cells. The recombinant proteins were purified by affinity chromatography and used in enzymatic assays. The products of reaction catalyzed by transketolase were characterized by GC/MS. The effect of the transketolase inhibitor oxythiamine was estimated during rehydration of *C. plantagineum* leaves. Oxythiamine was also used in the activity assay of enriched transktolase by $(NH_4)_2SO_4$ precipitation and in the enzymatic assay of recombinant transketolase proteins. Given the importance of possible phosphatases to hydrolyze D-g-D-i-oct phosphate to form D-g-D-i-oct, attempts were made to clone one of these phosphatase genes.

It has been well known that D-g-D-i-oct acts as the main sugar in *C. plantagineum* and it could be converted to sucrose when plants encounter desiccation. Relative to sucrose that was shown to play an important role in dehydrated resurrection plants, the occurrence of D-g-D-i-oct is not fully recognized. Additionally, in the genera *Linernia*, *Lindernia brevidens*, *L. subracemosa, L. philcoxii* and *L. numilarifolia* were found to produce D-g-D-i-oct. Only *L. brevidens* is desiccation tolerant and it accumulates much higher levels of D-g-D-i-oct than *L. subracemosa, L.*

philcoxii and L. numilarifolia (Kutzer, 2004). Thus it is necessary to study the role of D-g-D-i-oct and whether D-g-D-i-oct is associated with the ability of desiccation tolerance in *C. plantagineum*.

Carbohydrate acts as carbon source and provides the main energy in plant growth. There are various internal and external factors that affect the carbohydrate status in plants, including developmental stage, light and water etc. Although desiccation tolerance in resurrection plants involves a combination of molecular genetic mechanisms, metabolic and antioxidant systems as well as macromolecular and structural stabilizing processes (Moore *et al.*, 2009), the carbohydrate status is still fundamental for the achievement of desiccation tolerance in resurrection plants. As detached leaves and callus of some resurrection plants have complete tolerance to dehydration (Bartels *et al.*, 1990; Gaff and Loveys, 1984), they have to use stored carbohydrates to revive. However, no clear relationship has been established between the carbohydrate status and desiccation tolerance. In this study, the characteristic of D-g-D-i-oct in *C. plantagineum* was observed by comparing *C. plantagineum* plants in different development stages, estimating the localization of D-g-D-i-oct in cells, analyzing the periodic change of D-g-D-i-oct levels in leaves and analyzing the phloem exudate, as well as testing the antioxidant ability of D-g-D-i-oct. Also the change in sugar levels in *C. plantagineum* leaf tissues was determined to estimate plant responses to exogenous sugar, light and photosynthesis inhibitor.

Previous studies have proposed a potential function of transketolases in D-g-D-i-oct synthesis. However, there are still some questions to answer: whether the exchange reaction exists in *C. plantagineum* and whether the three different isoforms of transketolase in *C. plantagineum* have the same function, as well as how the three different isoforms are regulated in *C. plantagineum*? In this study, the protein sequences of transketolase from 50 angiosperm plant species and including the three different *C. planagineum* isofroms were analyzed phylogenetically. The proteins containing transketolase were extracted and enriched and the recombinant transketolase 3, 7 and 10 were purified from *E. coli* cells. All proteins were tested in the enzymatic assays to determine the reaction products. In addition, the inhibitor of transketolase oxythiamine, was used in the rehydration of leaves of *C. plantagineum* to determine the activity of transketolase and in the enzymatic assays of recombinant transketolases.

Given the fact that D-g-D-i-oct is accumulated very abundantly in *C. plantagineum*, it is reasonable to hypothesize that there is also a phosphatase that catalyzes the dephosphorylation of D-g-D-i-oct-8-phosphate or D-g-D-i-oct-1, 8-diphosphate to produce D-g-D-i-oct. Thus identification of the phosphatase that is involved in D-g-D-i-oct formation would also be an important task to shed light on the role of D-g-D-i-oct in *C. plantagineum*.

Chapter 2 Materials and methods

2.1 Materials

2.1.1 Plants and bacteria

C. plantagineum (Hochst.) plants were grown as previously described by Bartels *et al.* (1990). Plant seedlings were grown on MS medium for 2 weeks, and then transferred into plastic pots filled with artificial clay substrate. The plants were grown in a plant growth chamber with illumination of 100 μmol m^{-2} s^{-1} for 16 h and set at 22 °C in the light and 18 °C in the dark. *C. plantagineum* plants were sampled as "young plants" four weeks after transferring them into plastic pots and were sampled as "old plant" 15 weeks after transfer.

E. coli strains DH 10B and BL 21 (DE3) were obtained from the stock of the lab. The phage λ cDNA library of *C. plantagineum* was prepared by Bockel *et al.* (1998). The *E. coli* strain with the vector pET-22b containing the transketolase A gene of *E. coli* K12 was given by Professor Georg A. Sprenger, University of Stuttgart.

2.1.2 Media

Ingredients of Murashige and Skoog medium (MS medium): 1650 mg/L ammonium nitrate (NH_4NO_3), 440 mg/L calcium chloride ($CaCl_2 \cdot 2H_2O$), 370 mg/L magnesium sulfate ($MgSO_4 \cdot 7H_2O$), 170 mg/L potassium phosphate (KH_2PO_4), 1900 mg/L potassium nitrate (KNO_3), 6.2 mg/L boric acid (H_3BO_3), 0.025 mg/L cobalt chloride ($CoCl_2 \cdot 6H_2O$), 0.025 mg/L cupric sulfate ($CuSO_4 \cdot 5H_2O$), 27.8 mg/L ferrous sulfate ($FeSO_4 \cdot 7H_2O$), 22.3 mg/L manganese sulphate ($MnSO_4 \cdot 4H_2O$), 0.83 mg/L potassium iodide (KI), 0.25 mg/L sodium molybdate ($Na_2MoO_4 \cdot 2H_2O$), 8.6 mg/ zinc sulphate ($ZnSO_4 \cdot 7H_2O$) L, 37.2 mg/L Na_2EDTA $2H_2O$, 100 mg/L i-inositol, 0.5 mg/L niacin, 0.5 mg/L pyridoxine HCl and 0.1 mg/L thiamine HCl.

The composition of Luria Bertani Broth (LB medium): 10 g/L tryptone, 5 g/L yeast extract and 5 g/L NaCl (for the solid medium, 15 g agar added per L).

The composition of SOC medium: 2% (W/V) tryptone, 0.5% (W/V) yeast extract, 10 mM NaCl, 2.5 mM KCl, 10 mM $MgCl_2$, 10 mM $MgSO_4$ and 20 mM glucose.

2.1.3 Solutions and buffers

All the chemicals used in this study were purchased from Sigma-Aldrich or Roth if not specifically mentioned.

Percoll solution (P1644) was purchased from Sigma-Aldrich.

PBF Percoll (15 mL): 450 mg polyethylene glycol (PEG) 4000, 150 mg (bovine serum albumin) BSA and 150 mg Ficoll were dissolved in 15 mL Percoll solution.

70% Percoll gradient: 70% PBF Percoll (V/V), 330 mM sorbitol, 50 mM 4-(2-hydroxyethyl)-1-piperazineethanesulfonic acid (HEPES), 2 mM ethylenediaminetetraacetic acid (EDTA) (pH 8.0), 1 mM $MgCl_2$ and 1 mM $MnCl_2$.

30% Percoll gradient: 30 PBF Percoll (V/V), 330 mM sorbitol, 50 mM HEPES, 2 mM EDTA (pH 8.0), 1 mM $MgCl_2$ and 1 mM $MnCl_2$.

XPI buffer: 50 mM HEPES/KOH (pH 7.5), 330 mM sorbitol, 5 μM ascorbic acid, 1 mM $MgCl_2$, 1 mM $MnCl_2$ and 2 mM EDTA.

10× PCR buffer for routine PCR with $MgCl_2$: 100 mM tris(hydroxymethyl)aminomethane-HCl (Tris-HCl) (pH 8.3), 500 mM KCl, 15 mM $MgCl_2$ and 0.01% gelatin.

50× Tris-Acetate-EDTA (TAE) buffer: 2 M Tris base and 100 mM EDTA (pH 8.0, adjusted with glacial acetic acid).

10× DNA loading buffer (10 mL): 25 mg bromophenol blue, 25 mg xylen cyanol, 0.2 mL 50× TAE, 3 mL glycerol and 6.8 mL sterile distilled water.

Alkaline lysis solution Ⅰ: 25 mM Tris-HCl (pH8), 10mM EDTA (pH8) and 15% (W/V) glucose.

Alkaline lysis solution Ⅱ: 0.5M NaOH and 1% SDS.

Alkaline lysis solution Ⅲ: 3 M Potassium acetate (pH 5.0).

Buffer A of immobilized metal affinity chromatography: 50 mM HEPES/NaOH (pH 7.4), 300 mM NaCl, 5 mM imidazole, 10% (V/V) glycerol, 0.1% (V/V) Triton X-100 and 1.5 mM β-mercaptoethanol that was only added before use. The buffer was sterilized by filtration with 0.45 μm membrane.

Buffer B of immobilized metal affinity chromatography: 50 mM HEPES/NaOH (pH 7.4), 300 mM NaCl, 20 mM imidazole, 10% (V/V) glycerol, 0.1% (V/V) Triton X-100 and 1.5 mM β-mer captoethanol that was only added before use. The buffer was sterilized by filtration using a 0.45 μm membrane.

Buffer C of immobilized metal affinity chromatography: 50 mM HEPES/NaOH (pH 7.4), 300 mM NaCl, 250 mM imidazole, 10% (V/V) glycerol, 0 .1% (V/V) Triton X-100 and 1.5 mM β-mercaptoethanol that was only added before use. The buffer was sterilized by filtration with 0.45 μm membrane.

2× Laemmli buffer: 4% sodium dodecyl sulfate (SDS), 10% 2-mercaptoethanol, 20% (V/V) glycerol, 0.004% bromophenol blue and 0.125 M Tris-HCl. the pH was checked and adjusted to 6.8 if necessary.

Composition of 12% separating gel solution in sodium dodecyl sulfate polyacrylamide gel electrophoresis (SDS-PAGE) (12 mL for 2 gels) : 4.25 mL H_2O, 5 mL 30% Acrylamide/Bis-acrylamide (30%/0.8% W/V) (PAA-stock solution), 3.125 mL 1.5 M Tris-HCl (pH 8.8), 0.125 mL 10% (W/V) SDS, 62.5 μL 10% (W/V) ammonium persulfate (APS) and 6.25 μL tetramethylethylenediamine (TEMED).

Composition of 4% stacking gel solution in SDS-PAGE (6 mL for 2 gels): 6.1 mL dH_2O, 1.3 mL 30 % PAA-stock solution, 2.5 mL 0,5 M Tris-HCl, pH 6,8, 0.1 mL 10% (W/V) SDS, 50 μL 10% (W/V) APS and 10 μL TEMED.

TGS buffer in SDS-PAGE (1 L): 3 g Tris, 14 g glycine and 1 g SDS dissolved in 1000 mL dH_2O.

Composition of gel fixation solution in SDS- PAGE: 40 % (V/V) methanol and 10 % (V/V) acetic acid.

Composition of gel staining solution in SDS- PAGE: 0.08 % (W/V) coomassie brilliant blue G250, 0.8 % (V/V) 85% phosphoric acid, 8% (W/V) ammonium sulfate and 20% (V/V) methanol.

The transferring buffer in Western blotting: 25 mM Tris, 192 mM glycine and 20% (V/V) methanol; the pH was adjusted to 8.3.

Ponceau solution: 0.2% (W/V) Ponceau S and 5% (V/V) glacial acetic acid.

Tris-buffered saline with Tween 20 (TBST) buffer in Western blotting: 20 mM Tris (pH 7.5), 150 mM NaCl and 0.1% (V/V) Tween 20.

Blocking buffer in Western blotting: 3% BSA in TBST.

Antibody solution in Western blotting: primary or secondary antibody in 4% (W/V) skim milk in TBST.

The acid-molybdate reagent in phosphate determination: 13 g sodium molybdate dissolved in 1 L 1.25 M HCl.

Malachite green solution in phosphate determination: 126 mg/100mL.

2.1.4 Biochemical materials

PJET1.2 cloning Kit, Endonuclease (BamHⅠ, Hind Ⅲ and EcorⅠ), T4 DNA ligase, Phusion High-Fidelity DNA Polymerase, DNase-free RNase A and Gene Ruler 1Kb DNA ladder were purchased from Thermo Scientific.

NucleoSpin Gel and PCR Clean-up kit was purchased from MACHEREY-NAGEL.

Bio-Rad protein assay kit and the mixed bed resin AG 501-X8 and Bio-Rex MSZ 501(D) were purchased from Bio-Rad.

α-amyloglucosidase from *Aspergillus niger* (EC# 3.2.1.3, CAS: 9032-08-0), α-Amylase isolated from *Bacillus amyloliquefaciens* (EC#: 3.2.1.1, CAS: 9000-90-2) and acid phosphatase from wheat germ (EC#: 3.1.3.2, CAS: 9001-77-8) were all purchased from Sigma-Aldrich.

Miracloth was purchased from EMD Millipore.

Enhanced chemiluminescence (ECL) Western blotting detection reagent was purchased from GE Healthcare Life Sciences.

2.1.5 Primers

Primers used in this study were ordered from eurofins Genomics. The sequences of primers are shown in the following table.

Primer name	Sequence 5-3
SRG1 forward	AGTACGAATACGAACCGTGA
SRG1 reverse	GGCGTTCAGTCATAATCCAG
SRG2 forward	GAGTGGAAGAAGGTCAAGGG
SRG2 reverse	GGAAACAGCACAAGCAATCC
SRG3 forward	AACCCAAGCCTCGTATCCAC
SRG3 reverse	CAACCATCGTTCCTCGTAAT
SRG4 forward	GGGCAACGATTACCTCATG
SRG4 reverse	TTCCCAGCAACTTCAACAG
SnRK forward	ATAGTGGAGAAGGGAAGGC
SnRK reverse r	ACCAAGAGTGCGAACGAATC
HXK forward	TCACTTCCCTTGATCTATCC
HXK reverse	CCGAGCCATCGTTAGAGT
CDet11-24 forward	TCGGAAGACGAGCCTAAGAA
CDet11-24 reverse	ACAGCGCCTTGTCTTCATCT
EF1a forward	CACATCAACATTGTGGTCA
EF1a reverse	CTGAAGTGGGAGACGGAGAG
tk3-F-1	CGAGGATCCATGGAAGGGGTTTCTAACGAG
tk3-R-1	GCCAAGCTTTCAAATCAACTCCTTCGCAGC
t7-F-1	ATAGAATTCATGGCGCCCAAGACG
t7-R-1	CCGAAGCTTTCAGCAAATCTCCTT
t10-F-1	TAAGGATCCATGGCCAAGACTACG
t10-R-1	CCTAAGCTTCTAGCACAGCTCTTT
ta1-F-1	GTCGGATCCATGCTTGAGAAGATT
ta1-R-1	GACGAATTCCCACAGGCTAACTAG

PJET1.2 forward	CGACTCACTATAGGGAGAGCGGC
PJET1.2 reverse	AAGAACATCGATTTTCCATGGCAG
T7 promoter	TAATACGACTCACTATAGGG
T7 terminator	GCTAGTTATTGCTCAGCGG
SPP001de	KCTNGGYAGNTNNCCYAG
SPP002de	CANRAGCTRGGNNANCTRGG
M13 forward	TGTAAAACGACGGCCAGT
M13 reverse	CAGGAAACAGCTATGAACC

The sequences underlined are restriction enzyme cleavage sites. SPP001de and SPP002de are degenerate primers. R: A, G; Y: C, T; M: A, C; K: G, T; S: C, G; W: A, T; H: A, C, T; B: C, G, T; V: A, C, G; D: A, G, T; N: A, C, G, T.

2.2 Methods

2.2.1 Classification of leaves in *C. plantagineum*

C. plantagineum leaves were classified into two groups: inner leaves and outer leaves. The inner leaves developed two weeks later than the outer leaves, indicating they are younger than the outer leaves. Fig. 2.1 shows the distinction between inner leaves and outer leaves in *C. plantagineum*.

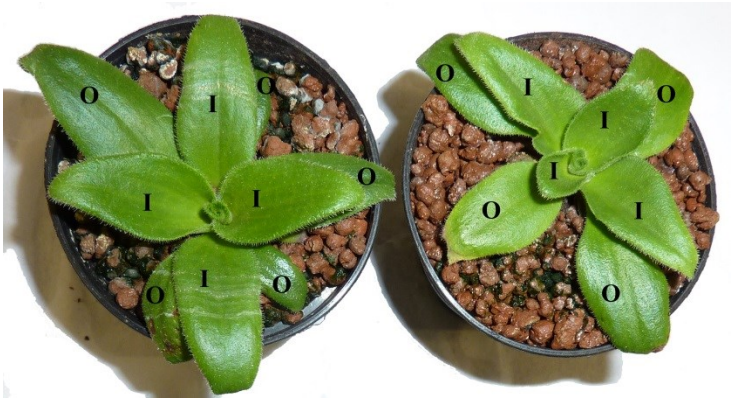

Fig. 2.1. Examples of classifying inner leaves (I) and outer leaves (O) in *C. plantagineum*.

2.2.2 The treatments of starvation, dehydration, rehydration and phosphate in plants

In the starvation treatment, Young plants kept in the dark in a fully hydrated state for nine days were sampled as “starved plants”.

C. plantagineum plants in pots were taken out of the tray and were subjected to dehydration by withholding water. Partially dehydrated plants were collected after 48 h and dehydrated plants collected after 20 days. For rehydration, dehydrated plants were removed from the substrate and submerged in water for 24 h.

To study the response of *C. plantagineum* plants to phosphate starvation in terms of sugar, plant seedlings growing on the MS medium were transferred to new MS medium or new phosphate-free MS medium. Samples were collected three days and seven days after the transfer. To study the effect of exogenous Pi on sugar accumulation, plants were grown in a hydroponic solution with 10 mM sodium phosphate or sprayed with 10 mM sodium phosphate three times per day. Water was used as control. Samples were collected four and eight days after the treatments.

2.2.3 The incubation of leaf pieces

C. plantagineum leaves were cut into pieces of 0.5 cm^2 and were firstly incubated overnight in water or 20 μM paraquat in Petri dishes for 12 h. Then the leaf pieces were transferred to water or 200 mM sucrose with or without 20 μM paraquat and kept in the dark or in continuous light at 22 °C. One, two and four days after the transfer, leaf pieces were collected and rinsed five times with water and then ground into powder with liquid nitrogen and subsequently used for carbohydrate extraction.

2.2.4 Chloroplast isolation

C. plantagineum chloroplasts were isolated according to Rowan and Bendich (2011). Details are the following:

1. Plant leaves were washed for three to five min with 70% ethanol and rinsed for three times with tap water, followed by three rinses with distilled water.

2. All solutions and plant tissue/chloroplasts were kept on ice. Four g plant leaves were cut into pieces and homogenized in 100 mL XPI buffer.

3. The homogenate was filtered through three layers of Miracloth. The plant tissue retained by the Miracloth was re-homogenized and filtered again.

4. The filtered was centrifuged for five min at 3000 g. After removing the supernatant, the pellet was re-suspended in XPI buffer with a small paintbrush.

5. The chloroplast suspensions were carefully layered onto the 30%-70% Percoll gradient and centrifuged for 30 min at 1500 g at 4 °C using a swing-up rotor.

6. The purified chloroplasts could be removed from the band at the inter-face between the 30 and 70% Percoll layers by a glass Pasteur pipette.

7. The purified chloroplasts were washed with 10 volumes of XPI buffer twice through centrifugation at 12,000 g for 20 s to get pellet.

Finally the isolated chloroplast was freezing dried and kept at -70 °C.

2.2.5 Determination of periodic change of sugar levels in *C. plantagineum* leaves

Morphologically uniform *C. plantagineum* plants (4 weeks old) were grown in a plant growth chamber with illumination of 100 μmol m^{-2} s^{-1} for 16 h. In a whole period of 24 h, leaves were collected each 4 h. The leaves were ground with liquid N_2 into powder for carbohydrate extraction.

2.2.6 Phloem exudate analysis

The analysis was performed according to Wingenter *et al.* (2010). At the end of the illumination, petiole ends of mature leaves from six weeks old plants were cut under water, and then transferred quickly into reaction tubes containing 100 μL of 15 mM EDTA solution (pH 7.25). The sugar export experiment was done in a water-saturated atmosphere overnight. Then the solution was heated to 95 °C for three min in the reaction tubes and cooled down for GC analysis. Five mM $CaCl_2$ contained into reaction tubes was used as control. To improve the sensitivity of GC, the solutions of leaf exudate were condensed to about 20 μL by evaporating under reduced pressure at 25 °C. The sugar content was presented as percentage of total sugars.

2.2.7 Carbohydrate extraction

Sugars were extracted from plant tissues of *C. plantagineum* as described by Willige *et al.* (2009). Plant material was extracted twice with 80% (v/v) methanol (3 mL/g) at 4°C. The homogenates were cleared by centrifugation (5 min at 5000 g, 4°C). The methanol was evaporated to dryness under reduced pressure at 25°C. The pellet was taken up in water and portioned three times against chloroform to remove lipophilic substances. The aqueous phase was centrifuged (30 min at 10,000 g, 4°C) to remove any particles. Cation (Dowex 50 WX8) and anion (Dowex IX8) exchange resins were added into the aqueous phase (5 g resin per 100 mL) to remove organic acids, amino acids or other charged molecules. After stirring for 1 h, the aqueous phase was transferred into a new reaction vial for GC analysis.

2.2.8 Thin layer chromatography and D-g-D-i-oct purification

Sugars were separated by TLC silica gel 60 (CAS 105553, Merck Millipore). The developing solution was n-butanol: H_2O: n-propanol (9:1:0.5). The duration of developing was about 2 h, then the plate was dried at 37 °C and sugars were detected by spraying plates with a mix of EtOH:H_2SO_4:HAc:anisaldehyde (90:5:1:5) and heating to 100 °C for 5 min (Kutzer, 2004).

The D-g-D-i-oct-containing area was excised from the silica gel and saturated in ethanol overnight, after centrifuging at 13000 g for 10 minutes and filtration through a 40 µm filter membrane, the ethanol solution was evaporated to dryness under reduced pressure at 25 °C. Finally the syrup was weighed and dissolved into water for hydroxyl radical scavenging assays.

2.2.9 Sugar analysis by GC/MS

Sugar extracts were further separated and identified by coupled gas chromatography (GC)–flame ionization detection (GC/FID) and coupled gas chromatography–mass spectrometry (GC/MS). Ten µL extract prepared as described above were dried at 60°C under N_2 gas. Twenty µL pyridine and 20 µL N,O-Bis(trimethylsilyl)trifluoroacetamide (BSTFA) were added, the sample was diluted with chloroform to reach a mass between 1 and 20 ng. Ten ng of xylitol was used as internal standard. The sugar derivatives were separated on a DB1 column (J&W Scientific, Folsom, CA, USA). Qualitative GC/MS analysis was performed with a gas chromatograph 6890 N, detector 5973 MS Detection HP (Agilent Technologies, Böblingen, Germany); quantitative

analysis was done with GC/FID (5890Series II Plus, HP, Agilent Technologies), (Willige *et al.*, 2009). The temperature program as follows: One microliter of each sample was injected. H_2 flow was set to 37 kpa. The initial temperature was 65˚C for 3 min, after which the temperature was raised at a rate of 8˚C per min to a temperature of 240˚C, after which the rate was increased by 12˚C per min to a final temperature of 310˚C for 35 min. Data analysis was performed with GC ChemStation [Rev.B.03.02(341), Agilent Technologies, Böblingen, Germany].

2.2.10 Starch assay

The methanol-extracted pellets obtained in carbohydrate extraction were dried at 50 °C, homogenized into 200 mL water and then heated to 100˚C for 10 min to gelatinize starch granules. After cooling down, half mL sodium acetate (200 mM, pH 5.5) was added. Then six units of a-amyloglucosidase and one units of a-amylase were added. The reactions were incubated at 37 °C for four h (Smith and Zeeman, 2006).

After incubation, the homogenate was centrifuged at 20000 rpm for 20 min. Ten µL of the aqueous phase was transferred to a new tube. Two hundred and forty µL water and 125 µL 4% (W/V) phenol were added into the tube. After mixing by vortex, 625 µL concentrated sulfuric acid were dropped slowly into the tube. The tube was placed on a heating block at 30 °C for 30 min. The absorption value of 490 nm was determined with a GENESYS 10 UV-vis spectrophotometer (Thermo Electron Scientific Instrument Corporation). Designated standard curve of glucose was used in calculating (Dubois *et al.*, 1951).

2.2.11 Hydroxyl radical scavenging assays of sugars

Hydroxyl radical scavenging activity was determined by measuring the ability of sugars to inhibit the formation of the fluorescent 2-hydroxyterephthalate (HTPA) in a Fenton reaction. The protocol of (Peshev *et al.*, 2013) was used with modifications. A 900 µl reaction mixture was prepared containing 125 µM terephthalate (TPA), 2.5 µM Na-EDTA, 2.5 µM $FeSO_4$, 25 µM ascorbic acid, and 25 µM hydrogen peroxide in 50 mM Na-phosphate buffer (pH 7.2). The reaction was mixed and incubated overnight at 30 °C. HTPA fluorescence was measured at room temperature with a F7000 fluorescence spectrophotometer (LABMATE) that was set to 315 nm

as excitation wavelength and 420 nm as emission wavelength. Hydroxyl radical scavenging was characterized by its half-inhibitory concentration (IC50) for HTPA formation.

2.2.12 Activity measurements of glucose-6-phosphate dehydrogenase and 6-phosphogluconate dehydrogenase

Glucose-6-phosphate dehydrogenase (G6PDH, EC 1.1.149) was assayed by the method of Yuan and Anderson (1987). Fifty milligrams of plant material was extracted in 0.5 mL of enzyme extraction buffer [10% (V/V) glycerol, 0.25% (W/V) BSA, 0.1% (V/V) Triton X-100 , 50 mM HEPES-KOH (pH 7.5), 10 mM $MgCl_2$, 1 mM EDTA, 1 mM EGTA, 1 mM benzamidine, 1 mM 6-aminocaproic acid, 1 mM phenylmethylsulfonylfluoride, and 10 µM leupeptin]. Fifty µL of enzyme extract was used in a 1 mL reaction that contains 2.5 mM glucose-6-phosphate (Na+), 0.2 mM NADP, 50 mM Hepes (K+), 10 mM KCl, 5 mM MgCl2, 1 mM EDTA (pH7.8) and 0.03% (V/V) Triton X-100. The assay temperature was 24°C. The reaction was started by adding 2.5 mmol/l glucose-6-phosphate. Absorbance at 340 nm was measured with a GENESYS 10 UV-vis spectrophotometer (Thermo Electron Scientific Instrument Corporation). The method for assaying 6-phosphogluconate dehydrogenase (6GPDL, 1.1.1.44) was same as that of glucose-6-phosphate dehydrogenase In the reaction the substrate glucose 6-phosphate was substituted by 6-phos-phogluconate (Devi *et al.*, 2007). Activities of G6PDH and 6GPDL were calculated in U/ min* µg protein. One unit of enzyme activity was defined as 0.01 absorption increase. Protein content was determined with the Bio-Rad protein assay kit.

2.2.13 Determination of protein concentrations

Protein concentration was determined with the Bio-Rad protein assay kit. Five µL of each protein sample was mixed with 100 µL 0.1 M potassium phosphate buffer (pH 6.8) by vortex. Water was used as control. The mixture was kept at room temperature for 10 min and then centrifuged for 5 min at 12000 g at room temperature. Ninety µL of the supernatant was pipetted into a new 1.5 mL Eppendorf tube and added with 710 µL dH_2O and 200 µL Bradford-reagent. The mixture was incubated for 5 min at room temperature. The absorption at 595 nm was measured using a spectrophotometer with the control as blank. Protein concentration was calculated by a standard curve built by testing designated concentrations of bovine serum albumin (BSA).

2.2.14 RNA isolation

Total RNA isolations were conducted according to Valenzuela-Avendaño *et al.* (2005). Plant tissue was ground to fine powder using liquid nitrogen. One hundred mg ground tissue was added 1.5 mL of the mixture of RNA extraction buffer and saturated phenol (62%: 38% v/v). The homogenate was incubated at room temperature for 10 min after vortex and then centrifuged at 10000 g for 10 min at room temperature. The supernatants were transferred into fresh tubes and added 300 µL of mixture of chloroform and isoamylalcohol (24:1, V:V). After shaking vigorously by vortex for 10 seconds, the tubes were centrifuged at 10000 g for 10 min at 4 °C. Then the aqueous phase was transferred to new tubes, mixed thoroughly with 375 µL isopropanol and 375 µL sodium citrate/sodium chloride (0.8 M/1 M). The mixture was kept at room temperature for 10 min. By centrifugation at 12000 g for 10 min at 4 °C, the pellet containing RNA was obtained. The pellet was washed with 1 mL cold (-20 °C) 70% ethanol, dried at room temperature and then dissolved with 100 µL sterile H_2O. Then 167 µL of 4 M LiCl was added and the tubes were incubated on ice for two hours. The RNA samples were centrifuged at 14000 g for 20 min at 4 °C to get RNA pellet. The pellet was washed with 1 mL of cold (-20 °C) 70% ethanol, dried and dissolved finally in 25 µL sterile H_2O.

2.2.15 Reverse transcription of RNA

Four µg of total RNA was mixed with 1 µL 10× DNase I reaction buffer with $MgCl_2$, 1 µL RNase-free DNase I and sterile H_2O to make total volume 10 µL. The mixture was incubated at 37 °C for 30 min. One µL of 25 mM EDTA was added and the mixture was incubated at 65 °C for 10 min. After briefly spinning down, the mixture was kept on ice.

The synthesis of the first strand cDNA was performed according to cDNA synthesis kits of Thermo scientific. Ten µL Dnase I-treated RNA was mixed with 1 µL 100 pmol/µL oligo-dT primer and 10 µL H_2O. The mixture was incubated for 5 min at 65 °C after gently centrifugation. Then the mixture was put on ice and added the following reagents: 4 µL 5 x First strand buffer, 1 µL RiboLockTM RNase Inhibitor, 2 µL 10 mM dNTP mix and 1 µL Reverse transcriptase. The mixture was incubated at 42 °C for 60 min. The reaction was terminated by heating at 70 °C for 5 min. The mixture was used directly for PCR or stored in freezer at -20 °C.

2.2.16 Polymerase chain reaction (PCR)

Primer design

Primers were designed with the software Oligo 7 (http://www.oligo.net/tutorials.html). The sequences of primers can be seen in section 2.1.5.

Composition and cycling condition for RT-PCR and bacterial colony PCR

Composition of a 20 µL PCR reaction: 2 µL 10× PCR Buffer containing 15 mM $MgCl_2$, 0.4 µL 10 mM dNTP mix, 0.8 µL 10 µM forward primer and 0.8 µL 10 µM reverse primer, 0.2 µL Taq polymerase, 14.8 µL H_2O and 1 µL cDNA or DNA template.

Cycling condition of RT-PCR: denaturing at 94 °C for 5 min; 30 cycles of amplification (94 °C, 30 sec of denaturation, 30 sec of primer binding at X °C and 1 min of elongation at 72 °C); 5 min for final elongation at 72 °C, pause at 4 °C for keeping the samples stable until they are collected. (X= Tm -5. Tm: melting temperature of certain primer.)

Cycling condition of colony PCR: 10 min of denaturing at 94 °C; 30 cycles of amplification (30 sec of denaturation at 94 °C, 30 sec of primer binding at 60 °C or 52 °C* and 1.5 min of elongation at 72 °C); 5 min for final elongation at 72 °C; pause at 4°C, for keeping the samples stable until they are collected. (* it is 60 °C when using the PJET forward primer and the PJET reverse primer and 52 °C when using the using the T7 promoter primer and the T7 terminator primer.)

Composition and cycling condition for PCR with high fidelity DNA polymerase

Composition of a 50 µL PCR: 10 µL 5× Phusion HF Buffer, 1.0 µL 10 mM dNTP mix, 2.5 µL 10 µM forward primer, 2.5 µL 10 µM reverse primer, 0.5 µL Phusion DNA polymerase, 32.5 µL H_2O and 1.0 µL cDNA template.

Cycling condition: 30 sec of denaturing at 98 °C; 35 cycles of amplification (10 sec of denaturation at 98 °C, 25 sec of primer binding at 60 °C or 57°C* and 30 sec of elongation at 72 °C); 10 min for final elongation at 72°C; pause at 4°C until they are collected. (* for the gene tkt3, it is 60 °C and for the genes tkt7 and tkt10, it is 57 °C)

2.2.17 Separation of RNA and DNA in agarose gels and analysis of the RT-PCR products

Agarose gel preparation

One g of agarose was measured out and poured into a glass flask with 100 mL of 1×TAE. The mixture was heated by microwave for 1-3 min until the agarose was completely dissolved. The agarose solution was placed at room temperature for 5 min to cool down. Ethidium bromide (EtBr) was added to the agarose solution (final concentration was approximately 0.5μg/mL). Then the agarose was poured in a gel tray with appropriate combs placed. Thirty min later, the gel was solidified and could be used for electrophoresis

Electrophoresis of RNA and DNA

To monitor the quality of RNA or DNA, appropriate volume of RNA or DNA mixed with loading buffer and water was loaded on a 1% agarose gel in 1× TAE buffer. Six μL of the 1 Kb DNA ladder (Thermo scientific, #SM1163) was also loaded to provide reference. The electrophoresis was set at 130 V and run for 30 min. The RNA or DNA fragments were visualized under ultraviolet (UV) light and recorded by an Intas gel iX imager.

Analysis of the expression levels of genes with regard to senescence

The sequences of four putative senescence-related genes (Assembly UniProt ID: Q9AVH2, Q5EMP6, Q45TE3 and B5TV63; all four genes are induced to express by dehydration), one gene encoding sucrose non-fermenting-1-related protein kinase-1 (SnRK1) (Assembly UniProt ID: contig11245) and one gene encoding hexose kinase (HXK) (Assembly UniProt ID: contig 02898) of *C. plantagineum* were obtained from the *C. plantagineum* transcriptome (Rodriguez *et al.*, 2010). The dehydration inducible gene *CDeT*11-24 gene was also included in gene expression analysis (van den Dries *et al.*, 2011). The EF1a gene was used as reference gene for equal amount of RNA and cDNA (Giarola *et al.*, 2015). The synthesis of cDNA and the setting of PCR composition and conditions were conducted as described above. The amplified DNA fragments were scanned and recorded using an Amersham Typhoon 9200 Imager. Detailed operation could be seen at: ttps://www.gelifesciences.com/gehcls _images/GELS/Related%20Content/Files/

1314742967685/litdoc375635_typhoon_userguide_20110831023220.pdf. Gene expression levels were calculated by analyzing signal intensities of bands in the gel using the software ImageJ2x (http://www.rawak.de/rs2012/) and presented relative to expression levels in inner leaves of young plants.

2.2.18 Extraction of DNA from agarose gels

The extraction of DNA from agarose gels were conducted using NucleoSpin® Gel and PCR Clean-up kit. The detailed operation could be seen at: http://www.mn-net.com/tabid/1452/default.aspx

2.2.19 Concentration measurement of RNA and DNA

The concentrations of RNA and DNA were measured by BioSpec-nano Micro-volume UV-Vis Spectrophotometer. Concrete operation could be seen at: http://www.ssi.shimadzu.com/products /product.cfm?product=biospec_nano.

2.2.20 Restriction enzyme digestions of DNA

For gene fragments of tkt3 and tkt10, the reaction system of double digestion with BamHI and HindIII composed of 2.5 μL 10× BamHI buffer, 1.0 μL BamHI, 2.0 μL HindIII and 19.5 μL plasmid DNA. The reaction was incubated at 37 °C for 3 h.

For gene fragments of tkt7 and ta1, the reaction system of double digestion with BamHI and EcoRI composed of 5.0 μL 10× Tango buffer, 1.0 μL EcoRI, 2.0 μL BamHI and 17 μL plasmid DNA. The reaction was incubated at 37 °C for 3 h.

2.2.21 Ligation reactions with T4 DNA ligase

The online NEBioCalculator was used to calculate molar ratios of insert DNA and vector for ligations (http://nebiocalculator.neb.com/#!/)

The 10 μL ligation reaction composed of: 1.0 μL 10× T4 DNA Ligase buffer, 0.020 pmol vector DNA, 0.060 pmol insert DNA, nuclease-free water and 0.5 μL T4 DNA Ligase. The reaction was incubated at room temperature for 1 h. Then the reaction was chilled on ice to transform the prepared competent cells.

2.2.22 Preparation of competent *E. coli* cells using calcium chloride

A single bacterial colony (*E. coli* strain DH10B or BL21 DE3) from a plate that has been incubated for 16-20 hours at 37 °C was growed into 100 mL LB medium. The culture was incubated for 3 hours at 37 °C with 200 r/min agitation. When the culture absorption at 600 nm reached 0.6, the culture was transferred into sterile, ice-cold 50-mL tubes. The tubes were stored on ice for 10 minutes. Bacterial cells were recovered by centrifugation at 2700 g for 10 minutes at 4 °C. After the LB medium was completely removed from the cell pellets, the pellets were resuspended by gently vortex in 30 mL of ice-cold $MgCl_2$-$CaCl_2$ solution. Then the bacterial cells were recovered again by centrifugation at 2700 g for 10 minutes at 4 °C. The $MgCl_2$-$CaCl_2$ solution (80 mM $MgCl_2$ and 20 mM $CaCl_2$) was completely removed from the cell pellets. The bacterial cells were resuspended in 2 mL of ice-cold 0.1 M $CaCl_2$ by gently vortex. The competent cells could be dispensed into aliquots (100 µL for each part) and stored at -70 °C.

2.2.23 Transformation of competent *E. coli* cells

Two hundred µL of competent cells was transferred to a sterile, 14 mL polypropylene tube and mixed with DNA (no more than 50 ng in a volume of 10 µL) by swirling gently. The tube was kept on ice for 30 min. Then, the tube was placed in a 42 °C water bath for exactly 90 sec (without shaking). The tube was transferred to an ice bath to chill cells for 1-2 min. 800 µL of SOC medium was added to the tube and the culture was incubated for 45 minutes in a water bath set at 37 °C. 200 µL of the culture was transferred onto solid LB medium containing the appropriate antibiotic. The plates was inverted and incubated at 37 °C. Transformed colonies would be observed in 12-16 hours.

2.2.24 Plasmid DNA isolation

Plasmid DNA was isolated by alkaline lysis with SDS according to the minipreparation protocol of Sambrook *et al.* (2001). A single colony of transformed bacteria was transferred into 2 mL LB medium and the culture was incubated overnight at 37 °C with vigorous shaking (200 rpm). 1.5 mL of the culture was centrifuged at 13000 rpm for 30 sec. After completely removing the medium, the bacterial pellet was resuspended in 100 µL of ice-cold alkaline lysis solution I by vigorous vortex. Two hundred µL of freshly prepared alkaline lysis solution II was added to the

bacterial suspension. The mixture was inverted rapidly five times and stored on ice for 5 min. 150 µL of ice-cold alkaline lysis solution III was added and the mixture was inverted several times and kept on ice for 5 min. The bacterial lysate was centrifuged at 13000 rpm for 5 min. The supernatant was transferred to a new tube and added 450 µL phenol: chloroform. The mixture was vortexed and then centrifuged at 13000 rpm for 2 min. The aqueous upper layer was transferred into a fresh tube and added 900 µL ethanol. The mixture stayed at room temperature for 2 min and then was centrifuged at 13000 rpm for 5 min to precipitate nucleic acids. The supernatant was removed completely and the pellet was washed with 1 ml of 70% ethanol. Through centrifugation at 13000 rpm for 2 min the pellet was recovered. The supernatant was removed completely again and the nucleic acids were dissolved in 50 µL of TE (pH 8.0) containing 20 µg/mL DNase-free RNase A. The DNA solution could be stored at -20 °C.

2.2.25 DNA Sequencing

The DNA samples were prepared as the requirement of eurofins company and sent to it for sequencing.

2.2.26 Sequence alignments

Sequences were aligned using the software MEGA 4 and blasted using the basic local alignment search tool of NCBI (http://blast.ncbi.nlm.nih.gov/Blast.cgi).

2.2.27 Induction of *E. coli* cultures expressing recombinant transketolase proteins

1. A single colony was incubated overnight in 10 mL LB medium containing 50 µg/mL kanamycin at 37 °C with vigorous shaking.

2. Five mL of the culture was transferred into 100 mL LB medium containing 50 µg/mL kanamycin at 37 °C with vigorous shaking.

3. When the culture absorption at 600 nm reached 0.6, the culture was incubated at 24 °C for 30 min. Then 1 µL of 100 mM Isopropyl β-D-1-thiogalactopyranoside (IPTG) was added and the cells were induced for 3 h at 24 °C with vigorous shaking.

4 cells were centrifuged at 3000 g at 4 °C for 20 min to obtain cells pellet. The pellet was frozen at -20 °C.

2.2.28 Immobilized metal affinity chromatography of recombinant transketolases

1. Cells pellet was thawed on ice and resuspended completely in 5 mL buffer A.

2. 50 µL 100 mg/L freshly prepared lysozyme was added and the suspension was incubated on ice for 30 min.

3. Cells were disintegrated by ultrasonic produced by an ultrasonic processor (UP200S, Hielscher – Ultrasound Technology) for 10 min. The ultrasonic device was set as: 0.5 cycles and 60% amplitude.

4. The cell suspension was centrifuged at 20000 g for 30 min and the supernatant was filtered through 0.45 µm membrane.

5. The pre-packed His-column (1 mL bed volume) was washed with 3 mL H_2O, followed by 5 mL 1× charge buffer (50 mM $NiSO_4$) and 3 mL buffer A.

6 Then, the filtered cell lysate was loaded on the column. When the cell lysate pass through the column, the column was washed with 10 mL buffer A and 8 mL buffer B.

7 The purified His-tag proteins were finally eluted with buffer C. Each 250 µL elution was collected and labeled one by one. The fractions of elution were frozen by liquid nitrogen and kept at −80 °C.

2.2.29 Extraction of transketolase from plant tissue

Hydrtated or rehydrated *C. plantagineum* leaves were homogenized with ice-cold extraction buffer (4 mL/g fresh weight) containing 50mM Tris-HCI (pH 7.5), 10% (v/v) glycerol, 10 mM $MgCl_2$, 0.1 mM thiamin diphosphate (ThDP), 1.5%(w/v) polyvinyl-polypyrrolidone, 5 mM dithiothreitol, 1 mM phenylmethylsulfonylfluoride, 1 mM benzamidine and 1 mM benzamide. The homogenate was filtered through Miracloth and centrifuged for 10 min at 10000 g followed by a centrifugation at 25000 g for 30 min. The supernatant was fractionated by ammonium

sulfate precipitation; active transketolase was contained in the 50-70% (w/v) $(NH_4)_2SO_4$ saturated pellet. The precipitate was dissolved in 10mL buffer E [50 mM Tris-HCI (pH7.5), 10% (v/v) glycerol and 10 mM $MgCl_2$) (Bernacchia *et al.*, 1995).

2.2.30 Protein extraction and sample preparation for SDS-PAGE

Total protein extraction

Total soluble proteins were extracted by Laemmli sample buffer. One hundred mg of plant powder ground in liquid nitrogen were extracted with 1 mL 1× Laemmli sample buffer by thorough vortex in a 1.5 mL Eppendorf tube. The extract was heated at 100 °C for 5 min in a heating block and centrifuged (13000 rpm, 5 min, room temperature) to separate insoluble material. The supernatant was transferred to a new Eppendorf tube. The obtained protein samples can be used in the protein concentration determination and in the loading of polyacrylamide gels.

Preparation of polyacrylamide gel

Polyacrylamide gels were prepared as follows: 1) join the glass plates with a U-shaped sealing belt to form a casting cassette and clamp the cassette in a vertical position; 2) mix the components of the 12% separating gel (add TEMED at the end) and shake gently; 3) pipette the separating gel mixture carefully into the casting cassette until it was1.5 cm far from the top of the shorter glass plates; lay 1 mL isopropanol on the gel mixture and let the cassette stand for 45 min; 4) remove the overlaying isopropanol from the separating gel with Whatman filter papers and add the stacking gel solution to the gel cassette until the solution reaches the cutaway edge of the gel plate; place combs into this solution without any air bubble produced; 5) after the stacking gel was set, remove the comb from the stacking gel and remove the unpolymerized acrylamide solution from the wells by wash with TGS buffer; separate the sealing belt from the gel cassette and fix the gel cassette to electrophoresis chamber with clamps; fill up the reservoir of electrophoresis chamber with TGS buffer; 6) load samples onto the gel and start electrophoresis at 25 mA.

Colloidal coomassie staining of proteins in polyacrylamide gels

The separated proteins were detected by staining with coomassie briliant blue G250. The process was the following: When the electrophoresis was finished, the cassette was disassembled and the separating gels were detached and placed in the fixation solution. The separating gels were incubated for 1 h with 60 r/min agitation. Then they were washed with dH_2O for three times (10 min for each washing) and stained by the coomassie staining solution (50 mL per gel). The stainning lasted overnight with 60 r/min agitation. The stained gels were washed with dH_2O for about 1 h to distinguish clearly protein bands from the background of the gel.

2.2.31 Western blotting

Western blot was conducted using Rio-Rad blotting system. After the SDS-PAGE, the cassette was disassembled and the separating gels were detached and washed simply with dH_2O. The gels were placed in 1× transfer buffer for 10 min. Then the transfer sandwich which composed of two Whatman filter papers, the separating gels, GE nitrocellulose membrane and another two Whatman filter papers from the anode to the cathode was assembled and fixed by a cassette. The cassette was placed in the transfer tank with an ice block to keep low temperature of the transfer buffer. The transferring of protein was performed for 4 h in a cold room at a constant current of 300 mA.

When the transfer was finished, the nitrocellulose membrane was rinsed briefly with water. The transfer quality could be checked by staining with Ponceau solution. The Ponceau stain was rinsed off with TBST buffer. The membrane was blocked in 4% skimmed milk powder in TBST overnight. The membrane was incubated in the primary antibody solution for 1 h at 4 °C. Being rinsed with TBST buffer 3 times (5 min each time), the membrane was incubated in the secondary antibody solution for 1 h at 4 °C. After rinsing with TBST buffer 3 times (5 min each time), the membrane was dried slightly and then incubated for 60 sec in a 1:1 mixture of the ECL-staining components (700 µL each). The membrane was placed in the chemiluminescence detector (Intellegent Dark Box II, Fujifilm) (keep the protein side upwards). Detection of signal was conducted using the program ImageReader LAS-1000 Lite 1.3.

2.2.32 Enzymatic reaction and product dephosphorylation

The enzymatic reactions were performed as described by Willige *et al.* (2009): 25 µg purified protein, 58 mM glycilglycin (pH 7.7), 0.01% (w/v) Na-azide, 5.3 mM acceptor substrate (ribose-5-phosphate or glucose-6-phosphate), 0.002% thiamine pyrophosphate, 15 mM $MgCl_2$ and 16 mM donor substrate (β-hydroxy-pyruvate or fructose-6-phosphate)

After the catalyzing reaction, sugar phosphates in the product were dephosphorylated according to Willige *et al.* (2009). The dephosphorylated products were purified through a column containing ion-exchanging bed resin AG 501-X8(D) (BIO-RAD). The filtrates were used for GC/MS analysis.

2.2.33 Activity assays of transketolase

Transketolase activity assay was conducted according to Bernacchia *et al.* (1995). Xylulose-5-phosphate and ribose-5-phosphate can be catalyzed by transketolase to generate glyceraldehyde-3-phosphate (GAP). The generated GAP could be catalyzed by triose phosphate isomerase (TIM) and glycerol-3-phosphate dehydrogenase (GAPDH) into a-glycerophosphate with the consumption of NADH. Transketolase activity was assayed spectrophotometrically by measuring the decrease in the concentration of NADH at 340 nm. The reaction system composed of appropriate amounts of proteins, 50 mM Tris-HCl (pH7.5), 10 mM $MgCl_2$, 0.1 mM ThDP, 0.2 mM NADH, 16 units/mL GAPDH, 50 units/mL TIM, 2 mM ribose-5-phosphate and 1 mM xylulose-5-phosphate. The volume of the reaction was 500 µL and the assay was conducted at room temperature (25 $^{\circ}$C). In the analysis regarding the inhibitor of transketolase, the inhibitor with appropriate concentration was added into the reaction system.

2.2.34 Cellular phosphate assays

The plant tissues were placed in 1% acetic acid followed by repeated freezing and thawing (Poirier *et al.*, 1991). Phosphate released in the solution was assayed by the method of Penney (1976). The assays were carried out in spectrophotometer cuvettes that contained 1.80 mL of the acid-molybdate reagent, 0.50 mL of water, 200 µL of the phosphate sample and 50 µL of the malachite green solution. The cuvette was shaken and the absorbance at 650 nm was read and

recorded two min after the addition of the malachite green solution. All measurements were conducted using a Thermo Scientific™ GENESYS 10S UV-Vis spectrophotometer.

2.2.35 Phylogenetic analysis of transketolase genes

Transketolse sequences were retrieved by blast from National Center for Biotechnology Information (www.ncbi.nlm.nih.gov/) and obtained from the RNA sequencing of *Lindernia brevidens* and *Lindernia subracemosa* (data unpublished). The phylogenetic tree was generated from aligned sequences of predicted proteins from 41 plant transketolase genes by maximum likelihood analysis using 2000 bootstrap predictions and 50% majority rule in MEGA6.

Chapter 3 Results

3.1 Preparation of the D-g-D-i-oct standard and sugar analysis by GC/MS

As there is no D-g-D-i-oct standard available, sugars extracted from *C. plantagineum* leaves were separated by thin layer chromatography (Fig. 2.2). Results showed that the mobility of D-g-D-i-oct was between glucose and sucrose. Thus the region where D-g-D-i-oct is found can be determined. The region containing D-g-D-i-oct was excised from the silicon plate. D-g-D-i-oct was extracted and then analyzed by GC/MS (Fig. 2.3). The m/z value of the most specific ion in the mass spectrum of the TMS derivative of D-g-D-i-oct is 641. The mass spectrum of the TMS derivative of D-g-D-i-oct purified by thin layer chromatography was similar as that of the TMS derivative of the most abundant sugar in plant samples (Fig. 2.4). The gas chromatography of TMS derivatives of sugars extracted from plant samples showed that five kinds of TMS derivatives of sugars were separated fully (Fig. 2.4). Thus this method was used in each sugar analysis in this study.

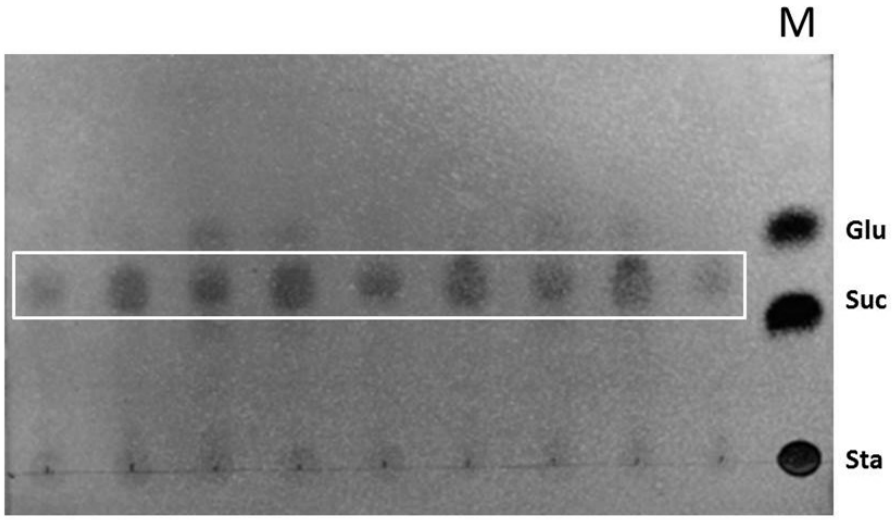

Fig 2.2. Thin layer chromatography of sugars extracted from *C. plantagineum* leaves. D-g-D-i-oct is marked by a rectangle. Glucose (Glu), sucrose (Suc) and stachyose (Sta) were used as reference standards.

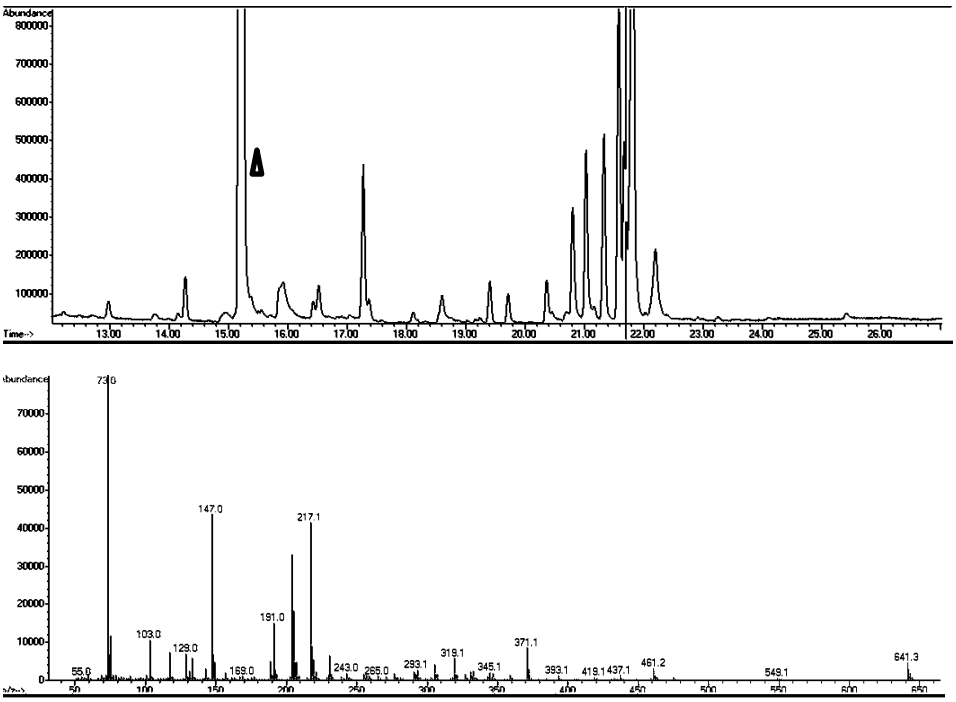

Fig. 2.3. Gas chromatography of the TMS derivatives of D-g-D-i-oct purified from *C. plantagineum* leaves (upper part) and the mass spectrum of the TMS derivative of D-g-D-i-oct (lower part). The TMS derivative of the internal standard xylitol is labeled by a triangle and that of D-g-D-i-oct is labeled by a vertical line.

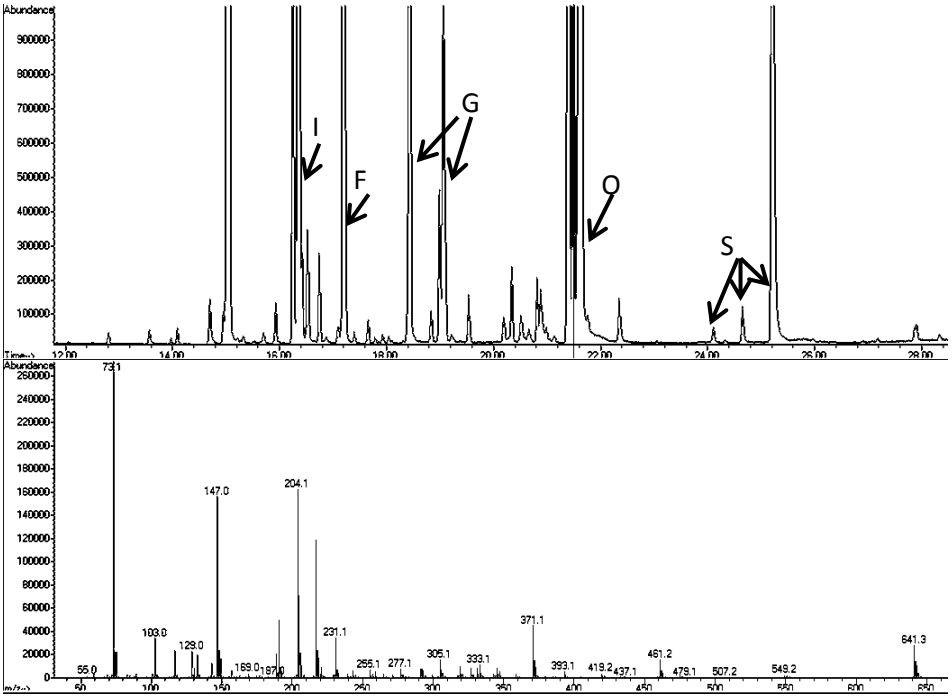

Fig. 2.4. Gas chromatography (upper part) of TMS derivatives of xylitol (I), fructose (F), glucose (G), D-g-D-i-oct (O) and sucrose (S) and the spectrum of the TMS derivative of D-g-D-i-oct (lower part) extracted from plant samples (lower part). Xylitol was used as internal standard.

3.2 The levels of sugars in different leaves of *C. plantagineum*

Sugars are important energy-carriers, their distribution may reflect their functions. Experimental results showed that D-g-D-i-oct is the dominant sugar in leaves of *C. plantagineum* in hydrated conditions, D-g-D-i-oct is 10-20 times more abundant than fructose, glucose and sucrose (Fig. 2.5). However, D-g-D-i-oct levels depend on the physiological conditions of the leaves. The levels of ocutlose in old plants were lower than in young plants both in inner and outer leaves. Starvation in the dark led to a significant decrease of the D-g-D-i-oct level both in inner and outer leaves. Except in old plants, the D-g-D-i-oct level of inner leaves was higher than that of outer leaves. It is interesting that the sucrose level in outer leaves of old plants was higher than in young plants. Similarly, starvation treatments also promoted an increase of the sucrose level both in inner and in outer leaves of young plants.

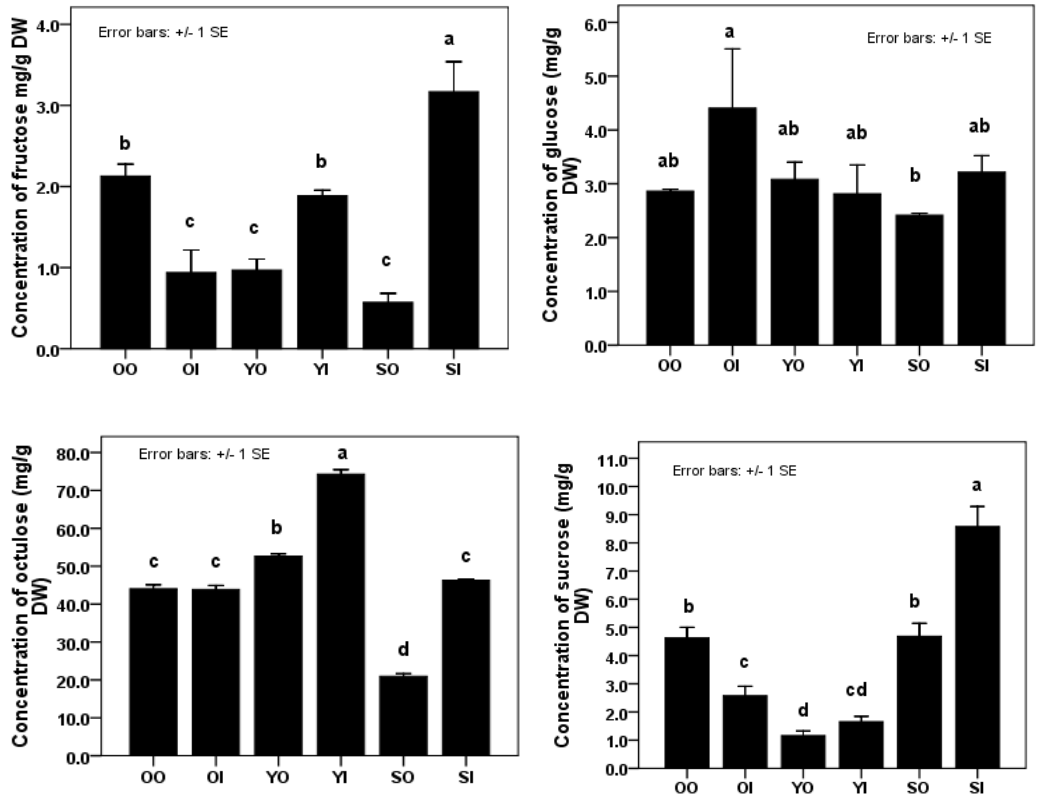

Fig. 2.5. Concentrations of sugars in different leaves of *C. plantagineum*. OO: outer leaves of old plants; OI: inner leaves of old plants; YO: outer leaves of young plants; YI: inner leaves of young plants; SO: outer leaves of starved plants; SI: inner leaves of starved leaves.

3.3 Sucrose accumulating rates in *C. plantagineum* leaves

Sucrose plays an important role in desiccation tolerance of resurrection plants, its accumulating rate reflects the intensity of the response of the plant to dehydration. Results showed that the sucrose accumulating rate of outer leaves of young plants was significantly higher than those of old plants and starved plants. The sucrose accumulating rates of inner leaves did not change in the plants of the different physiological conditions (Fig. 2.6). It is interesting that the sucrose accumulating rates did not correlate with the D-g-D-i-oct levels in hydrated leaves of *C. plantagineum*.

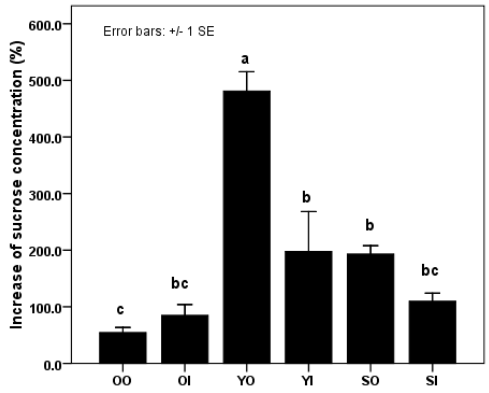

Fig. 2.6. The sucrose accumulating rates in different leaves of *C. plantagineum* plants that were dehydrated for 2 days. OO: outer leaves of old plants; OI: inner leaves of old plants; YO: outer leaves of young plants; YI: inner leaves of young plants; SO: outer leaves of starved plants; SI: inner leaves of starved leaves. The sucrose accumulating rates were calculated with sucrose levels in leaves of plants dehydrated for 2 days divided by sucrose levels in leaves of plants in hydrated conditions and are presented as percentage increase.

3.4 Carbohydrate status and plant performance in desiccation experiments

Old, young and starved plants were dehydrated and then rehydrated to investigate the relationship between sugar status and the ability of the plant to tolerate desiccation. Some outer leaves of old plants and starved plants could not fold or curl-up during dehydration compared to young plants (Fig. 2.7). After rehydration, the inner leaves of both young and old plants could recover to resume full physiological activities. Some tissue necrosis was observed at the edge of outer leaves of young plants, whereas the outer leaves of old plants died completely (Fig. 2.8). This indicates that the acquisition of desiccation tolerance depends on the age of the leaf. Senescence

can also lead to the loss of desiccation tolerance in *C. plantagineum*. Starvation for 9 days could lead to the death of some outer leaves of young plants (Fig. 2.7). Although some outer leaves were viable after starvation, they were not desiccation tolerant. Relative to outer leaves, some inner leaves of starved plants revive after rehydration (Fig. 2.8). This might indicate that water stress is also regulated by the overall energy status in *C. plantagineum*. Water is a vital factor for plants, *C. plantagineum* evolves desiccation tolerance to cope with extreme water deficiency. But when resources and energy are limited, plants have to utilize resources and energy in an optimized way for maximum survival. The occurrence of leaf senescence and loss of desiccation tolerance may be the result of this survival strategy.

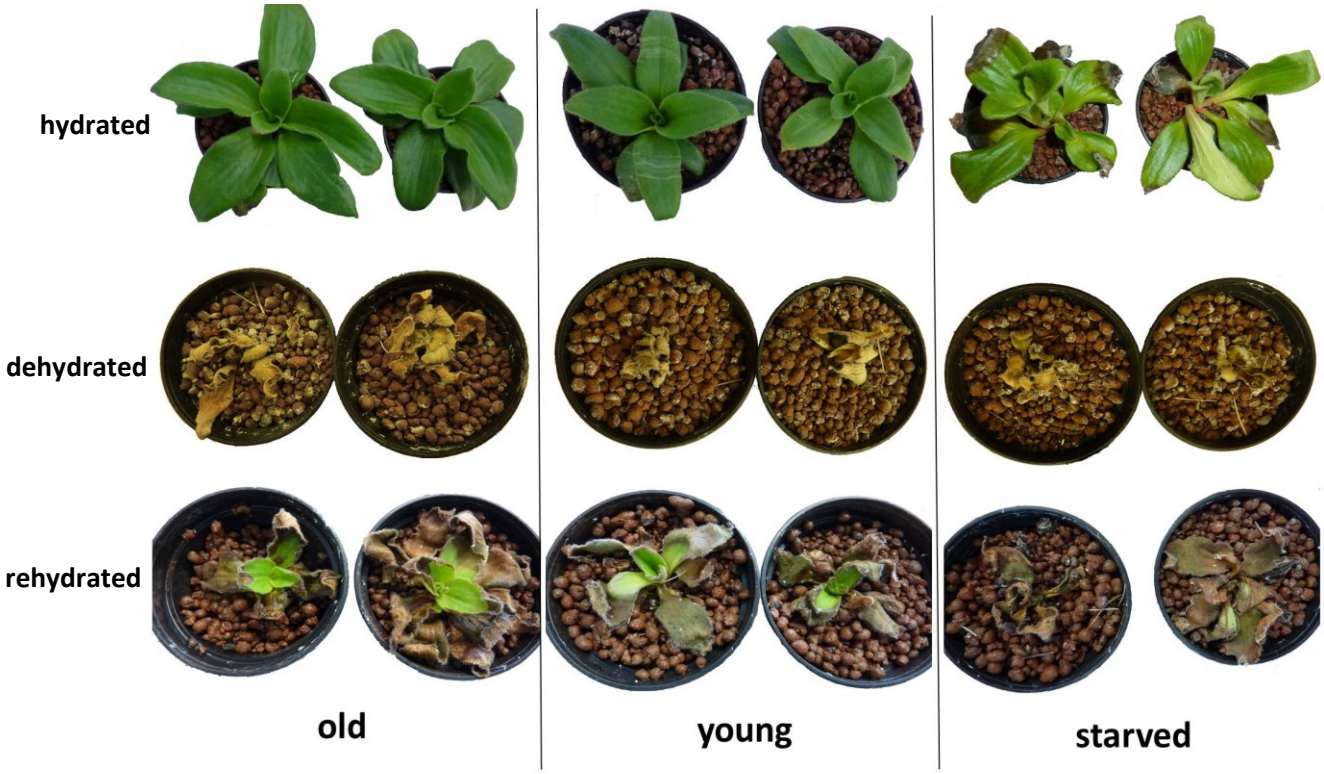

Fig. 2.7. Plants performance in dehydration and rehydration. a-c: hydrated, dehydrated and rehydrated old plants; d-f: hydrated, dehydrated and rehydrated young plants; g-i: hydrated, dehydrated and rehydrated starved plants (dehydration cost 2 weeks and rehydration cost 48 hours)

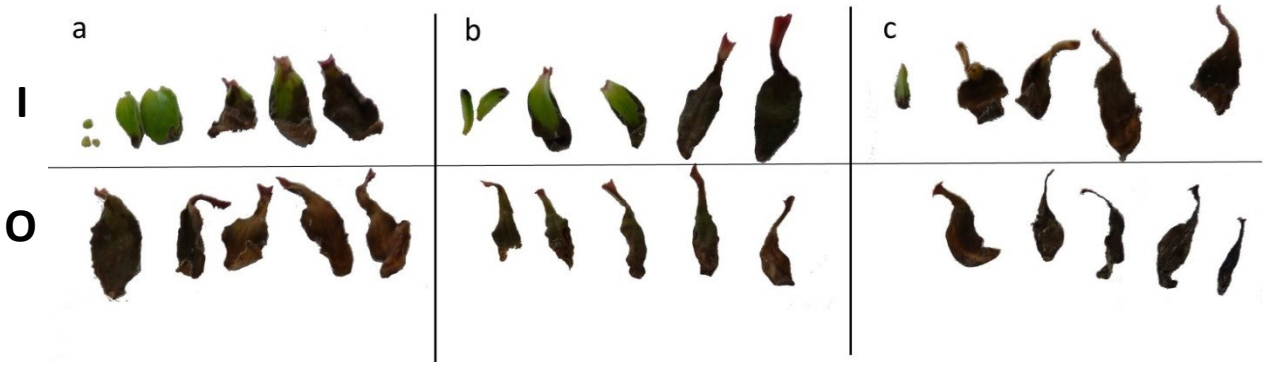

Fig. 2.8. Detached leaves of rehydrated old plants (a), young plants (b) and starved plants (c). Inner leaves (**I**) are rowed on the top of outer leaves (**O**).

3.5 Gene expression during senescence

The leaves of *C. plantagineum* senesce and die in nature (Fig. 2.9). The analysis of gene expression demonstrated that expression patterns differ with regards to senescence or desiccation tolerance in young and old plants (Fig. 2.9). The transcript levels of SRG2, SRG4, SnRK, HXK and *CDeT11-24* were lower in old plants than in young plants for both inner and outer leaves. In contrast, SRG3 was expressed higher in young plants than in old plants. The transcript levels of SRG2, SRG4 and *CDeT11-24* in inner leaves were lower than in outer leaves.

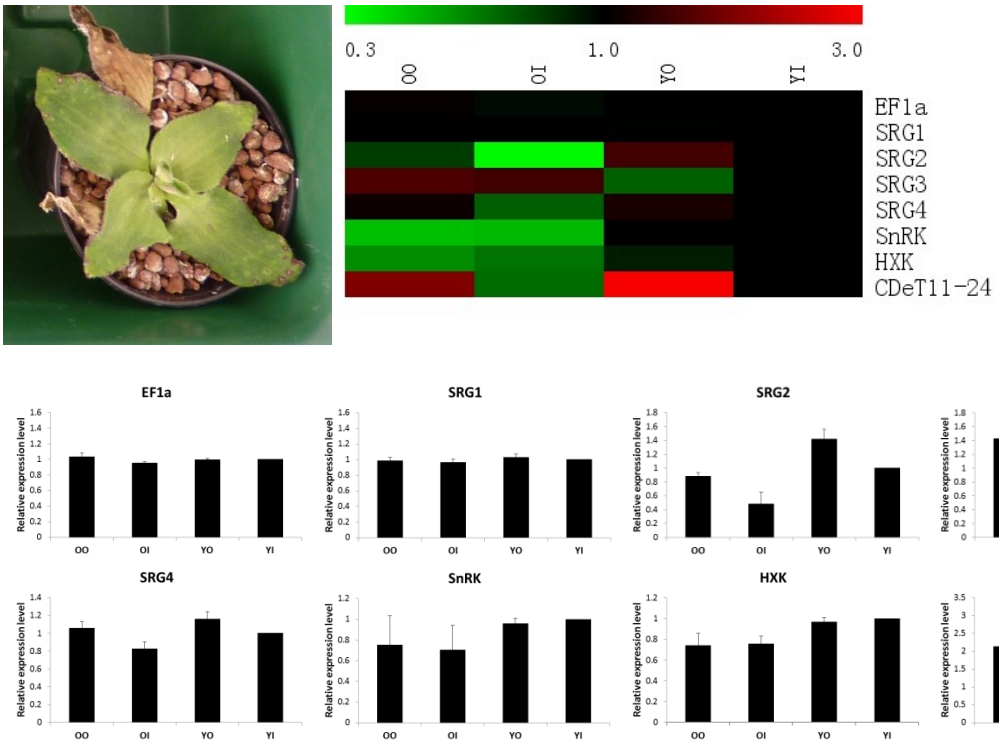

Fig. 2.9. The aging and death of *C. plantagineum* leaves and gene expression analysis during senescence in *C. plantagineum*. YO: outer leaves of young plants; YI: inner leaves of young plants; OO: outer leaves of old plants; OI: inner leaves of old plants. Gene expression levels are presented as relative to expression levels in inner leaves of young plants.

3.6 Sugar metabolism of *C. plantagienum* plants exposed to exogenous sucrose and other factors

Results had revealed that starvation (darkness treatment) could result in the difference in sugar status of young plants. To further explore the sugar metabolism in *C. plantagienum* plants, a range of experiments were conducted with leaf tissues. Results showed that when the leaf tissues ware incubated with sucrose, the levels of fructose, glucose and sucrose in leaf tissues increased more than ten times during one day compared with the control. In contrast, the level of D-g-D-i-oct declined during one day, although the level was still higher than that in control plants. In the period from the second day to the fourth day the levels of fructose, glucose and sucrose in leaf tissues incubated with sucrose stayed at the same level as those of the first day. The levels of D-g-D-i-oct in leaf tissue continuously decreased for both the treatment with sucrose supply and the control (Fig. 2.10). This indicates that the level of D-g-D-i-oct was not sensitive to excess exogenous sucrose.

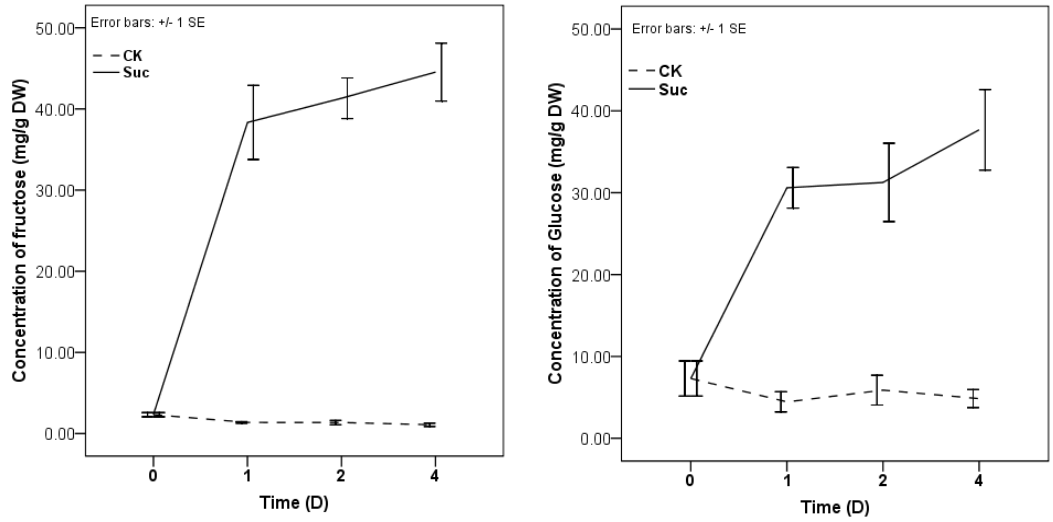

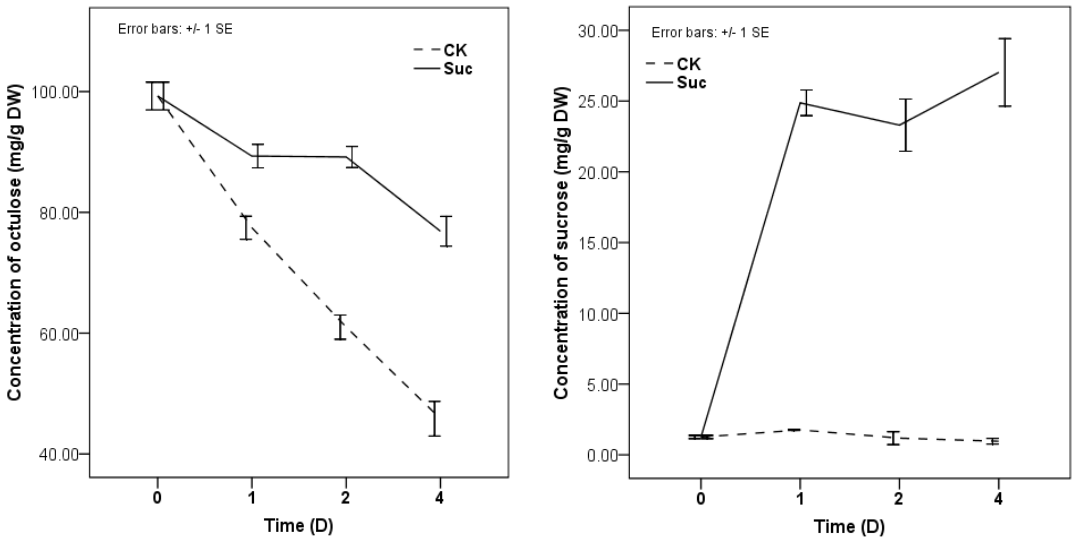

Fig. 2.10. Concentrations of sugars in leaf tissues of *C. plantagineum*. Leaves were cut into pieces and incubated with 200 mM sucrose (Suc) or water (CK).

To further explore the mechanism that regulates D-g-D-i-oct levels, other factors were analyzed. Experimental results showed that, both in dark and in light, the levels of fructose, glucose and sucrose increased more than ten times after supply of exogenous sucrose (Fig. 2.11). D-g-D-i-oct levels of leaf tissues incubated with exogenous sucrose did not change significantly in the dark, but they doubled in the light. The levels of glucose and sucrose in leaves treated with exogenous sucrose were also higher in the light than in the dark. This means light is required for the hydrolysis of sucrose and the production of D-g-D-i-oct. To analyze whether the production of D-g-D-i-oct driven by light is associated with the process of photosynthesis, paraquat was used as a ROS producer to inhibit photosynthesis. Paraquat treatment reduced the level of D-g-D-i-oct in leaf tissues of *C. plantagineum* without exogenous sugar, and this influence was enhanced by light (Fig. 2.11). When exogenous sucrose was supplied, the concentration of D-g-D-i-oct was slightly reduced by paraquat in the dark, whereas it decreased dramatically when the paraquat treatment was done in the light. From this we hypothesize that D-g-D-i-oct would be produced from fructose and glucose, and this process is supported by light; paraquat inhibits the pathway and the inhibitory effect was enhanced by light.

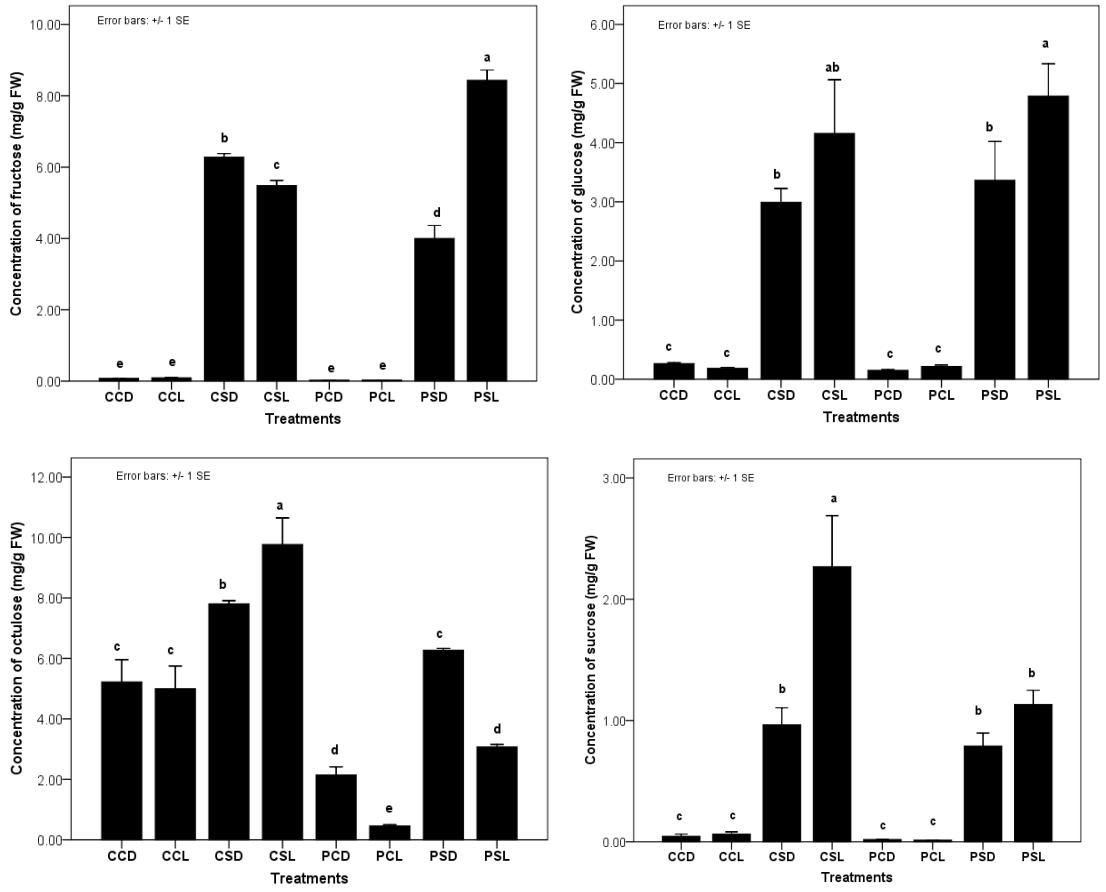

Fig. 2.11. Concentrations of sugars in leaf tissues of *C. plantagineum*. CCD: leaf tissues incubated in water in dark; CCL: leaf tissues incubated in water in light; CSD: leaf tissues incubated in sucrose solution in dark; CSL: leaf tissues incubated in sucrose solution in light; PCD: leaf tissues incubated in water with paraquat in dark; PCL: leaf tissues incubated in water with paraquat in light; PSD: leaf tissues incubated in sucrose solution with paraquat in dark; PSL: leaf tissues incubated in sucrose solution with paraquat in light.

3.7 Localization and transport of D-g-D-i-oct

Although D-g-D-i-oct accumulates to a high amount, its cellular localization is so far unknown. Therefore we attempted to identify the cellular compartment where D-g-D-i-oct accumulates and how it is transported. Experimental results showed that both in hydrated and partially dehydrated conditions, D-g-D-i-oct was the most abundant sugar both in the isolated chloroplasts and the intact leaves (Fig. 2.12). There were significant differences of the levels of fructose, glucose and D-g-D-i-oct between chloroplasts and the whole leaves in hydrated conditions. When *C. plantagineum* plants were partially dehydrated, the levels of fructose, glucose, D-g-D-i-oct and sucrose in chloroplasts did not significantly change while the levels of fructose, glucose and

sucrose in the whole leaves increased. The concentration of D-g-D-i-oct in isolated chloroplasts was lower than in whole leaf tissues either in dehydrated conditions or partially dehydrated conditions (Fig 2.12). This demonstrates that D-g-D-i-oct mainly accumulates in the cytosol, probably in the vacuole (It was not possible to establish a protocol for vacuole isolation for *C. plantagineum*).

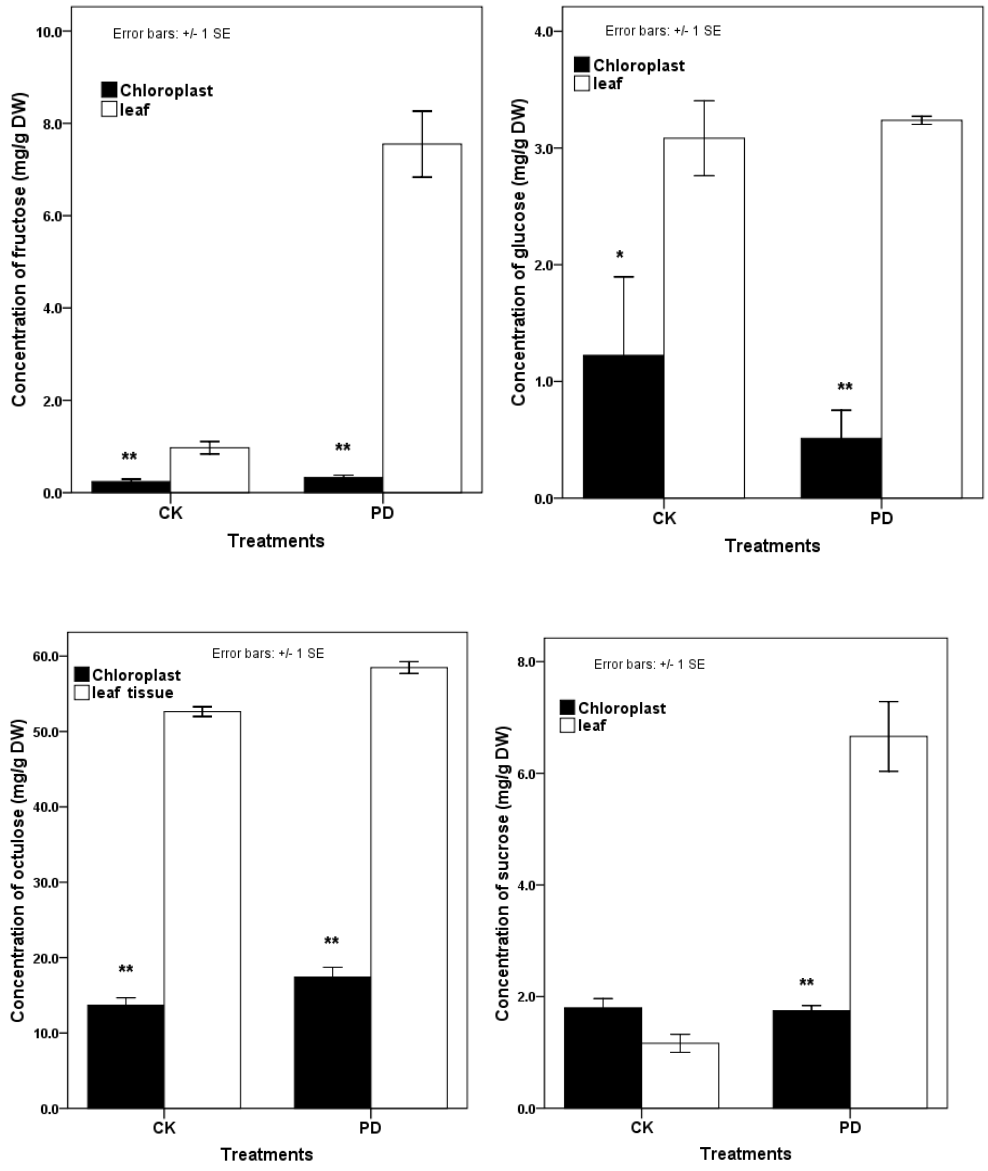

Fig. 2.12. Concentrations of sugars in chloroplasts and leaf tissues in hydrated (CK) and partially dehydrated (PD) conditions. In PD, plants were slowly dehydrated for two days while an RWC of 75% in leaves was reached. For partial dehydration plants were dehydrated slowly for 2 days and an RWC of 75% was reached in leaves.

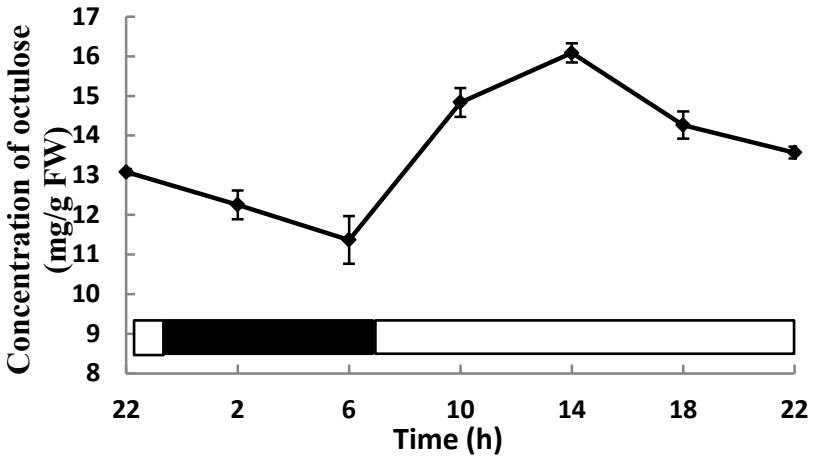

Fig. 2.13. Concentrations of D-g-D-i-oct in leaves of *C. plantagineum* plants within a 24-h period. The black bar represents the dark period and the transparent bar the light period.

The results of periodic determination of sugar levels in *C. plantagineum* leaves (Fig. 2.13) showed that D-g-D-i-oct levels in leaves of *C. plantagineum* increased from the onset of illumination and reached a peak in the middle of the illumination (14:00). Then the levels of D-g-D-i-oct are reduced and the trend continued during darkness until the light period started again. This indicates that the levels of D-g-D-i-oct are subjected to a circadian rhythm and might be regulated by the inner clock of *C. plantagineum* plants.

As the most abundant sugar in fully hydrated *C. plantagienum* plants, the levels of D-g-D-i-oct showed periodic changes. It is reasonable to hypothesize that D-g-D-i-oct could be exported to other organs from leaves during certain times. By analyzing the phloem exudate of leaves, it was found that leaves of *C. plantagineum* export glucose, fructose, D-g-D-i-oct and sucrose and D-g-D-i-oct occupied 75%-80% of the total exported sugars (Fig. 2.14). This indicates that D-g-D-i-oct represents a potential transport form in *C. plantagineum* plants.

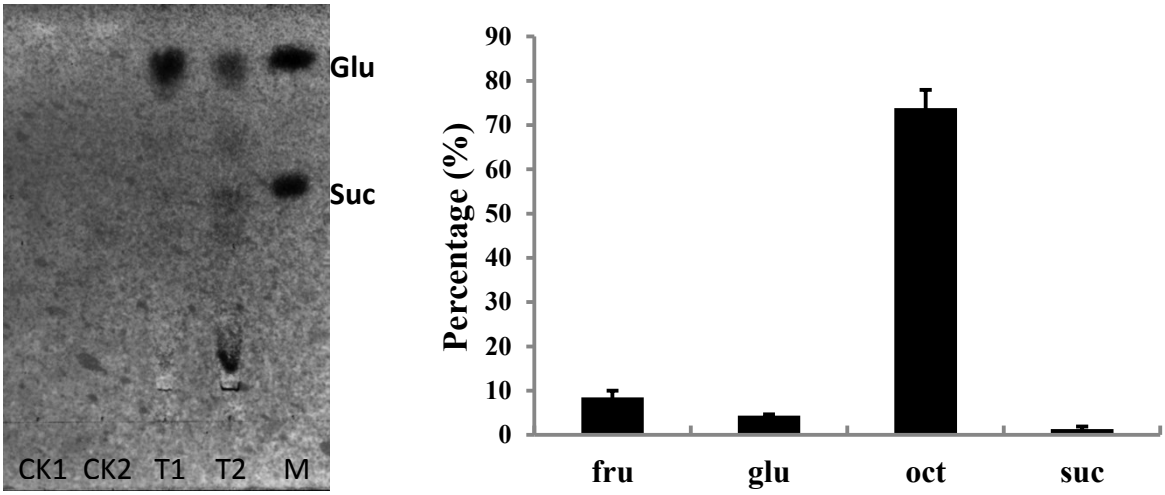

Fig. 2.14. Thin layer chromatogram (left panel) and GC analysis of leaf exudates (right panel) of *C. plantagineum*. CK1 and CK2 are the sugars exported into 5 mM $CaCl_2$ from leaves (control); T1 and T2 are sugars exported into 15 mM EDTA (leaf exudates); Lane M contains glucose (Glu) and sucrose (Suc) standards. The GC analysis shows the percentage of sugars relative to total sugars.

3.8 D-g-D-i-oct is synthesized by the oxidative pentose phosphate pathway?

D-g-D-i-oct is speculated to be localized in the cytosol according to the result above. In addition, its monophosphate is a component of the oxidative pentose phosphate pathway. To evaluate the relationship between D-g-D-i-oct accumulation and the intensity of the oxidative pentose phosphate pathway, the activities of the key enzymes of the pentose phosphate pathway, glucose-6-phosphate dehydrogenase and 6-phosphogluconate dehydrogenase, were determined. Results (Fig. 2.15) showed that the light enhanced the activity of G6PDH and the activity of 6GPDL without exogenous sugar supply. Although sugar supply did not affect the activities of G6PDH and 6GPDL, the combination of sugar supply and light significantly reduced the activity of G6PDH and 6GPDL compared to the treatment with sugar only. This means that the key enzymes of the oxidative pentose phosphate pathway are regulated by light and sugar. With the absence of paraquat, the activity of G6PDH and 6GPDL were not affected in the dark, but were significantly reduced in light. The activity of G6PDH increased with sugar supply even in the presence of paraquat in both dark and light, while in the presence of paraquat, the activity of 6GPDL increased with sugar supply in the dark and did not change in light. The total activity of dehydrogenase represents the ability of the plant to provide NADPH for reductive biosynthesis and maintenance of the cellular redox state. Results showed that the influence of light and sugar supply on total dehydrogenase activity in the absence of paraquat was similar as on G6PDH and

6GPDL. With the presence of paraquat, light reduced total dehydrogenase activity without sugar supply, but the total dehydrogenase activity increased when sugar was supplied in both dark and light in the presence of parquat. This indicates that light enhances the production of NADPH through the oxidative pentose phosphate way, while sugar delays this process in the light. Paraquat in light could reduce the production of NADPH through the oxidative pentose phosphate pathway, but sugar enhances the production of NADPH in the presence of paraquat in both dark and light. However, it appeared that there is no positive correlation between D-g-D-i-oct content and the activities of key enzymes in the oxidative pentose phosphate pathway.

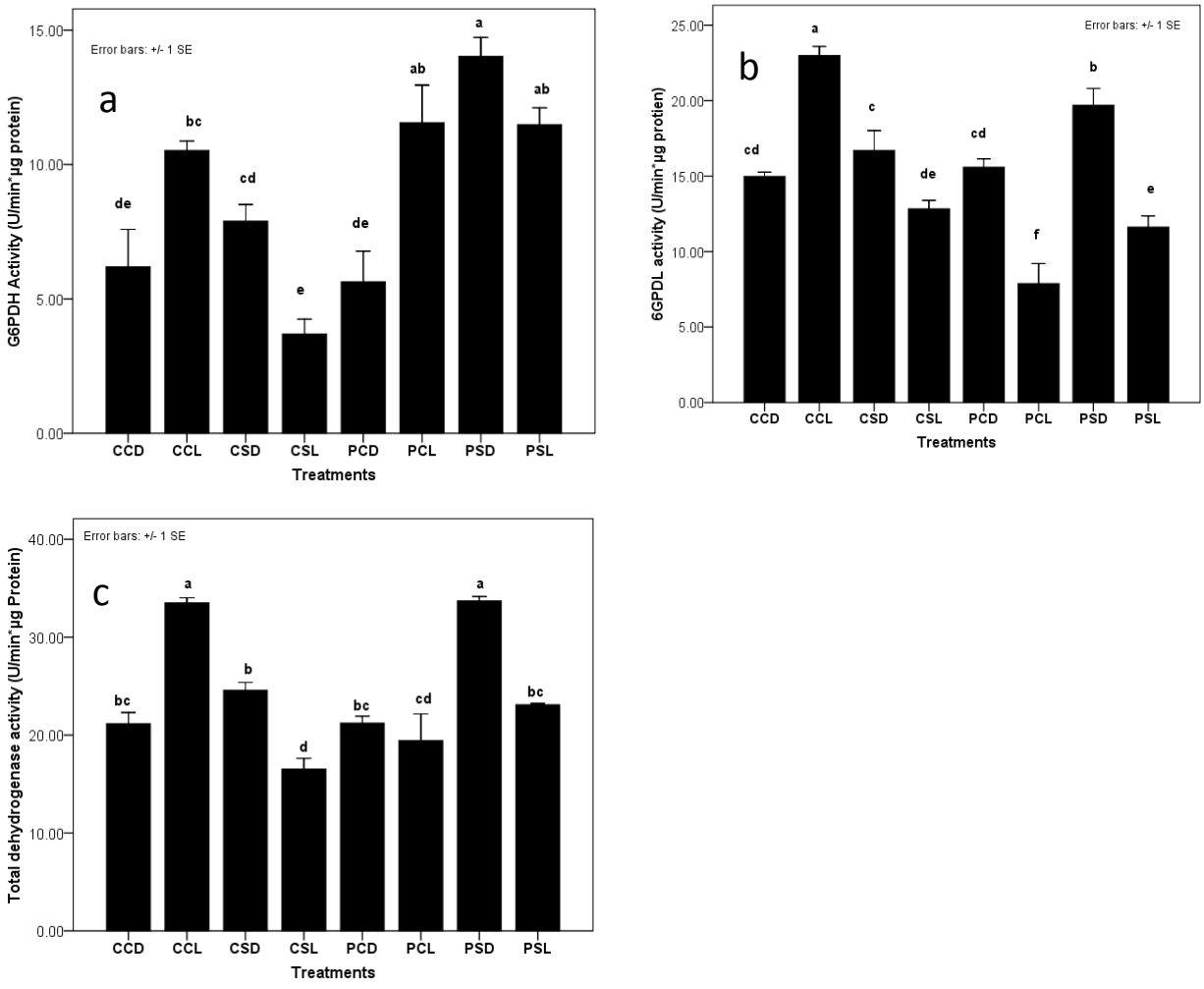

Fig. 2.15. The activities of glucose-6-phosphate dehydrogenase (a) and 6-phosphogluconate dehydrogenase (b) as well as the total activity of the dehydrogenase (c) that produces NADPH.

3.9 Hydroxyl scavenging ability of D-g-D-i-oct

Research provides novel perspectives for highly accumulated sugars in the cytosol or vacuole of plants, including proposing that sugars function as antioxidants. By testing the hydroxyl radical scavenging ability of D-g-D-i-oct that was obtained by TLC, we found that D-g-D-i-oct had a better hydroxyl scavenging ability than sucrose (Table 1.1). The hydroxyl scavenging ability of D-g-D-i-oct was about 4 times that of sucrose. In addition we analyzed the antioxidant capacity of the oligosaccharide stachyose that accumulates to high levels in roots of *C. plantagineum*. The hydroxyl scavenging ability of stachyose was similar to sucrose.

Table 1.1 Hydroxyl radical scavenging ability of sugars presented by half-inhibitory concentration (IC_{50}) for HTPA formation.

Hydroxyl scavenging ability	IC_{50} (mM)
D-g-D-i-oct	0.05
stachyose	0.18
sucrose	0.20

3.10 Starch metabolism in *C. plantagineum*

Though *C. plantagineum* plants accumulate high amounts of D-g-D-i-oct, starch is also synthesized. By periodic analysis, it was observed that the synthesis of starch in *C. plantagineum* plants was also subjected to circadian rhythm (Fig. 2.16). The starch concentration increased 2 h after illumination, peaked at 14 h and then decreased until 6 h of the next day when it reached a minimum value.

When starch concentrations were compared in leaves of old and young plants, as well as leaves of starved plants, no significant difference was found between outer leaves and inner leaves for both old and young plants. Starvation treatment led to a decline of starch levels in outer leaves but did not affect that of inner leaves (Fig. 2.17). No correlation was seen between the ability of desiccation tolerance and starch concentration in *C. plantagineum* plants.

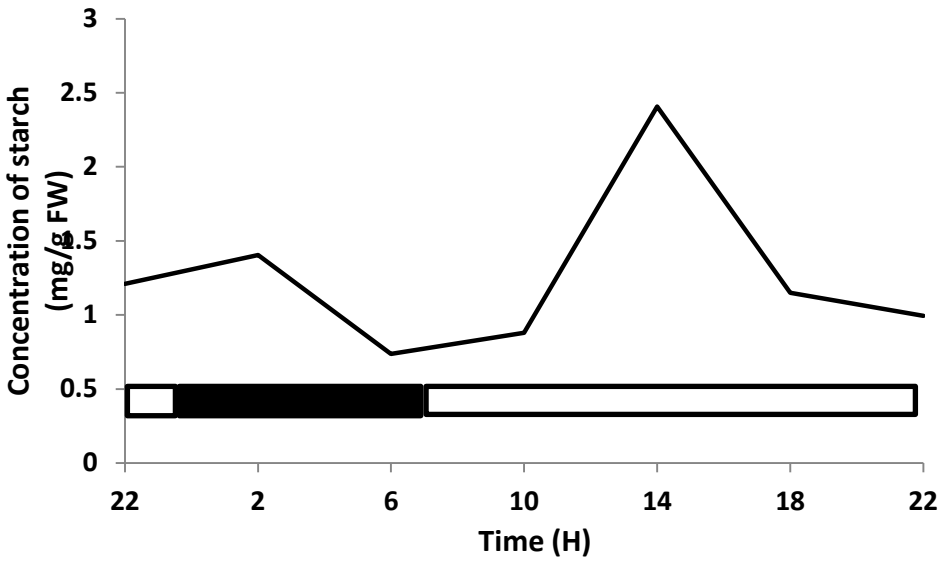

Fig. 2.16. Concentrations of starch in *C. plantagineum* leaves during a 24-h period. Samples were collected each four hours and first sampling began at 22:00. The black bar represents the dark period and the transparent bar the light period.

The metabolism of starch involves various enzymes. RNA sequencing of *C. plantagineum* plants in hydrated, partial dehydrated, total dehydrated and rehydrated conditions revealed the expression pattern of potential genes regarding the metabolism of starch, including soluble starch synthases (STS), granule-bound starch synthases (GBS), starch branching enzymes (SBE), starch debranching enzymes isoamylase and limit dextrinase (ISA and LDA, respectively), α-glucan phosphorylases (PHS), disproportionating enzymes (DPE), α-amylases (AMY) and β-amylases (BAM) (Fig. S2). Results showed that the expression patterns of most genes were not significantly regulated by dehydration, though a few genes were inducible by partial dehydration or total dehydration. In control, dehydrated, desiccated and rehydrated treatments, the maximum relative expression of genes was 5.3 times of that in control (Assembly UniProt ID: Q41058) and the minimum was 0.34 times of that in control (Assembly UniProt ID: B2ZGN0). This indicates that starch metabolism does not significantly contribute to the mechanism of desiccation tolerance.

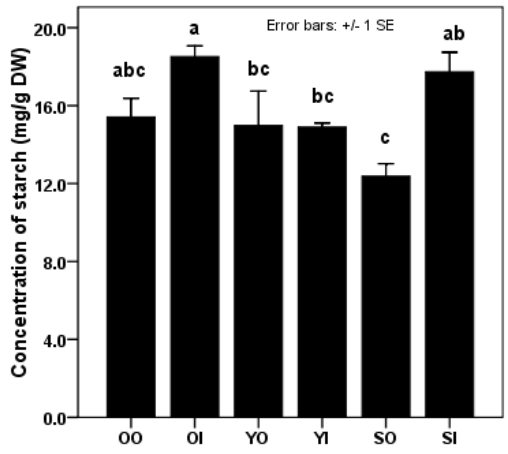

Fig. 2.17. Starch concentrations in leaves of *C. plantagineum* plants. OO: outer leaves of old plants; OI: inner leaves of old plants; YO: outer leaves of young plants; YI: inner leaves of young plants; SO: outer leaves of starved plants; SI: inner leaves of starved leaves.

3.11 Molecular phylogeny of plant transketolases

Phylogeny analysis of transketolase genes demonstrates that TKT7 and TKT10 are closely related in *C. plantagineum* (Fig. 3.1).TKT7 and TKT10 in *C. plantagineum* have diverged from other transketolase genes of many desiccation sensitive species in the phylogenetic tree, while TKT3 shares higher identity with other plant species. Through RNA sequencing, we have found eight possible homologous genes for TKT3 TKT7 and TKT10 of *C. plantagineum* in another two often D-g-D-i-oct-producing plants *Lindernia brevidens* and *Lindernia subracemosa*. In the phylogenetic tree, TKT7 and TKT10 and their five homologs from *L. brevidens* and *L. subracemosa* (con 8 lb, con 3 ls, con 2 lb, con 1 lb and con 5 ls) form a branch. Three homologs from *L. brevidens* and *L. subracemosa* (labeled as con 6 LS, con 1 LS and con 2 LS) show highly similar evolutionary characteristics with TKT3 in another branch. The branch with *C. plantagineum* TKT3 appears closer to the big group composed of another 40 species of angiosperms. This shows the specificity of the TKT7 and TKT10 of these D-g-D-i-oct-producing plants in evolution.

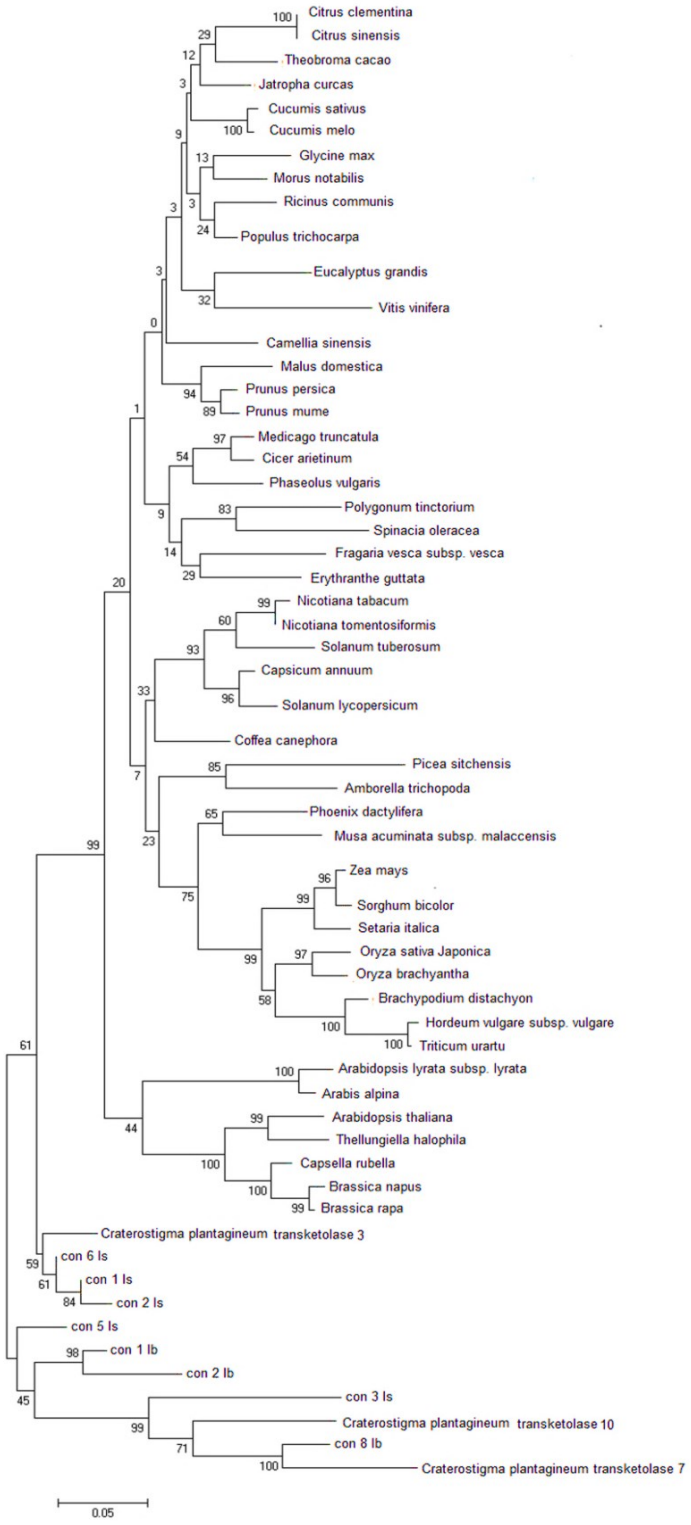

Fig. 3.1. Phylogenetic tree of plant transketolases constructed by Mega 6 software using amino acid sequences. The genes con 1 lb, con2 lb and con 8 lb are possible transketolase genes from *Lindernia brevidens* and the genes con 1 ls, con 2 ls, con 3 ls, con 5 ls and con 6 ls are possible transketolase genes from *Lindernia subracemosa*.

3.12 Extraction of transketolase from *C. plantagineum* leaves and immune blotting

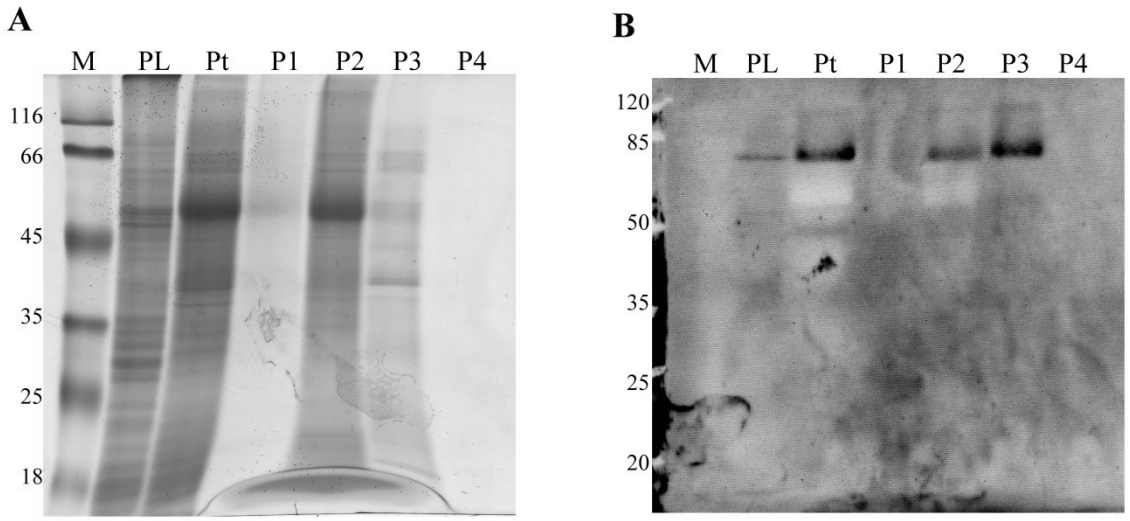

Fig. 3.2. SDS-PAGE (A) and immuno blotting (B) of proteins extracted from leaves of *C. plantagineum*. Note: M, protein size markers (given in kDa); PL: proteins not soluble in extraction buffer; Pt: total proteins extracted by the extraction buffer; P1, proteins precipitated with 0-25% (w/v) $(NH_4)_2SO_4$; P2, proteins precipitated with 25-50% (w/v) $(NH_4)_2SO_4$; P3, proteins precipitated with 50-70% (w/v) $(NH_4)_2SO_4$; P4, proteins remained in extraction buffer after precipitation with 50-70% (w/v) $(NH_4)_2SO_4$; all pellets were dissolved in buffer A. Samples were loaded with SDS buffer on the gel. The volume loaded was 20 μL.

Results showed that proteins in leaves of *C. plantagineum* could not completely be extracted by the extraction buffer (Fig. 3.2). After $(NH_4)_2SO_4$ precipitation, most proteins soluble in the extraction buffer were enriched in the fraction obtained through 25-50% (w/v) $(NH_4)_2SO_4$ precipitation. The result of Western blotting using transketolase anti-serum showed that a few transketolase proteins remained in the plant tissues, most transketolase proteins that were extracted by the extraction buffer were enriched in the fraction obtained by 50-75% (w/v) $(NH_4)_2SO_4$ precipitation although the amount of total proteins in this fraction was rather low. Additionally, some transketolase proteins were observed in the fraction obtained by 25-50% (w/v) $(NH_4)_2SO_4$ precipitation, but the amount of them was low (signal was weak). Thus it could be concluded that $(NH_4)_2SO_4$ precipitation can enrich transketolase proteins effectively and these proteins are contained in the fraction obtained by 50-75% (w/v) $(NH_4)_2SO_4$ precipitation.

3.13 Gene cloning and protein purification of recombinant *C. plantagineum* transketolases

The open reading frames of genes tkt3, tkt7 and tkt10 of *C. plantagineum* were amplified by PCR with restriction enzyme sites added at both 5' end and 3' end (Fig. 3.3). The results of electrophoresis showed that the sizes of tkt3, tkt7 and tkt10 were about 1.5 kb, 2.0 kb and 2.0kb, respectively. The *C. plantagineum* transaldolase 1(tal) was obtained from *C. plantagineum* transcriptome. The available fragment length of ta1 was about 500 bp. The sizes of the fragments were consistent with the information of these genes or gene fragments.

The PCR products were ligated to blunt end pJET1.2 vector. The ligation products were used to transform competent cells of *E. coli* DH10B. The transformed cells of *E. coli* were grown on solid LB medium with ampicillin. The colonies of *E. coli* DH10B grown on the LB medium were picked and directly used as template in PCRs for selecting the positive transformations (Fig. 3.4). By analyzing the lengths of the PCR products, eight positive colonies containing pJET1.2 vector with tkt3 inserted were observed. Similarly, one colony regarding tkt7 and two colonies regarding tkt10 were observed.

After the verification of the PCR, the positive colonies were grown in LB medium with ampicillin to isolate plasmid DNAs. Isolated plasmid DNAs were digested with specific restriction enzymes (Fig. 3.5) to obtain gene fragments. The results showed that the lengths of the gene fragments obtained by digestion were consistent with those of PCR products (The lengths of tkt3, tkt7 and tkt10 were of about 1.5, 2.0 and 2.0 kb, respectively).

The digested gene fragments were ligated to digested expression vector pet28a+ (Fig. 3.5). The ligation products were firstly used to transform *E. coli* DH10B (Fig. 3.6). After PCR verification, positive colonies were grown in LB medium with kanamycin and the isolation of plasmid DNAs was done as above. The pet28a+ vectors inserted by genes tkt3, tkt7 and tkt10 were transformed into competent cells of *E. coli* BL21. Similarly, PCRs were conducted to select and verify positive transformations (Fig. 3.7). The positive transformations were grown for protein purification after sequencing the inserted plasmid DNAs.

In addition, as control of enzymatic assays, the fragment of the *C. plantagineum* transaldolase gene was amplified by PCR with restriction enzyme sites added at both 5' ends and 3' ends (Fig. 3.3). The PCR product was digested with restriction enzymes and ligated directly to digested pet28a+ vector. The ligation product was transformed into competent DH10B cells. After PCR verification (Fig. 3.6), the positive colonies were grown and plasmid DNAs were isolated. Finally the vector pet28a+ containing the ta1 fragment was transformed into competent *E. coli* BL21 cells. The positive colonies were verified by PCRs (Fig. 3.7) and DNA sequencing and subsequently used for protein purification.

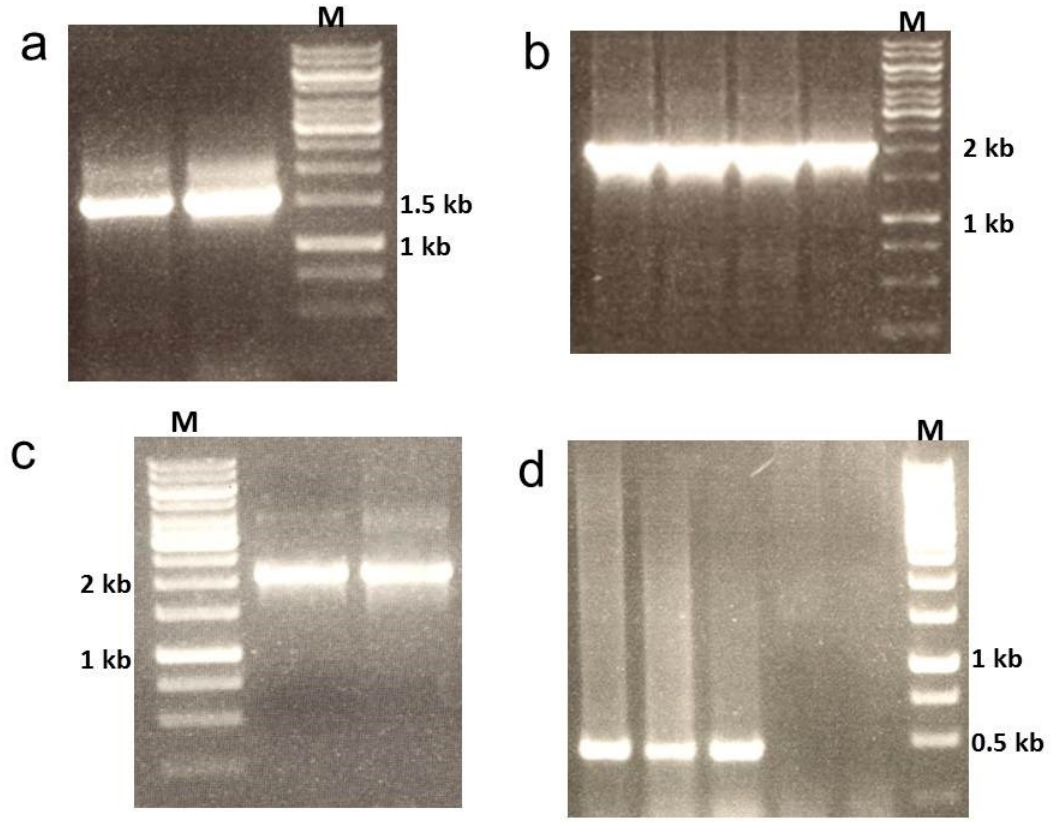

Fig. 3.3. Electrophoresis of PCR products for amplifying the open reading frames of tkt3 (a), tkt7 (b), tkt10 (c) and the partial fragment of ta1 (d).The Gene Ruler 1Kb DNA ladder (M) of Thermo scientific was loaded in each gel.

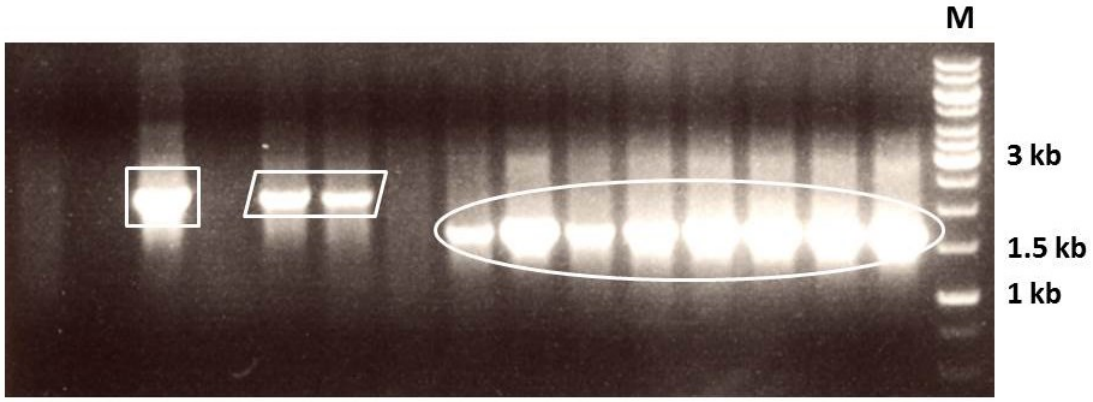

Fig. 3.4. Electrophoresis of the products of colony PCR for selecting positive transformations of tkt3, tkt7 and tkt10 ligated to blunt pJET1.2 vector. Competent cells of *E. coli* DH10B were used for transformations. Colonies picked from solid LB medium containing ampicillin were directly used as templates in PCRs. The Gene Ruler 1Kb DNA ladder (M) of Thermo scientific was loaded on each agarose gel. Positive transformants of tkt3, tkt7 and tkt10 were marked by circles, squares and parallelograms, respectively.

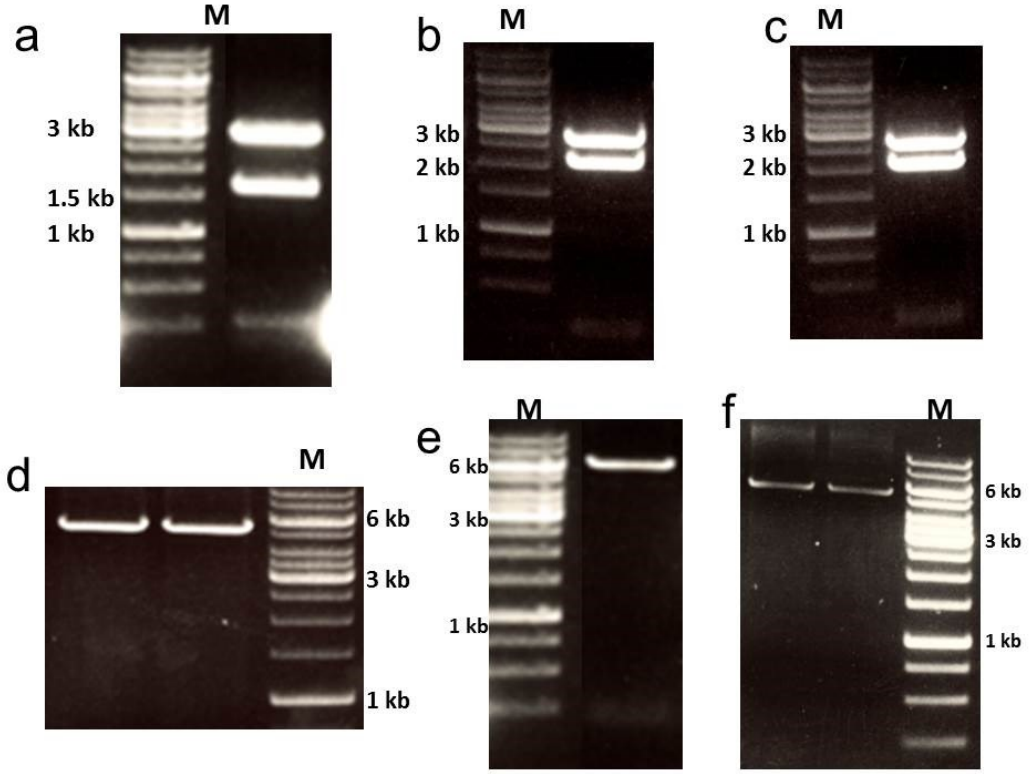

Fig 3.5. Electrophoresis of digestion products of plasmid DNA isolated from positive transformations of tkt3 (a), tkt7 (b) and tkt10 (c) that were ligated to blunt pJET1.2 vector, as well as empty vector pet28a+ digested with different enzyme combinations (d-f). The Gene Ruler 1Kb DNA ladder (M) of Thermo scientific was loaded on each agarose gel.

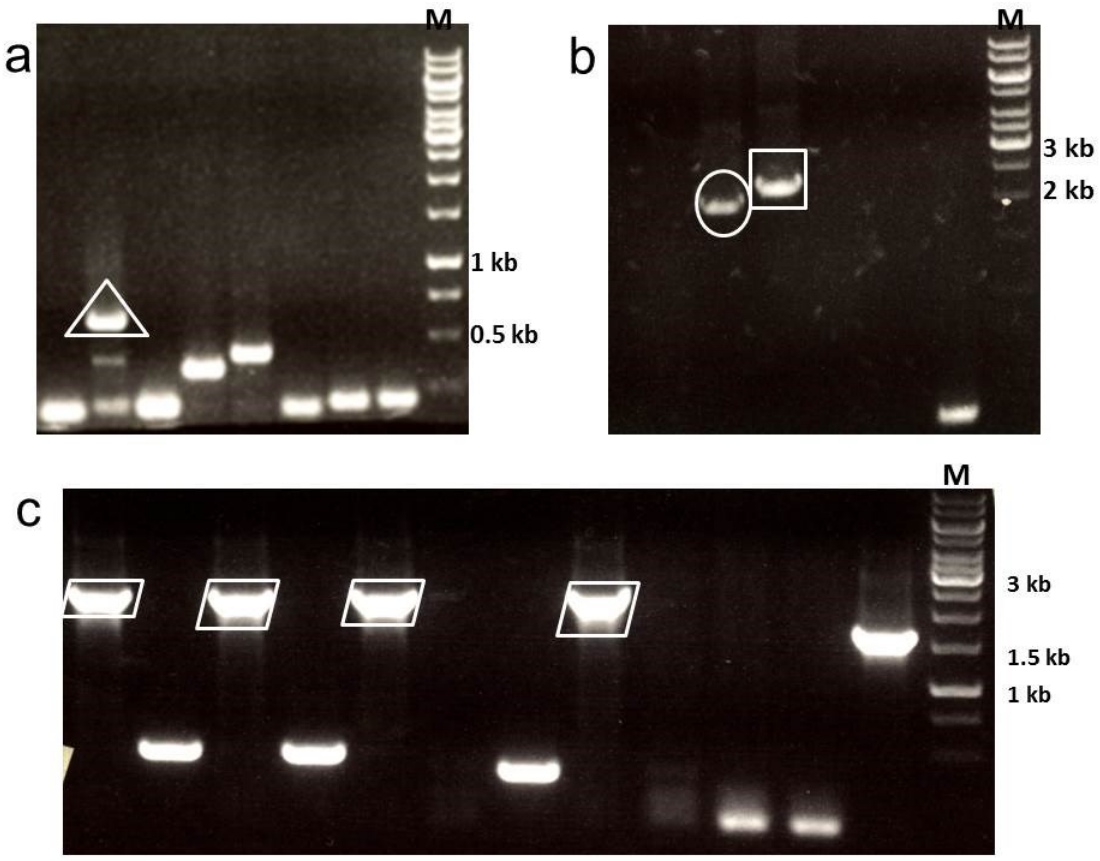

Fig. 3.6. Electrophoresis of the products of colony PCR for selecting positive transformations of pta1, tkt3, tkt7 and tkt10 that were all ligated to vector pet28a+. Competent cells of *E. coli* DH10B were used for transformation. Colonies picked from solid LB medium containing ampicillin were directly used as templates in PCR reactions. The Gene Ruler 1Kb DNA ladder (M) of Thermo scientific was load on each agarose gel. Positive transformations of tkt3, tkt7 and tkt10 are marked by a triangle, a circle, a square and parallelograms, respectively.

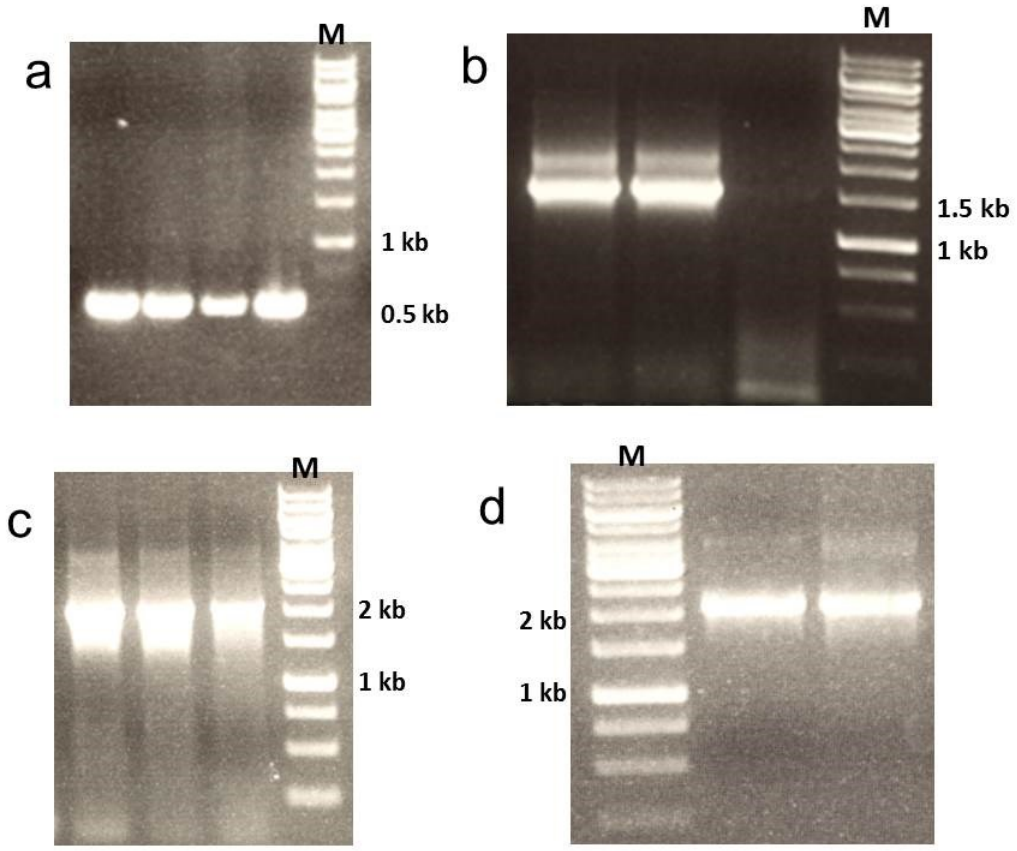

Fig. 3.7. Electrophoresis of the products of colony PCR for selecting positive transformations of pta1 (a), tkt3 (b), tkt7 (c) and tkt10 (d) that were all ligated to vector pet28a+. Competent cells of *E. coli* BL21 (DE3) were used for transformation. Colonies picked from solid LB medium containing kanamycin were directly used as templates in PCR reactions. The Gene Ruler 1Kb DNA ladder (M) of Thermo scientific was loaded on each agarose gel. Positive transformants of tkt3, tkt7 and tkt10 are marked by triangle, circles, squares and parallelograms, respectively.

The *E. coli* BL21cells transformed with the pet28a+ vector containing the inserted genes were grown and induced by IPTG for protein expression. Recombinant proteins of the ta1 fragment, tkt3, tkt7 and tkt10 were purified (Fig. 3.8) after cell disruption, membrane filtration and affinity chromatography. The results of SDS-PAGE showed that the concentrations of purified proteins were highest in the second elution fraction. The sizes of the proteins of recombinant ta1 fragment, tkt3, tkt7 and tkt10 were about 15 kDa, 66 kDa, 66 kDa and 66 kDa, respectively.

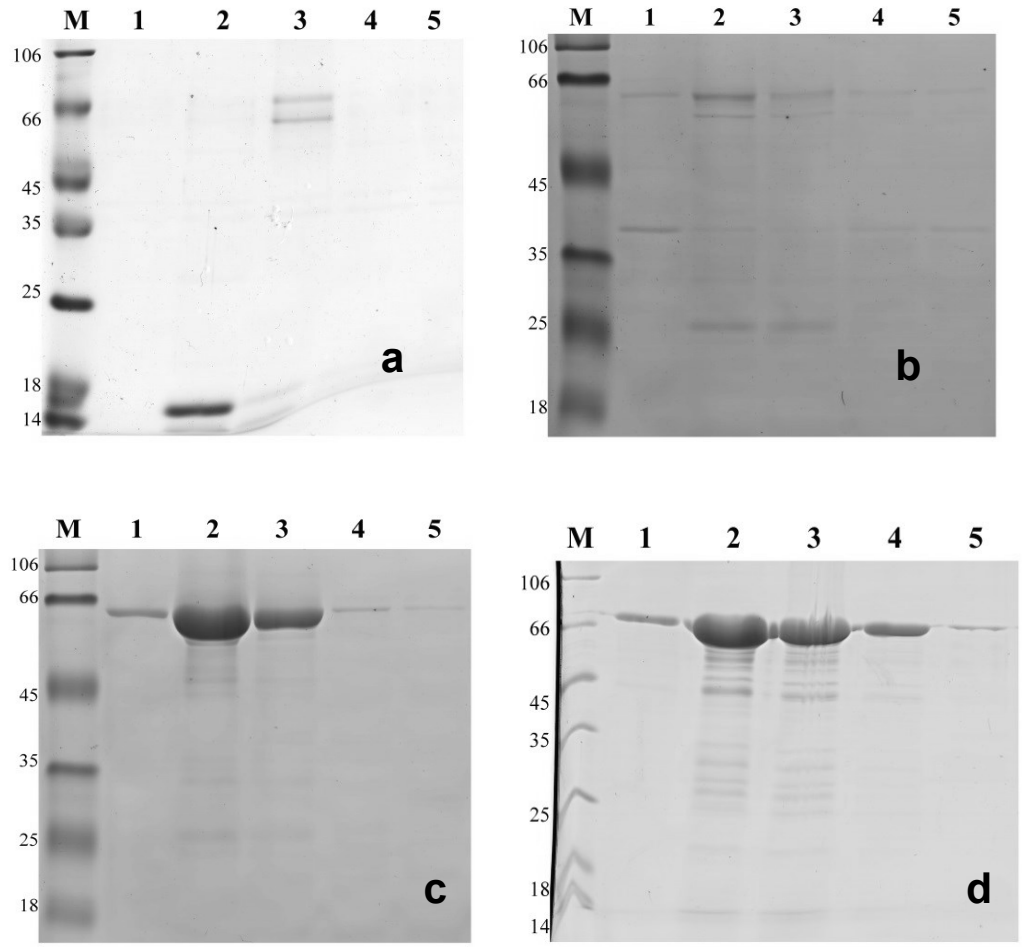

Fig. 3.8. SDS-PAGE of purified proteins: partial fragment of transaldolase 1 (a), transketolase 3 (b), transketolase 7 (c) and transketolase 10 (d). From left to right in each sub-figure lanes represent the protein size markers and the eluted fractions 1 to 5. The protein size markers are given in kDa.

3.14 Dephosphorylation of reaction products

In this study, nearly all the enzymatic assays use sugar phosphates as substrates and target products are also sugar phosphate. In order to evaluate the influence of the phosphate group of the sugar on the identification of sugars by GC/MS, two target sugars D-g-D-i-oct and seduheptulose and their phosphates were derivatized by TMS and detected by GC/MS (Fig. 3.9). By comparison of the MS spectrum of the derivative of sedoheptulose and that of the derivative of sedoheptulose-7-phospahte, it was found that the derivatized phosphate group was not separated in the process of ionization. Since two important ions (m/z 299.1 and 691.3) of the MS spectrum of the derivative of sedoheptulose-7-phosphate could be deduced from the ions

(m/z147.2 and 539.3) of the MS spectrum of the derivative of sedoheptulose (Fig. 3.9). In contrast, a similar phenomenon was observed for D-g-D-i-oct. When D-g-D-i-oct was phosphorylated, there was no typical ion peak in the spectrum of the TMS derivative as that observed for D-g-D-i-oct (Fig. 3.9 c-d). This indicated that the molecule of D-g-D-i-oct-8-phosphate would be more easily split into fragments with lower molecular weight than D-g-D-i-oct in the ionization of MS. Thus it makes the detection of D-g-D-i-oct is more difficult. Based on this fact, all the sugar phosphates in the reaction products were detected after dephosphorylation by acid phosphatase.

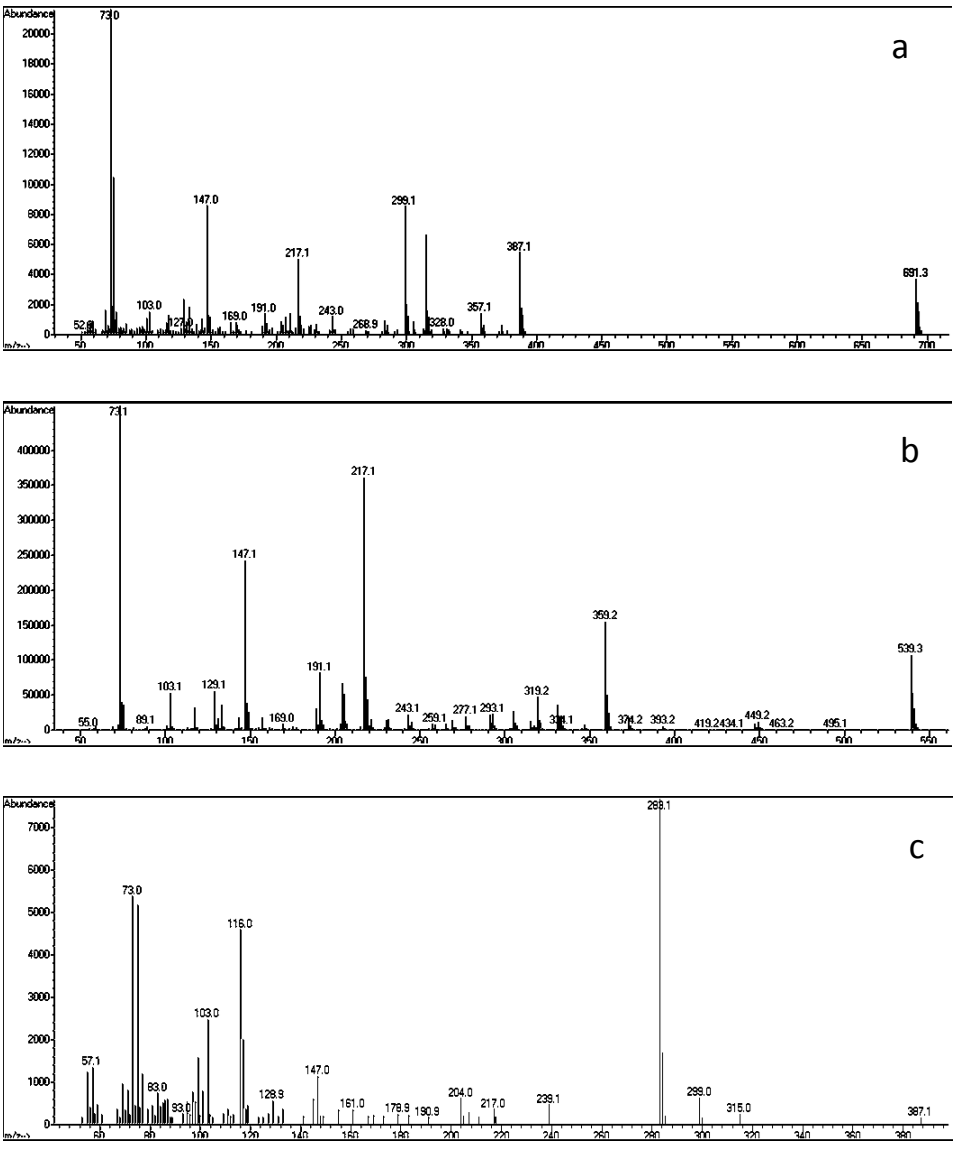

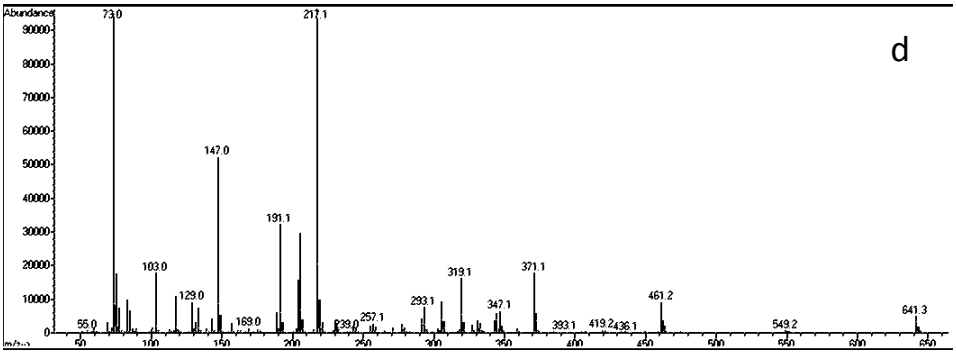

Fig. 3.9. The MS spectrum of the derivatives of sedoheptulose-7-phosphate (a), sedoheptulose hydrolyzed from sedoheptulose-7-phosphate by acid phosphatase (b), D-g-D-i-oct-8-phosphate (c) and D-g-D-i-oct hydrolyzed from sedoheptulose-7-phosphate by acid phosphatase (d). Sedoheptulose-7-phospahte was synthesized by the transketolase extracted from *C. plantagineum* leaves and enriched by $(NH_4)_2SO_4$ precipitation with ribose-5-phospahte and xylulose-5-phosphate as substrates. Ocutolse-8-phosphate was synthesized by the transketolase extracted from *C. plantagineum* leaves and enriched by $(NH_4)_2SO_4$ precipitation with hydroxypyruvate and glucose-6-phosphate as substrates.

3.15 Enzymatic assays of transketolase

The transketolase extracted form *C. plantagineum* and the recombinant proteins purified form *E. coli* cells were used in the enzymatic assays with different donor and acceptor substrates.

3.15.1 Performance of transketolase extracted from *C. plantagineum* leaves

Given the specificity of the anti-serum of transketolase used in this study, the transketolase proteins extracted form *C. plantagineum* leaves and enriched by 50-70% (w/v) $(NH_4)_2SO_4$ precipitation should be the mixture of three isoforms of *C. plantagineum* transketolases. The results of enzymatic assays using the transketolase mixture suggested that this mixture could catalyze the formation of D-g-D-i-oct-8-phosphate using hydroxypyruvate as donor substrate and glucose-6-phosphate as acceptor substrate (Fig. 3.10). In similar conditions, when the acceptor substrate was changed to ribose-5-phosphate, sedoheptulose was observed in the dephosphorylated reaction products (Fig. 3.11). According to a previous study (Kutzer, 2004), sedoheptulose-7-phosphate was proposed to be formed in this reaction.

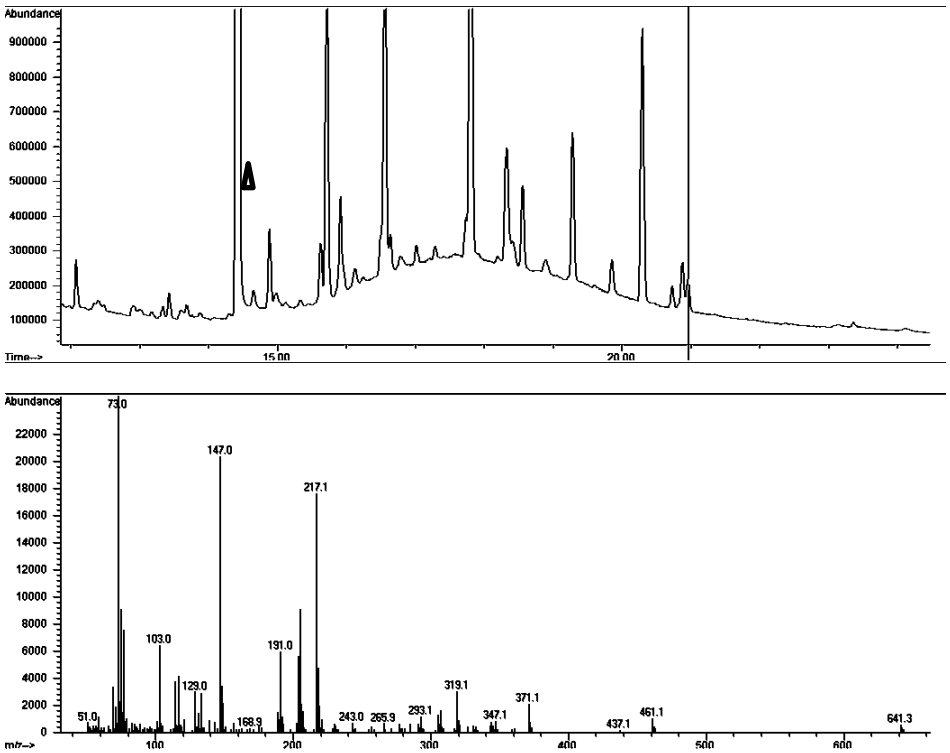

Fig. 3.10. The chromatogram of the TMS derivatives of the dephosphorylated reaction product with **glucose-6-phosphate** as acceptor substrate and **hydroxypyruvate** as donor (upper part) and the mass spectrum of the TMS derivative of D-g-D-i-oct (lower part). The TMS derivative of the internal standard xylitol is labeled by a triangle and that of D-g-D-i-oct is labeled by a vertical line. The reaction contains 25 μg transketolase proteins extracted form **rehydrated** *C. plantagineum* leaves and enriched by 50-70% (w/v) $(NH_4)_2SO_4$ precipitation, 58 mM glycylglycine (pH 7.7), 0.01% (w/v) Na-azide, 0.002% thiamine pyrophosphate, 15 mM $MgCl_2$, 5.3 mM donor and 16 mM acceptor. After 24 h of the catalyzing reaction, sugar phosphates in the product were dephosphorylated using acid phosphatase. The dephosphorylated products were purified on a column containing ion-exchange bed resin AG 501-X8(D) (BIO-RAD). The flow-through fractions were used for GC/MS analysis.

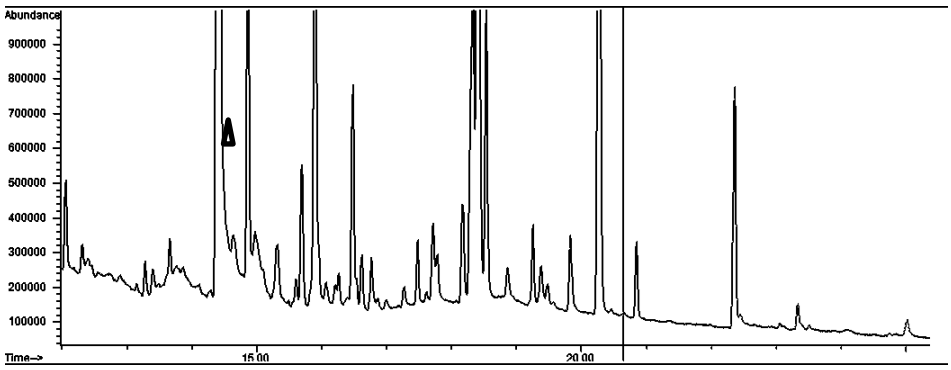

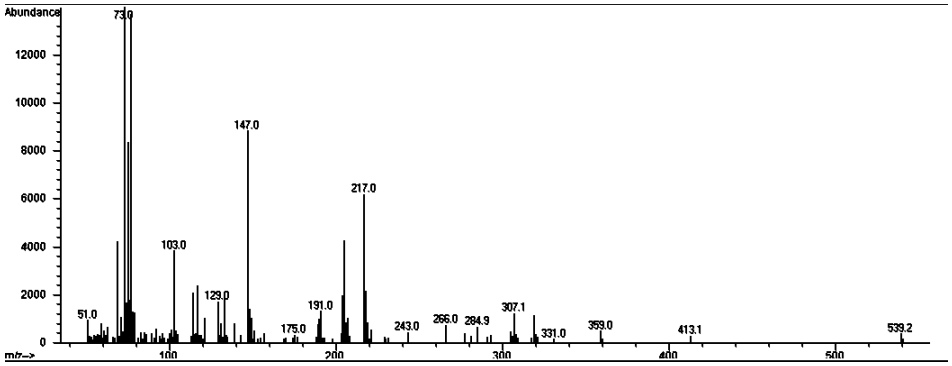

Fig. 3.11. The chromatogram of the TMS derivatives of the dephosphorylated reaction product with **ribose-5-phosphate** as acceptor substrate and **hydroxypyruvate** as donor (upper part) and the mass spectrum of the TMS derivative of sedoheptulose (lower part). The TMS derivative of the internal standard xylitol is labeled by a triangle and that of sedoheptulose is labeled by a vertical line. The reaction condition is the same as described in Fig 3.10.

To confirm the existence of the exchange reaction, the mixture of different isoforms of *C. plantagineum* transketolases were used in the exchange reaction in which glucose-6-phosphate was used as acceptor substrate and fructose-6-phosphate was used as donor substrate. Besides, glucose-6-phosphate was substituted by ribose-5-phosphate to observe the reaction products in the same reaction conditions. The results demonstrated that D-g-D-i-oct-8-phosphate was formed in the reaction catalyzed by the transketolase mixture when using glucose-6-phosphate as acceptor substrate and fructose-6-phosphate as donor (Fig. 3.12). Additionally, sedoheptulose-7-phosphate was formed in the reaction in which the acceptor substrate glucose-6-phosphate was substituted by ribose-5-phosphate (Fig. 3.13).

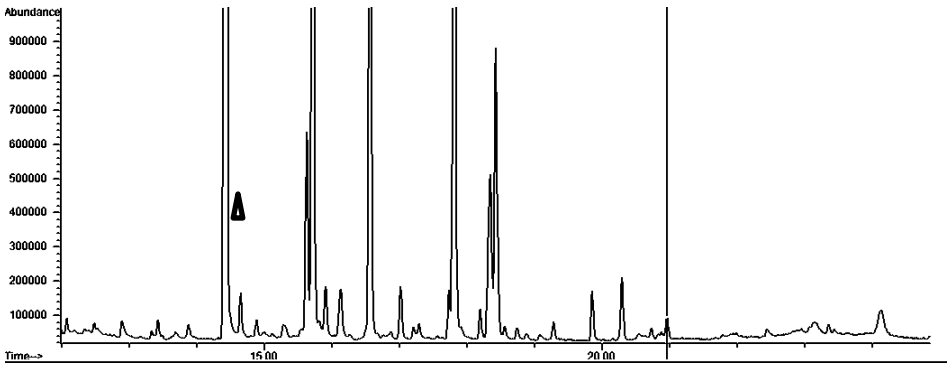

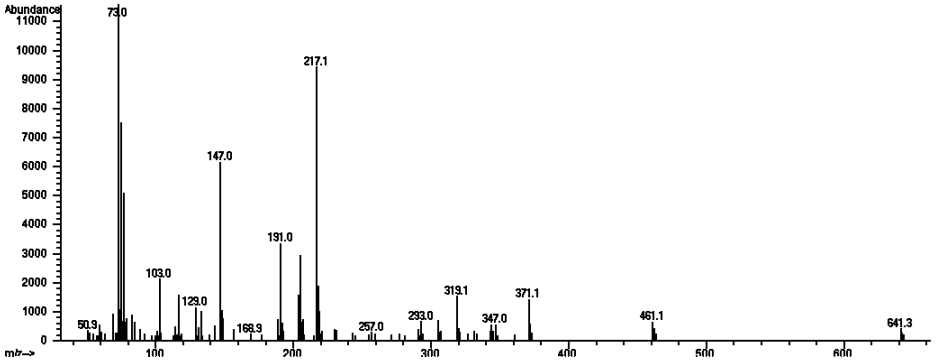

Fig. 3.12. The chromatogram of the TMS derivatives of the dephosphorylated reaction product with **glucose-6-phosphate** as acceptor substrate and **fructose-6-phosphate** as donor (upper part) and the mass spectrum of the TMS derivative of D-g-D-i-oct (lower part). The TMS derivative of the internal standard xylitol is labeled by a triangle and that of D-g-D-i-oct is labeled by a vertical line. The reaction condition is the same as described in Fig 3.10.

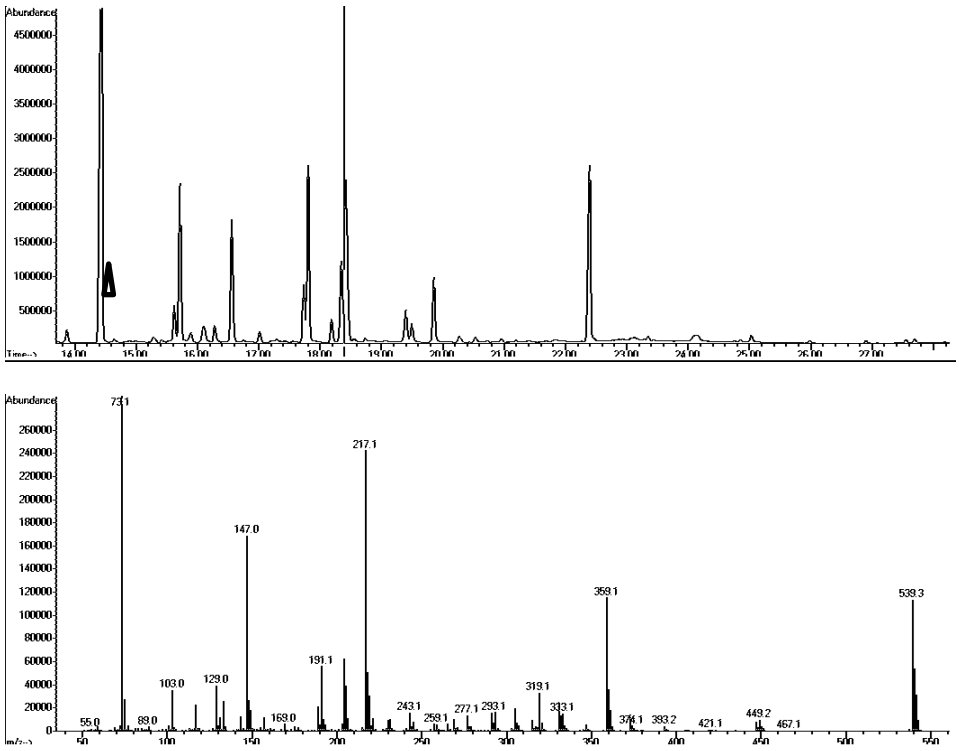

Fig. 3.13. The chromatogram of the TMS derivatives of the dephosphorylated reaction product with **ribose-5-phosphate** as acceptor substrate and **fructose-6-phosphate** as donor (upper part) and the mass spectrum of the TMS derivative of sedoheptulose (lower part). The TMS derivative of the internal standard xylitol is labeled by a triangle and that of sedoheptulose is labeled by a vertical line. The reaction condition is the same as described in Fig 3.10.

The study of Willige *et al.* (2009) showed the transketolse proteins extracted from rehydrated *C. plantagineum* leaves possessed catalytic activity. Based on the possible relationship between transketolase and D-g-D-i-oct in *C. plantagineum* and the fact that D-g-D-i-oct accumulates in

normal growth conditions, it is necessary to explore the possibility that transketolse proteins extracted from hydrated *C. plantagineum* leaves could also catalyze the exchange reaction. Results (Fig. 3.14) showed that the transketolase proteins extracted form hydrated *C. plantagineum* leaves and enriched by 50-70% (w/v) $(NH_4)_2SO_4$ precipitation can also catalyze the exchange reaction.

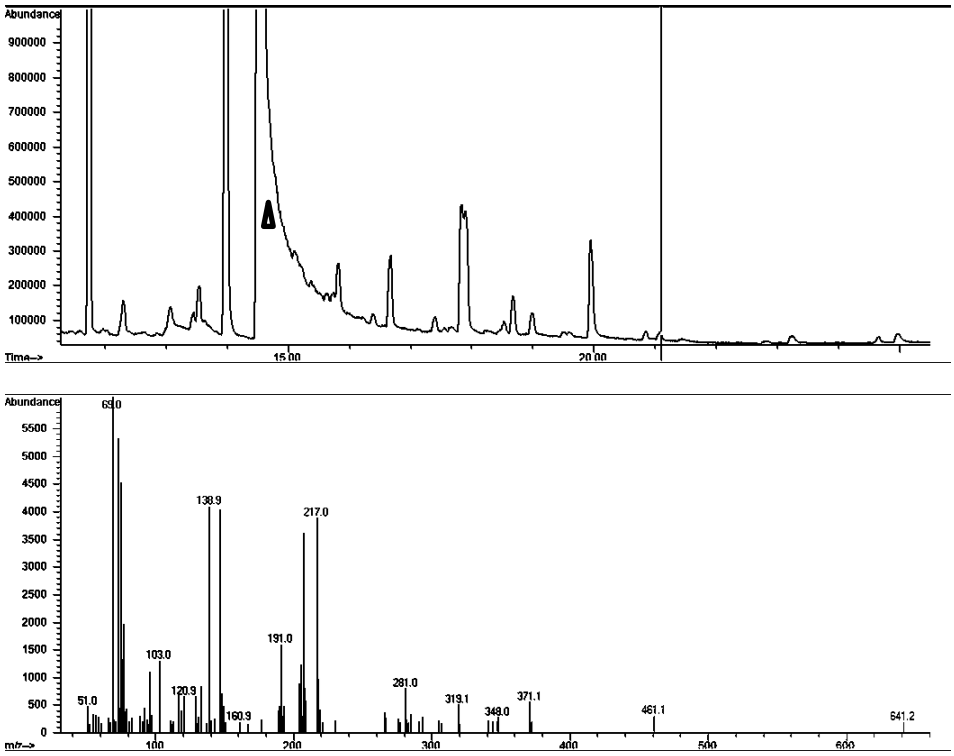

Fig. 3.14. The chromatogram of the TMS derivatives of the dephosphorylated reaction product with **glucose-6-phosphate** as acceptor substrate and **fructose-6-phosphate** as donor (upper part) and the mass spectrum of the TMS derivative of D-g-D-i-oct (lower part). The TMS derivative of the internal standard xylitol is labeled by a triangle and that of D-g-D-i-oct is labeled by a vertical line. The reaction contains 25 µg transketolase proteins extracted from **hydrated** *C. plantagineum* leaves and enriched by 50-70% (w/v) $(NH_4)_2SO_4$ precipitation, 58 mM glycylglycine (pH 7.7), 0.01% (w/v) Na-azide, 0.002% thiamine pyrophosphate, 15 mM $MgCl_2$, 5.3 mM donor and 16 mM acceptor. After 24 h of the catalyzing reaction, sugar phosphates in the product were dephosphorylated using acid phosphatase. The dephosphorylated products were purified on a column containing ion-exchange bed resin AG 501-X8(D) (BIO-RAD). The flow-through fractions were used for GC/MS analysis.

3.15.2 Performance of recombinant transketolases

Like the transketolase proteins extracted from *C. plantagineum* leaves and enriched by $(NH_4)_2SO_4$ precipitation, the recombinant tkt3, tkt7 and tkt10 purified from *E. coli* cells were also used in the enzymatic assays. Results demonstrated that the recombinant tkt3 could not catalyze

the synthesis of D-g-D-i-oct-8-phosphate using hydroxypyruvate as donor substrate and glucose-6-phosphate as acceptor substrate (Fig. 3.15). Specifically, the possible peaks in the gas chromatogram of the TMS derivatives of the dephosphorylated reaction products could not be verified by their mass spectrum to be the TMS derivative of D-g-D-i-oct. When the donor substrate was changed to fructose-6-phosphate, the reaction could also not synthesize D-g-D-i-oct (Fig. 3.17). In contrast, the recombinant tkt3 was capable of catalyzing the formation of sedoheptulose-7-phoshpate using hydroxypyruvate as donor substrate and ribose-5-phosphate as acceptor substrate (Fig. 3.16). When fructose-6-phosphate was used as donor substrate, this reaction was still possible. Sedoheptulose was observed in the dephosphorylated reaction products (Fig.3.18).

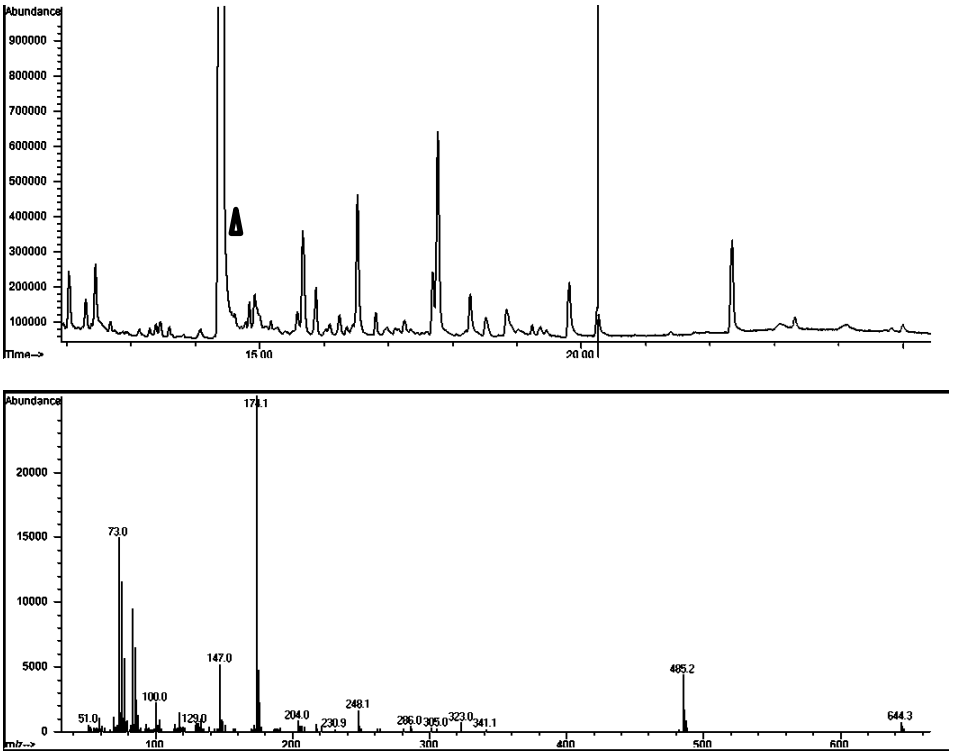

Fig. 3.15. The chromatogram of the TMS derivatives of the dephosphorylated reaction product with glucose-6-phosphate as acceptor substrate and **hydroxypyruvate** as donor (upper part) and the mass spectrum of the TMS derivative of D-g-D-i-oct candidate (lower part). The TMS derivative of the internal standard xylitol is labeled by a triangle and that of D-g-D-i-oct candidate is labeled by a vertical line. The reaction contains 25 µg recombinant **tkt3** proteins purified from *E. coli* cells, 58 mM glycylglycine (pH 7.7), 0.01% (w/v) Na-azide, 0.002% thiamine pyrophosphate, 15 mM $MgCl_2$, 5.3 mM donor and 16 mM acceptor. After 24 h of the catalyzing reaction, sugar phosphates in the product were dephosphorylated using acid phosphatase. The dephosphorylated products were purified on a column containing ion-exchange bed resin AG 501-X8(D) (BIO-RAD). The flow-through fractions were used for GC/MS analysis.

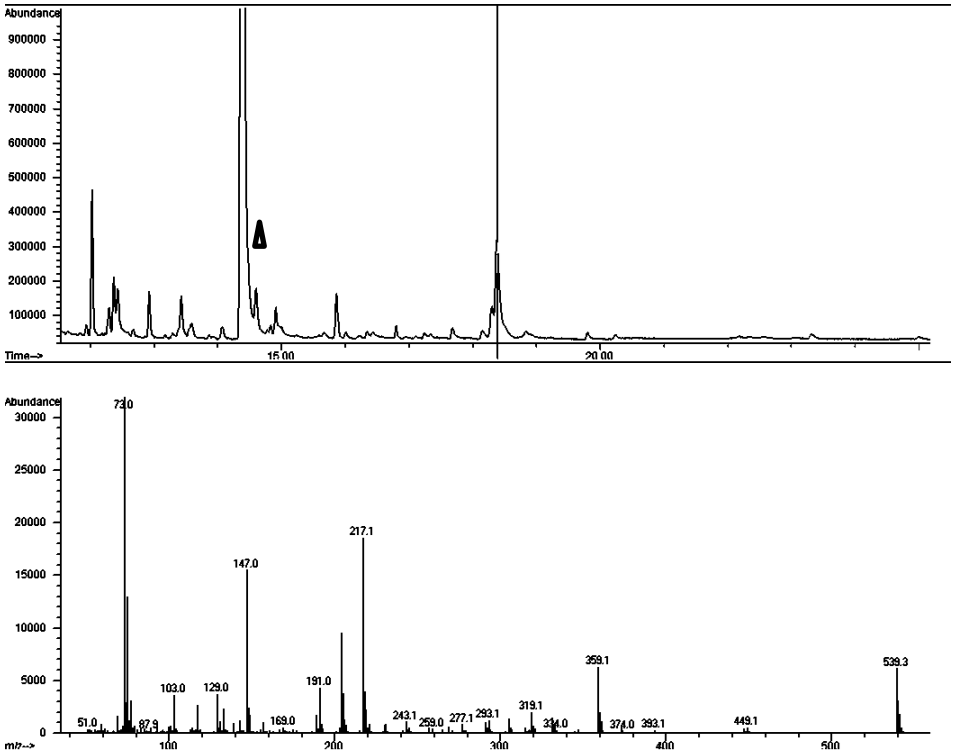

Fig. 3.16. The chromatogram of the TMS derivatives of the dephosphorylated reaction product with **ribose-5-phosphate** as acceptor substrate and **hydroxypyruvate** as donor (upper part) and the mass spectrum of the TMS derivative of sedoheptulose candidate (lower part). The TMS derivative of the internal standard xylitol is labeled by a triangle and that of the sedoheptulose candidate is labeled by a vertical line. The reaction condition is the same as described in Fig. 3.15.

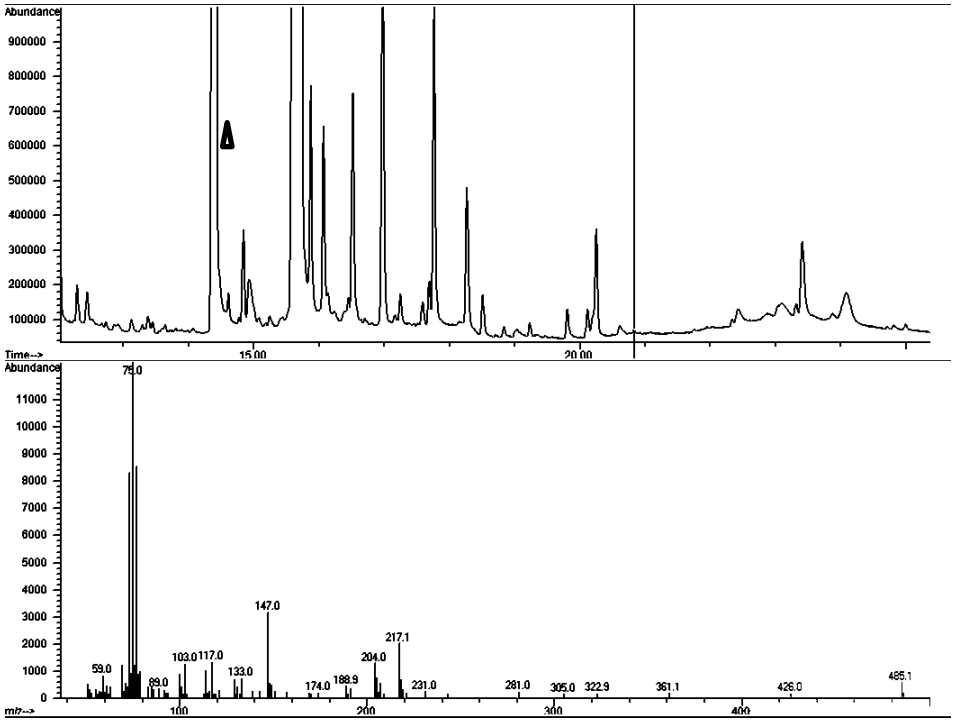

Fig. 3.17. The chromatogram of the TMS derivatives of the dephosphorylated reaction product with **glucose-6-phosphate** as acceptor substrate and **fructose-6-phosphate** as donor (upper part) and the mass spectrum of the TMS derivative of D-g-D-i-oct candidate (lower part). The TMS derivative of the internal standard xylitol is labeled by a triangle and that of the D-g-D-i-oct candidate is labeled by a vertical line. The reaction condition is the same as described in Fig. 3.15.

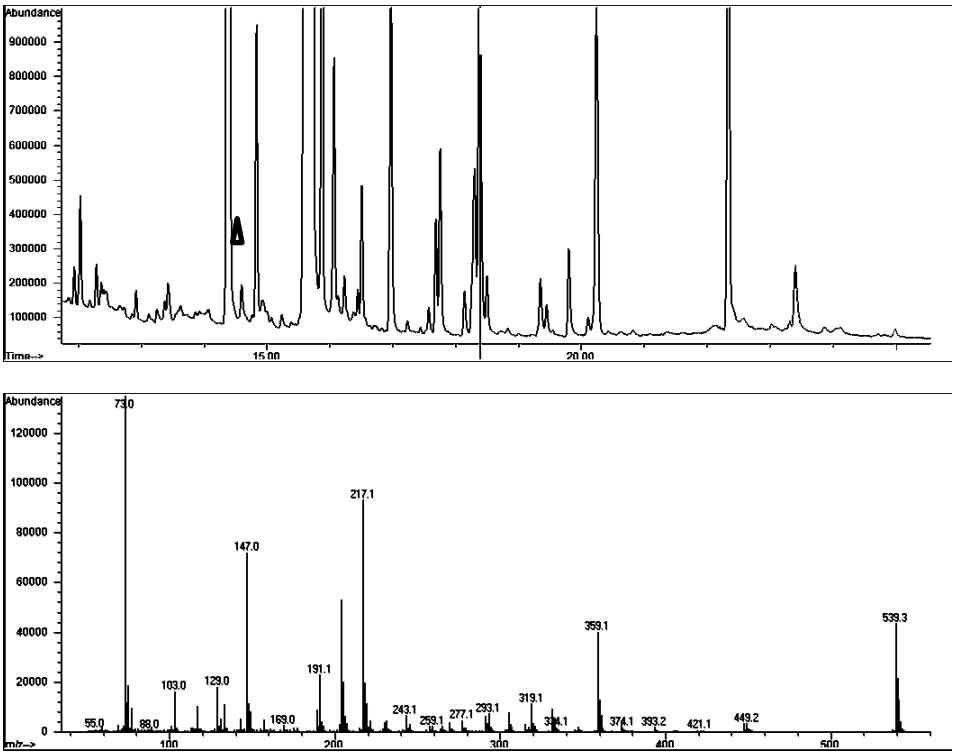

Fig. 3.18. The chromatogram of the TMS derivatives of the dephosphorylated reaction product with **ribose-5-phosphate** as acceptor substrate and **fructose-6-phosphate** as donor (upper part) and the mass spectrum of the TMS derivative of sedoheptulose candidate (lower part). The TMS derivative of the internal standard xylitol is labeled by a triangle and that of the sedoheptulose candidate is labeled by a vertical line. The reaction condition is the same as described in Fig. 3.15.

The results of the reaction using recombinant tkt7 showed that D-g-D-i-oct-8-phosphate was formed in the reaction with hydroxypyruvate as donor substrate and glucose-6-phosphate as acceptor substrate (Fig. 3.19), and sedoheptulose-7-phosphate was formed in the reaction with hydorxylpyruvate as donor substrate and ribose-5-phosphate as acceptor substrate (Fig. 3.20). The reaction with fructose-6-phosphate as donor substrate and glucose-6-phosphate as acceptor substrate catalyzed by the recombinant tkt7 also synthesized D-g-D-i-oct-8-phosphate (Fig. 3.21). Sedoheptulose-7-phosphate was synthesized by the recombinant tkt7 in the reaction that used fructose-6-phosphate as donor substrate and ribose-5-phosphate as acceptor substrate (Fig. 3.22).

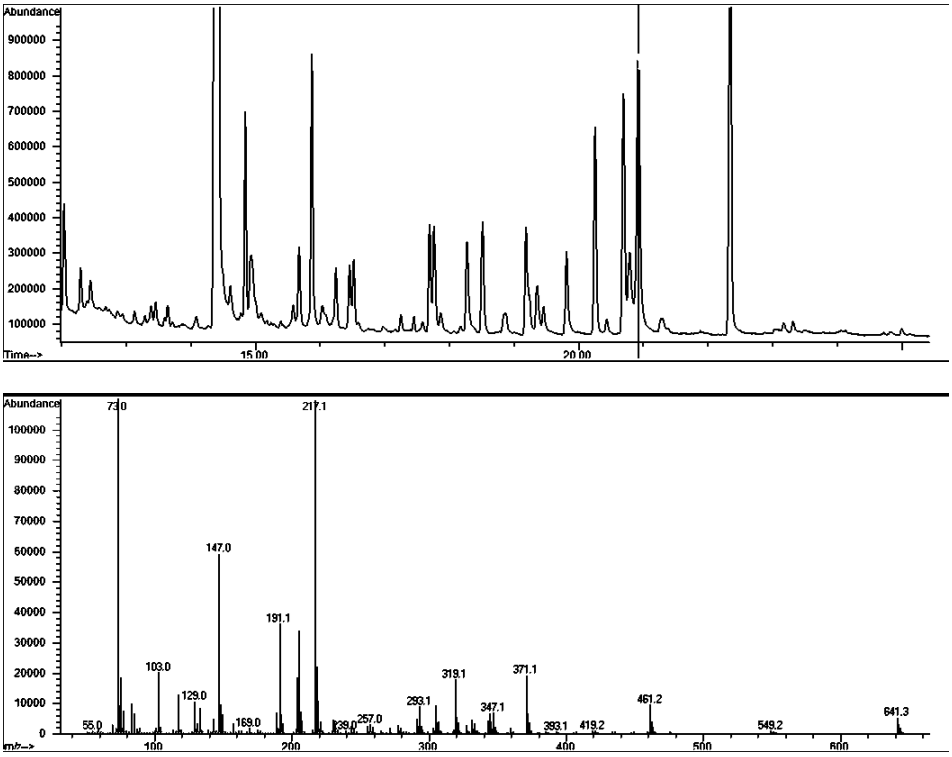

Fig. 3.19. The chromatogram of the TMS derivatives of the dephosphorylated reaction product with **glucose-6-phosphate** as acceptor substrate and **hydroxypyruvate** as donor (upper part) and the mass spectrum of the TMS derivative of D-g-D-i-oct candidate (lower part). The TMS derivative of the internal standard xylitol is labeled by a triangle and that of D-g-D-i-oct candidate is labeled by a vertical line. The reaction contains 25 µg recombinant **tkt7** proteins purified from *E. coli* cells, 58 mM glycylglycine (pH 7.7), 0.01% (w/v) Na-azide, 0.002% thiamine pyrophosphate, 15 mM $MgCl_2$, 5.3 mM donor and 16 mM acceptor. After 24 h of the catalyzing reaction, sugar phosphates in the product were dephosphorylated using acid phosphatase. The dephosphorylated products were purified on a column containing ion-exchange bed resin AG 501-X8(D) (BIO-RAD). The flow-through fractions were used for GC/MS analysis.

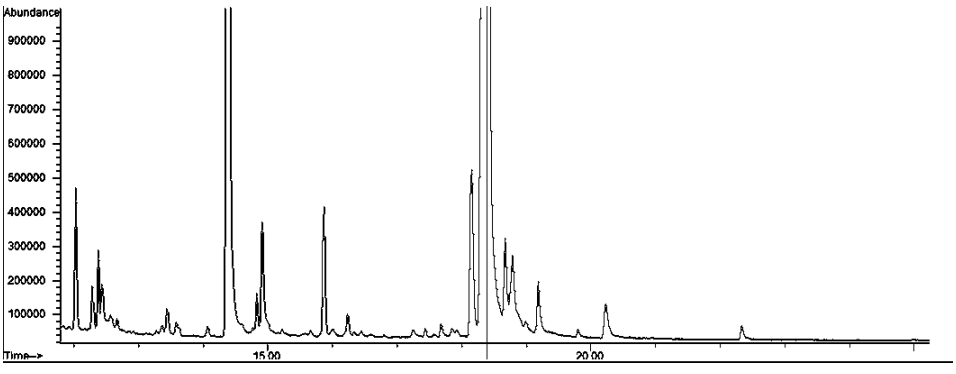

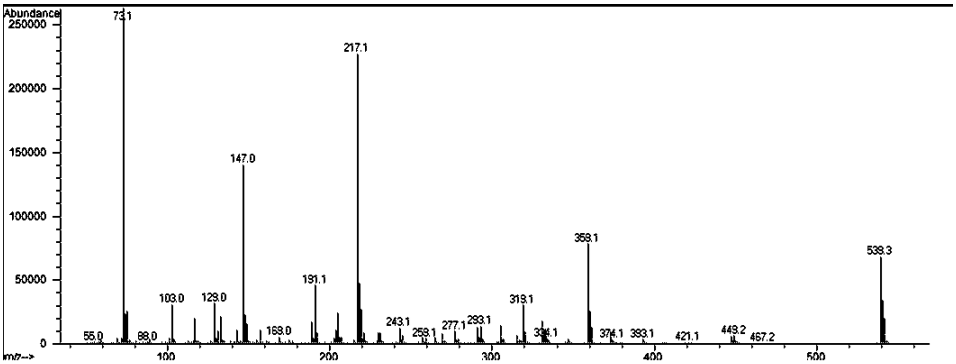

Fig. 3.20. The chromatogram of the TMS derivatives of the dephosphorylated reaction product with **ribose-5-phosphate** as acceptor substrate and **hydroxypyruvate** as donor (upper part) and the mass spectrum of the TMS derivative of the sedoheptulose candidate (lower part). The TMS derivative of the internal standard xylitol is labeled by a triangle and that of sedoheptulose candidate is labeled by a vertical line. The reaction condition is the same as described in Fig. 3.19.

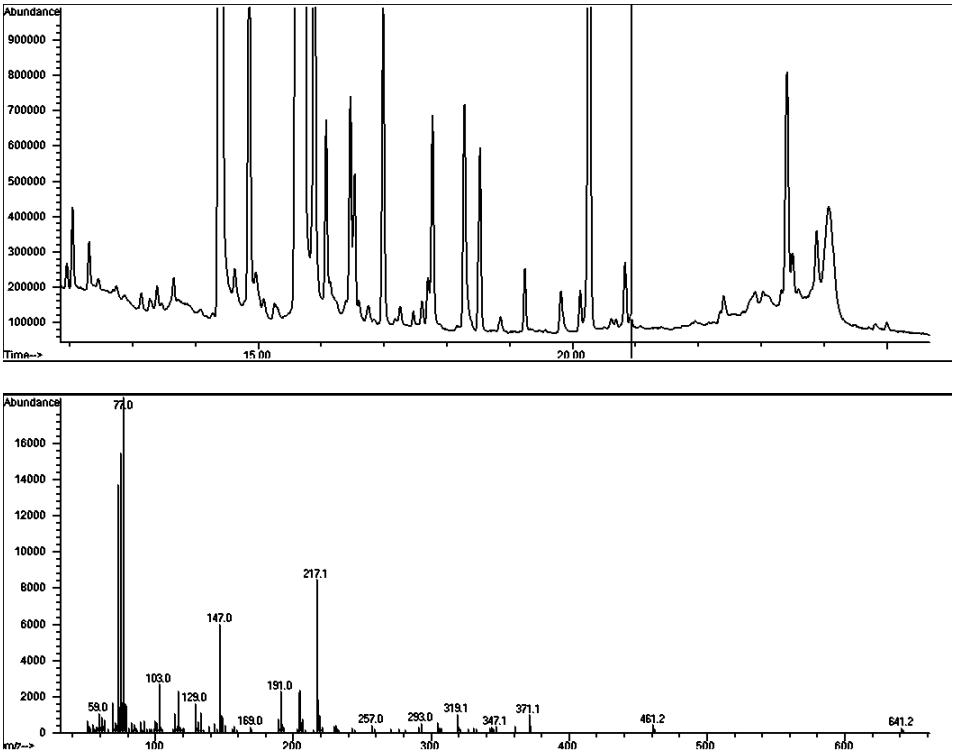

Fig. 3.21. The chromatogram of the TMS derivatives of the dephosphorylated reaction product with **glucose-6-phosphate** as acceptor substrate and **fructose-6-phosphate** as donor (upper part) and the mass spectrum of the TMS derivative of the D-g-D-i-oct candidate (lower part). The TMS derivative of the internal standard xylitol is labeled by a triangle and that of D-g-D-i-oct candidate is labeled by a vertical line. The reaction condition is the same as described in Fig. 3.19.

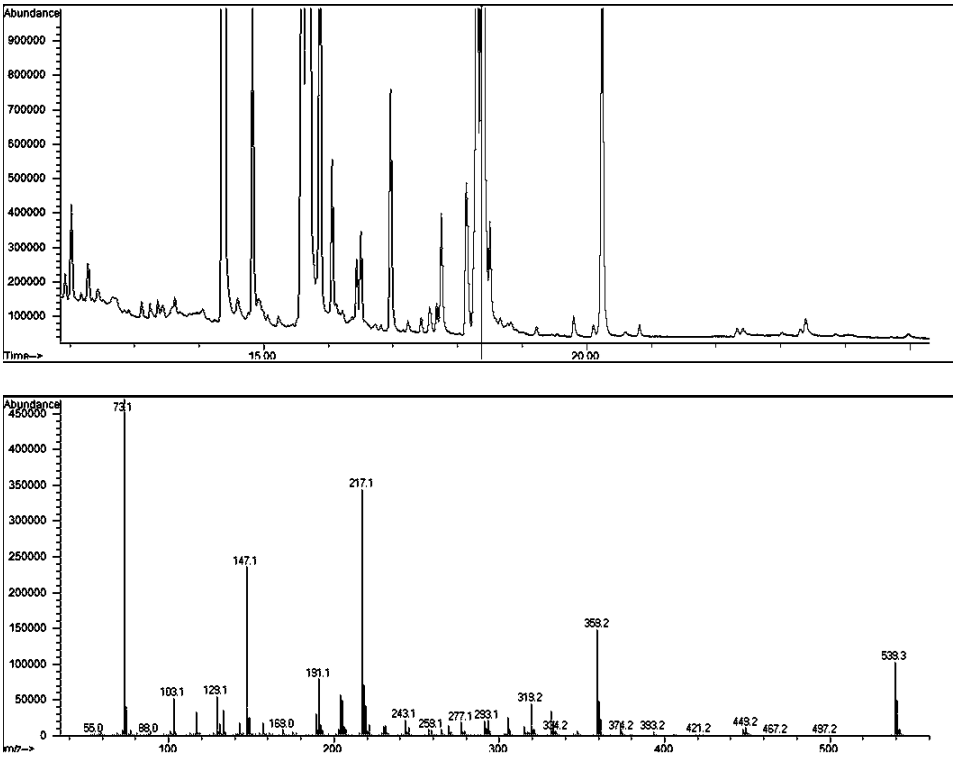

Fig. 3.22. The chromatogram of the TMS derivatives of the dephosphorylated reaction product with **ribose-5-phosphate** as acceptor substrate and **fructose-6-phosphate** as donor (upper part) and the mass spectrum of the TMS derivative of the sedoheptulose candidate (lower part). The TMS derivative of the internal standard xylitol is labeled by a triangle and that of sedoheptulose candidate is labeled by a vertical line. The reaction condition is the same as described in Fig. 3.19.

The enzymatic assay using recombinant tkt10 showed that the recombinant tkt10 had similar function as tkt7. D-g-D-i-oct can be observed in the dephosphorylated products of reactions using glucose-6-phosphate as acceptor substrate and hydroxypyruvate/fructose-6-phosphate as donor substrate (Fig. 3.23 and Fig. 3.25). Sedoheptulose-7-phosphate was synthesized by the recombinant tkt10 in the reaction that used ribose-5-phosphate as acceptor substrate and hydroxypyruvate/fructose-6-phosphate as donor substrate (Fig. 3.24 and Fig. 3.26).

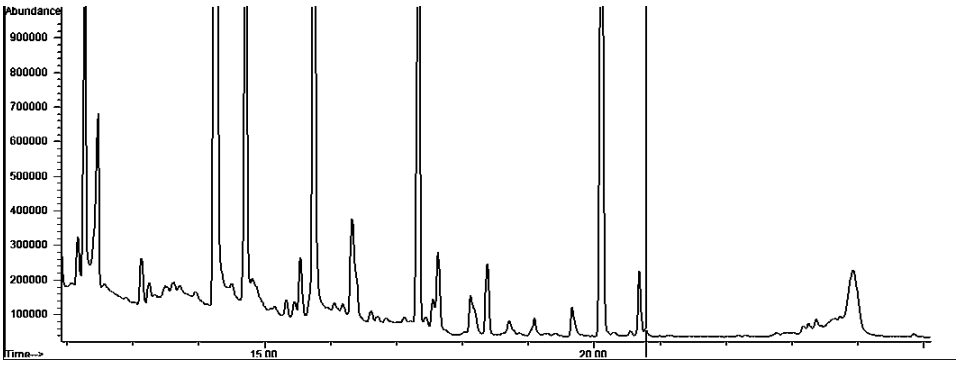

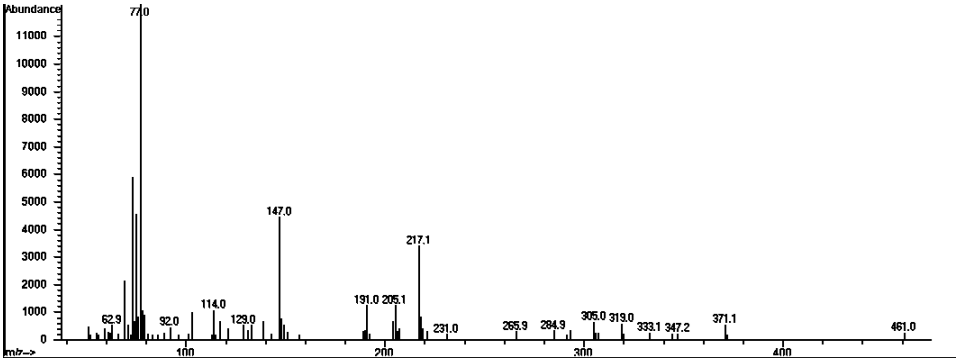

Fig. 3.23. The chromatogram of the TMS derivatives of the dephosphorylated reaction product with **glucose-6-phosphate** as acceptor substrate and **hydroxypyruvate** as donor (upper part) and the mass spectrum of the TMS derivative of the D-g-D-i-oct candidate (lower part). The TMS derivative of the internal standard xylitol is labeled by a triangle and that of D-g-D-i-oct candidate is labeled by a vertical line. The reaction contains 25 µg recombinant **tkt10** protein purified from *E. coli* cells, 58 mM glycylglycine (pH 7.7), 0.01% (w/v) Na-azide, 0.002% thiamine pyrophosphate, 15 mM $MgCl_2$, 5.3 mM donor and 16 mM acceptor. After 24 h of the catalyzing reaction, sugar phosphates in the product were dephosphorylated using acid phosphatase. The dephosphorylated products were purified on a column containing ion-exchange bed resin AG 501-X8(D) (BIO-RAD). The flow-through fractions were used for GC/MS analysis.

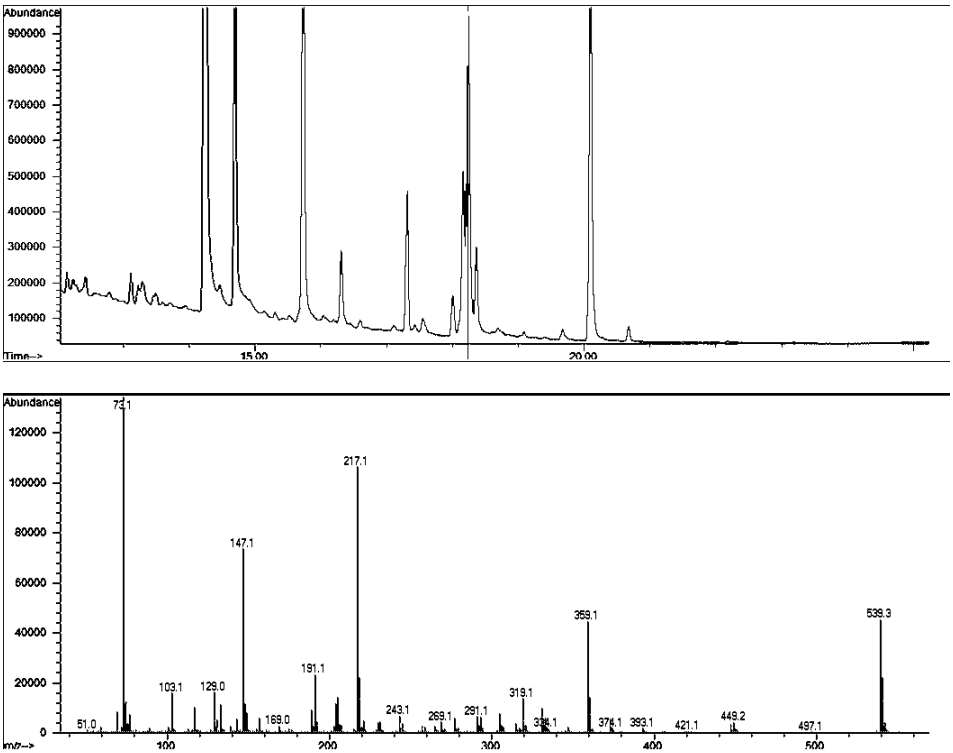

Fig. 3.24. The chromatogram of the TMS derivatives of the dephosphorylated reaction product with **ribose-5-phosphate** as acceptor substrate and **hydroxypyruvate** as donor (upper part) and the mass spectrum of the TMS derivative of the sedoheptulose candidate (lower part). The TMS derivative of the internal standard xylitol is labeled by a triangle and that of the sedoheptulose candidate is labeled by a vertical line. The reaction condition is the same as described in Fig. 3.23.

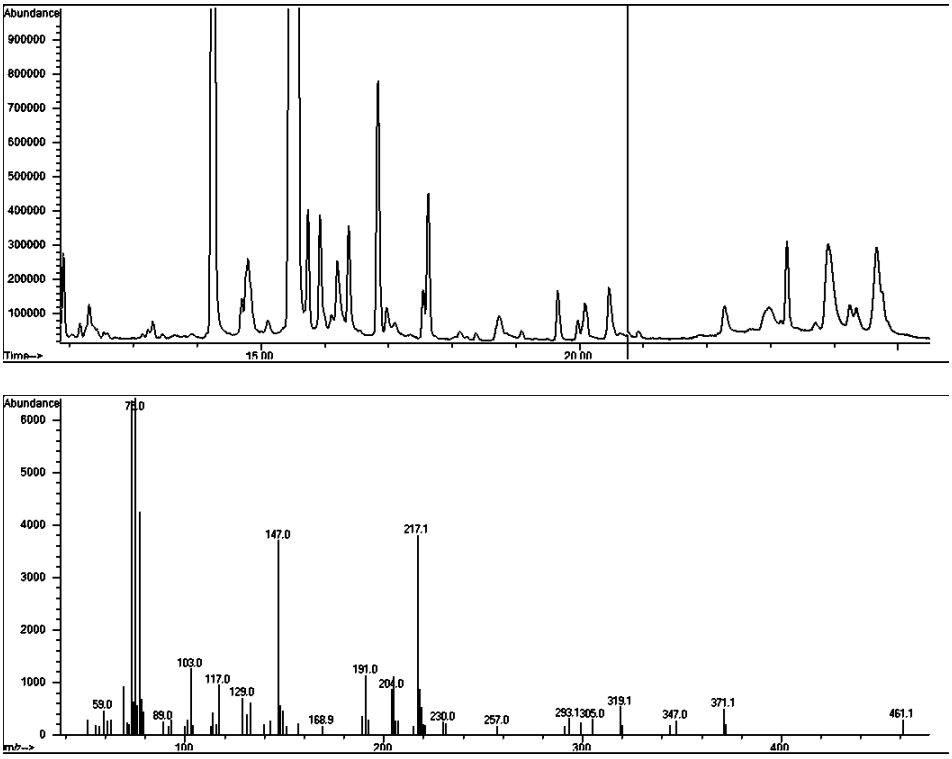

Fig. 3.25. The chromatogram of the TMS derivatives of the dephosphorylated reaction product with **glucose-6-phosphate** as acceptor substrate and **fructose-6-phosphate** as donor (upper part) and the mass spectrum of the TMS derivative of the D-g-D-i-oct candidate (lower part). The TMS derivative of the internal standard xylitol is labeled by a triangle and that of the D-g-D-i-oct candidate is labeled by a vertical line. The reaction condition is the same as described in Fig. 3.23.

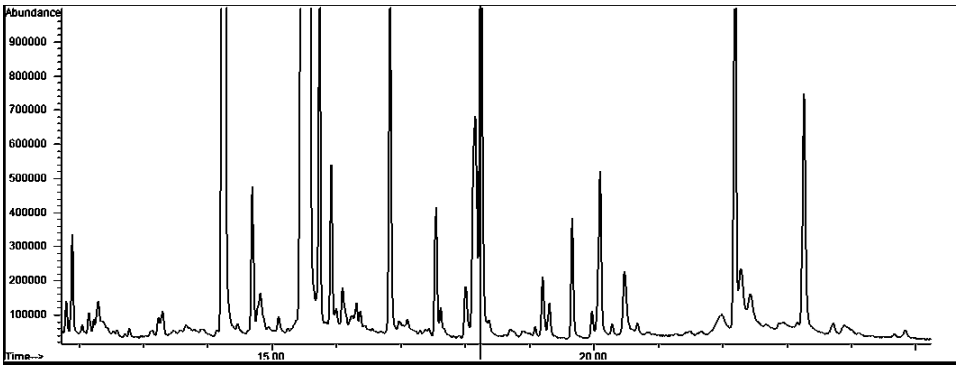

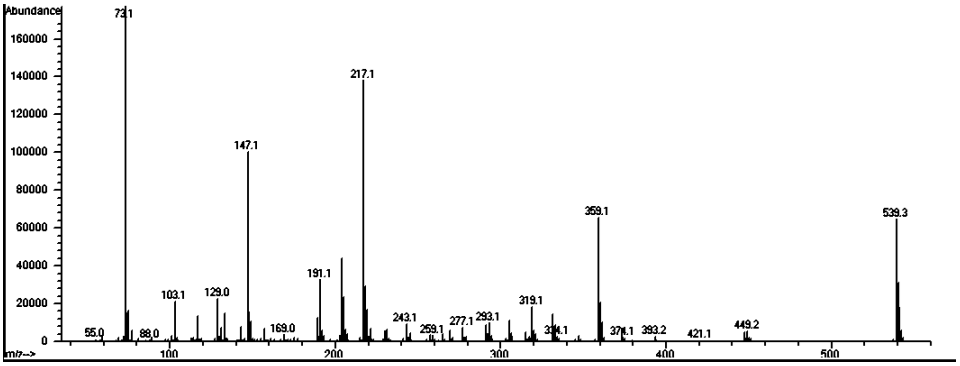

Fig. 3.26. The chromatogram of the TMS derivatives of the dephosphorylated reaction product with **ribose-5-phosphate** as acceptor substrate and **fructose-6-phosphate** as donor (upper part) and the mass spectrum of the TMS derivative of the sedoheptulose candidate (lower part). The TMS derivative of the internal standard xylitol is labeled by a triangle and that of the sedoheptulose candidate is labeled by a vertical line. The reaction condition is the same as described in Fig. 3.23.

The control of enzymatic assays in which proteins purified from E.coli cells transformed with the empty vector pet28a+ and the vector pet28a+ containing the tal fragment showed that neither D-g-D-i-oct-8-phosphate or sedoheptulose-7-phosphate was synthesized in the reactions despite of the presence of donor substrate and acceptor substrate (see supplementary data).

Table 2 Summary of products detected in enzyme reactions using different combinations of acceptor and donor substrates

Enzyme	donor	acceptor	donor	acceptor	donor	acceptor	donor	acceptor
	HP	Glu-6-P	HP	Rib-5-P	Fru-6-P	Glu-6-P	Fru-6-P	Rib-5-P
CK	--		--		--		--	
CKe	--		--		--		--	
TA1	--		--		--		--	
Tkt3	--		Sed		--		Sed	
Tkt7	Oct		Sed		Oct		Sed	
Tkt10	Oct		Sed		Oct		Sed	
Tktp	Oct		Sed		Oct		Sed	

HP refers to hydroxypyruvate, Glu-6-P to glucose-6-phosphate, Rib-5-P to ribose-5-phosphate and Fru-6-P to fructose-6-phosphate. Sed: sedoheptulose; Oct: D-g-D-i-oct; --: no sedoheptulose or D-g-D-i-oct found. CK: reaction without protein; Cke: proteins purified from *E. coli* (BL21) transformed with the empty vector Pet28a+; Ta1: partial fragment of potential transaldolase 1 of *C. plantagineum*; Tktp: the protein enriched from plant leaves of *C. plantagienum*.

3.16 Effect of the transketolase inhibitor oxythiamine

Oxythiamine was proposed as transketolase inhibitor. It was used in this study to explore the function of *C. plantagineum* transketolase. Firstly, the dried *C. plantagineum* leaves were rehydrated in 100 uM oxythiamine solution to analyze the influence of oxythiamine on the sugar content during rehydration. Results (Fig. 3.27) demonstrated that oxythiamine significantly affected the sugar levels of rehydrated *C. plantagineum* leaves. Two days after rehydration, both the levels of fructose and D-g-D-i-oct were lower in leaves rehydrated in oxythiamine solution than those rehydrated in water only.

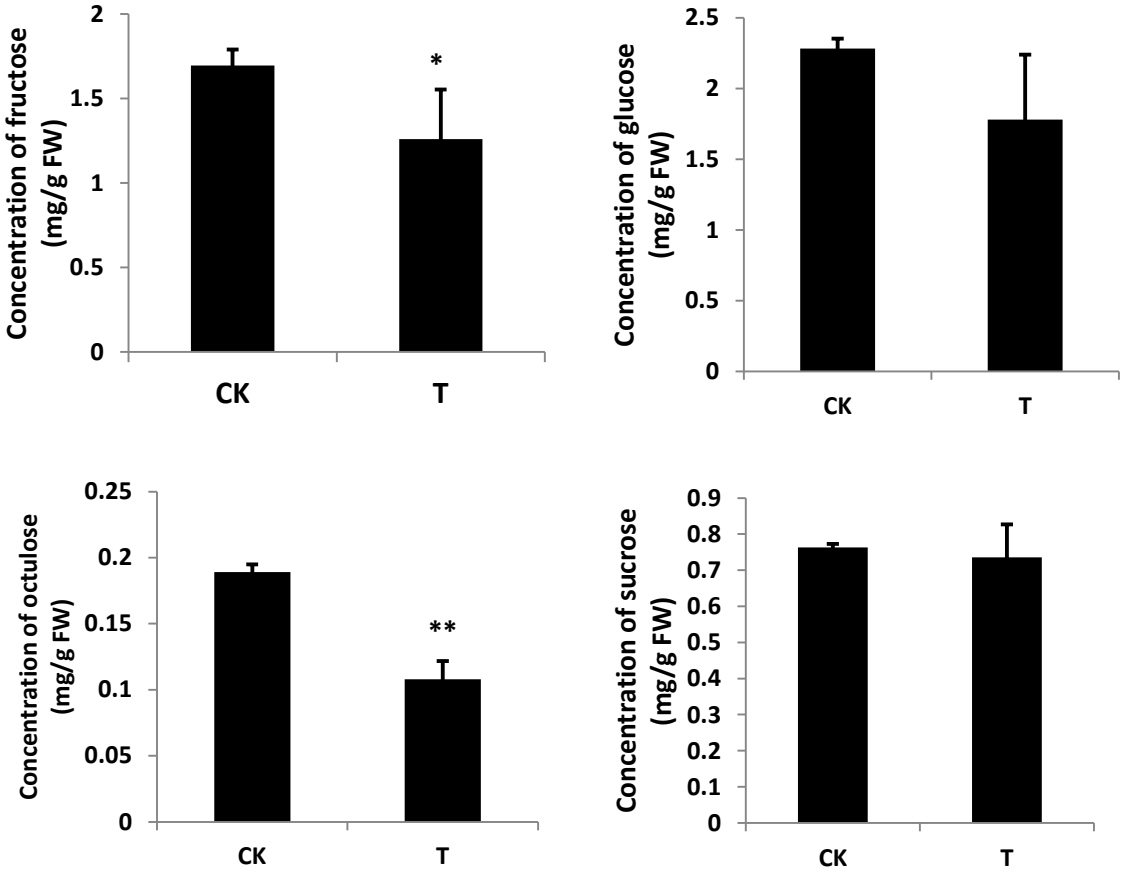

Fig. 3.27. Sugar concentration of *C. plantagineum* leaves that were rehydrated for 2 days in water (CK) or in 100 uM oxythiamine solution (T). Samples were collected 2 days after starting rehydration. (* indicates that the difference is evaluated at $P_{0.05}$ level and ** at $P_{0.01}$ level.)

As there are various enzymes that are thiamin diphosphate-dependent, it is still hard to confirm that transketolase of *C. plantagineum* is inhibited by oxythiamine. Thus the activity of the

transketolase extracted from *C. plantagineum* leaves was tested and oxythiamine was used in the test. The result showed that the activity of *C. plantagineum* transketolase was inhibited by oxythiamine. With higher concentrations of oxythiamine, the inhibition effect was stronger (Fig. 3.28).

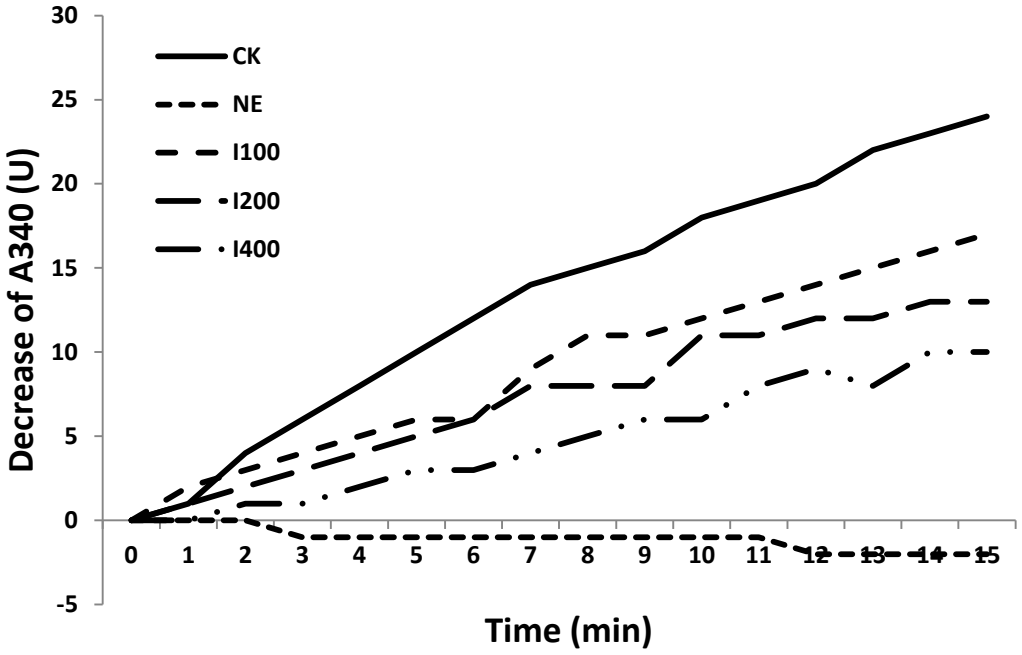

Fig. 3.28. The effect of oxythiamine on transketolase activity. CK: the control reaction; NE: the reaction without transketolase; I100: the reaction with 100 μM oxythiamine; I200: the reaction with 200 μM oxythiamine; I400: the reaction with 400 μM oxythiamine. The activity of transketolase is presented as the decrease of absorption at 340 nm. (1U = 0. 001 absorption decrease)

To further confirm the inhibition effect of oxythiamine, the products of the reaction that contained oxythiamine were analyzed by GC/MS. The result showed that the activity of *C. plantagineum* tkt7 in the reaction without thiamine pyrophosphate was only 12.7% of that with thiamine pyrophosphate. This indicated that *C. plantagineum* tkt7 is thiamine pyrophosphate dependent. In addition, oxythiamine can effectively inhibit the activity of *C. plantagineum* tkt7. One seventieth concentration of oxythiamine could decrease the activity of *C. plantagineum* tkt7 to 11.6% of the normal reaction (Fig. 3.29a and Fig. 3.29b).

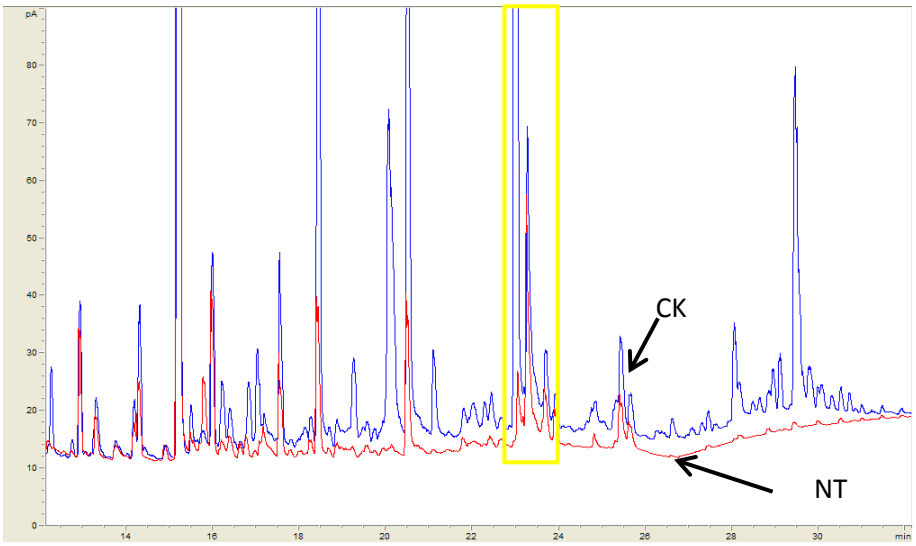

Fig. 3.29a. The chromatogram of the TMS derivatives of the products in reactions with ribose-5-phosphate as acceptor substrate and hydroxypyruvate as donor. The peaks of the TMS derivative of sedoheptulose-7-posphate are labeled by a yellow rectangle. NT refers to the reaction without thiamine pyrophosphate.

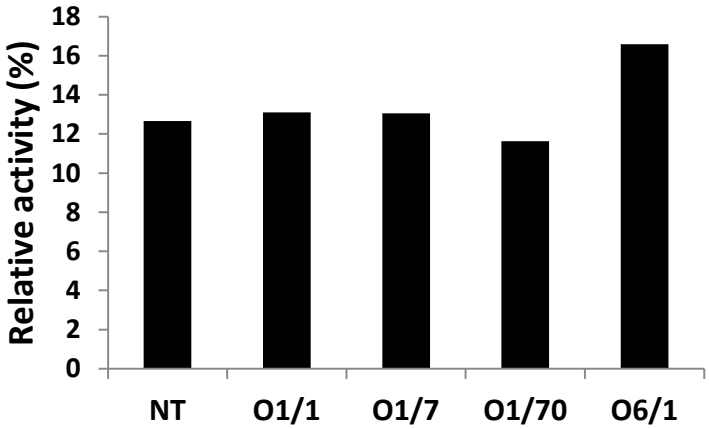

Fig. 3.29b. The inhibition effect of oxythiamine on the formation of sedoheptulose-7-phosphate catalyzed by *C. plantagineum* tkt7. Ribose-5-phosphate and hydroxypyruvate are used as substrates. The products were analyzed by GC/MS. NT: the reaction without thiamine pyrophosphate; O1/1: the reaction with 0.002% TPP and 0.002% oxythiamine; O1/7: the reaction with 0.002% TPP and 0.00033% oxythiamine; O1/70: the reaction with 0.002% TPP and 0.000033% oxythiamine; O6/1: the reaction with 0.002% TPP and 0.002% oxythiamine;

3.17 Study of *E.coli* K12 transketolase A

The transketolase A gene of *E. coli* K12 was inserted into in the vector pET-22b and the vector was transformed into competent cells of *E.coli* DH10B by the providers Professor Georg A. Sprenger at University of Stuttgart. After bacterial culture, the plasmid DNA were isolated and used to transform the competent cells of *E. coli* BL21 (DE3). The recombinant transketolase A

was also purified by immobilized affinity chromatography from IPTG-induced cells of *E. coli* BL21 (DE3) (Fig. 3.30).

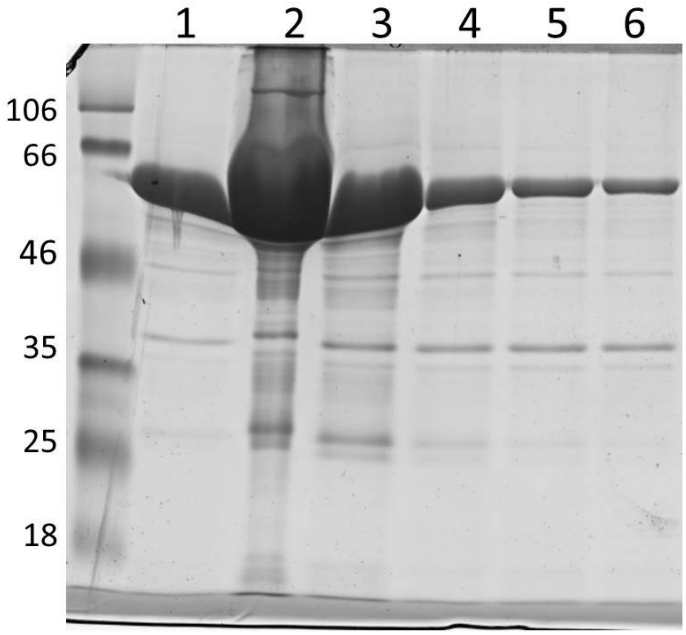

Fig. 3.30. SDS-PAGE of purified transketolase A of *E. coli* K12. Lanes from left to right represent the protein size markers and the eluted fractions 1 to 6. The protein size markers are given in kDa.

The purified recombinant transketolase A of *E. coli* K12 was also used in the enzymatic assays. The results showed that D-g-D-i-oct was observed in the dephosphorylated product of the reaction using hydroxypyruvate as donor substrate and glucose-6-phosphate as acceptor substrate (Fig. 3.31). This indicates that transketolase A of *E. coli* K12 could also catalyze the synthesis of D-g-D-i-oct-8-phosphate. When the acceptor substrate hydroxypyruvate was substituted by fructose-6-phosphate, sedoheptulose was detected in the dephosphorylated reaction products (Fig. 3.32) It is intriguing that ocutolse was also detected in the dephosphorylated product of the reaction using hydroxypyruvate as donor substrate and glucose-6-phosphate as acceptor substrate (Fig.3.33). Similarly, when fructose-6-phosphate was used as the donor substrate and ribose-5-phosphate as acceptor substrate, sedoheptulose was observed in the dephosphorylated reaction products (Fig. 3.34).

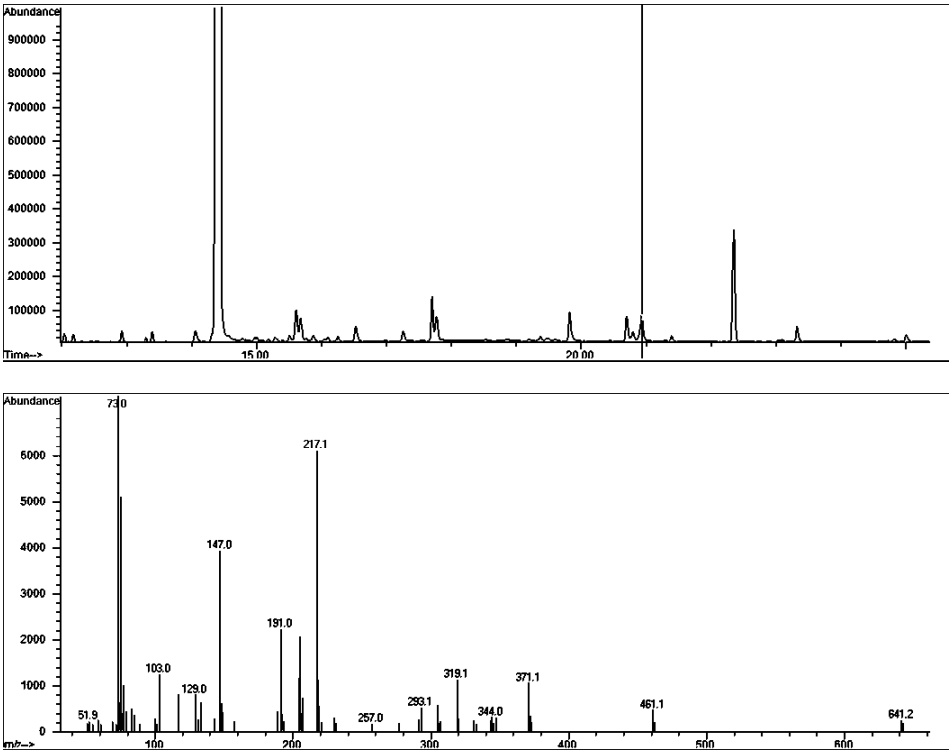

Fig. 3.31. The chromatogram of the TMS derivatives of the dephosphorylated reaction product with **glucose-6-phosphate** as acceptor substrate and **hydroxypyruvate** as donor (upper part) and the mass spectrum of the TMS derivative of the D-g-D-i-oct candidate (lower part). The TMS derivative of the internal standard xylitol is labeled by a triangle and that of the D-g-D-i-oct candidate is labeled by a vertical line. The reaction contains 25 μg recombinant **transketolase A** protein purified from *E. coli* cells, 58 mM glycylglycine (pH 7.7), 0.01% (w/v) Na-azide, 0.002% thiamine pyrophosphate, 15 mM $MgCl_2$, 5.3 mM donor and 16 mM acceptor. After 24 h of the catalyzing reaction, sugar phosphates were dephosphorylated using acid phosphatase. The dephosphorylated products were purified on a column containing ion-exchange bed resin AG 501-X8(D) (BIO-RAD). The flow-through fractions were used for GC/MS analysis.

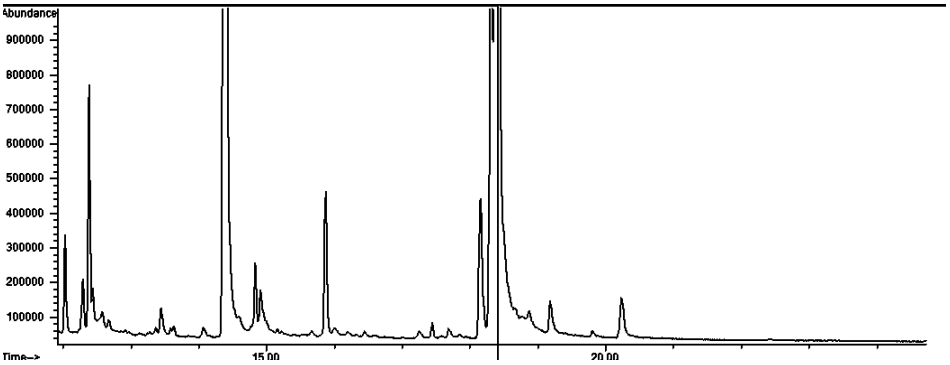

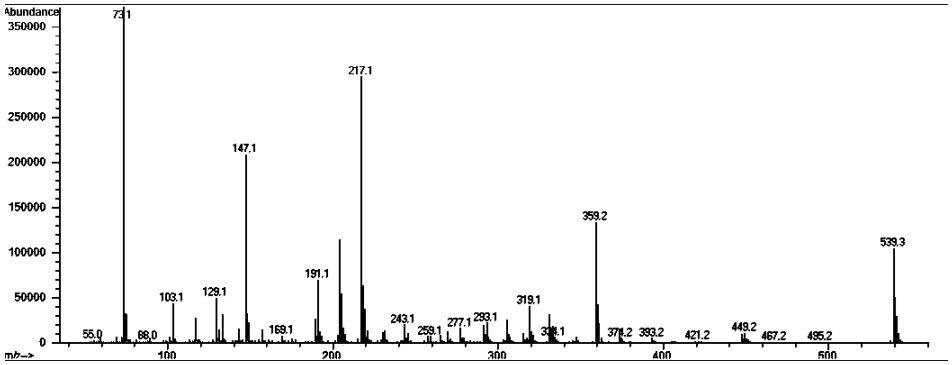

Fig. 3.32. The chromatogram of the TMS derivatives of the dephosphorylated reaction product with **ribose-5-phosphate** as acceptor substrate and **hydroxypyruvate** as donor (upper part) and the mass spectrum of the TMS derivative of the sedoheptulose candidate (lower part). The TMS derivative of the internal standard xylitol is labeled by a triangle and that of the sedoheptulose candidate is labeled by a vertical line. The reaction condition is the same as described in Fig. 3.31.

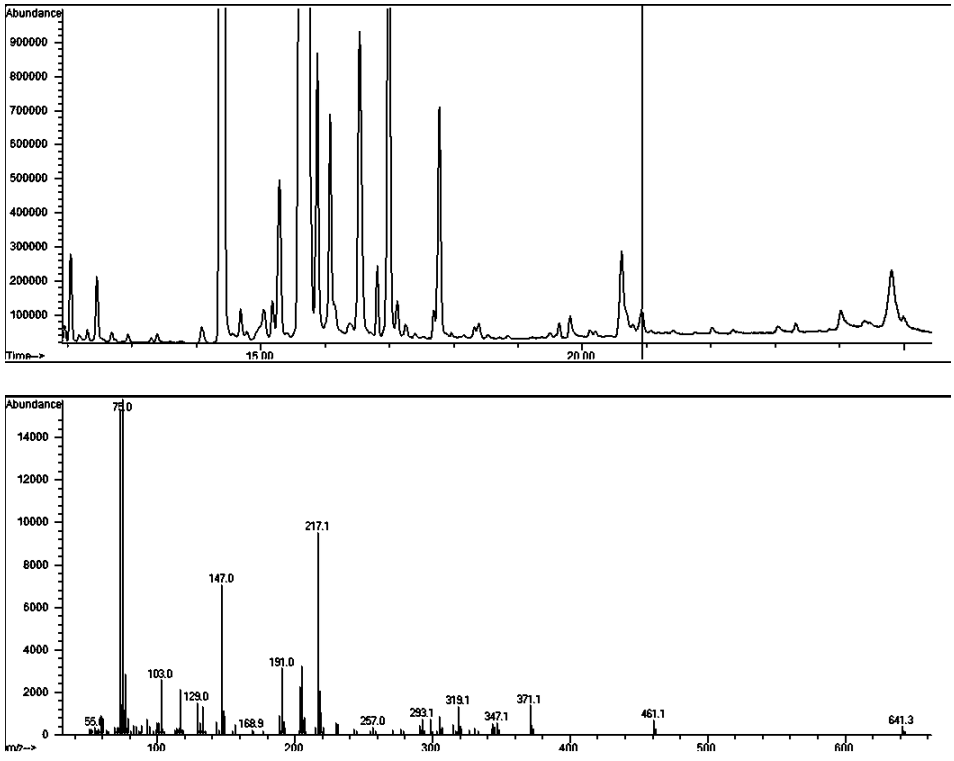

Fig. 3.33. The chromatogram of the TMS derivatives of the dephosphorylated reaction product with **glucose-6-phosphate** as acceptor substrate and **fructose-6-phosphate** as donor (upper part) and the mass spectrum of the TMS derivative of the D-g-D-i-oct candidate (lower part). The TMS derivative of the internal standard xylitol is labeled by a triangle and that of the D-g-D-i-oct candidate is labeled by a vertical line. The reaction condition is the same as described in Fig. 3.31.

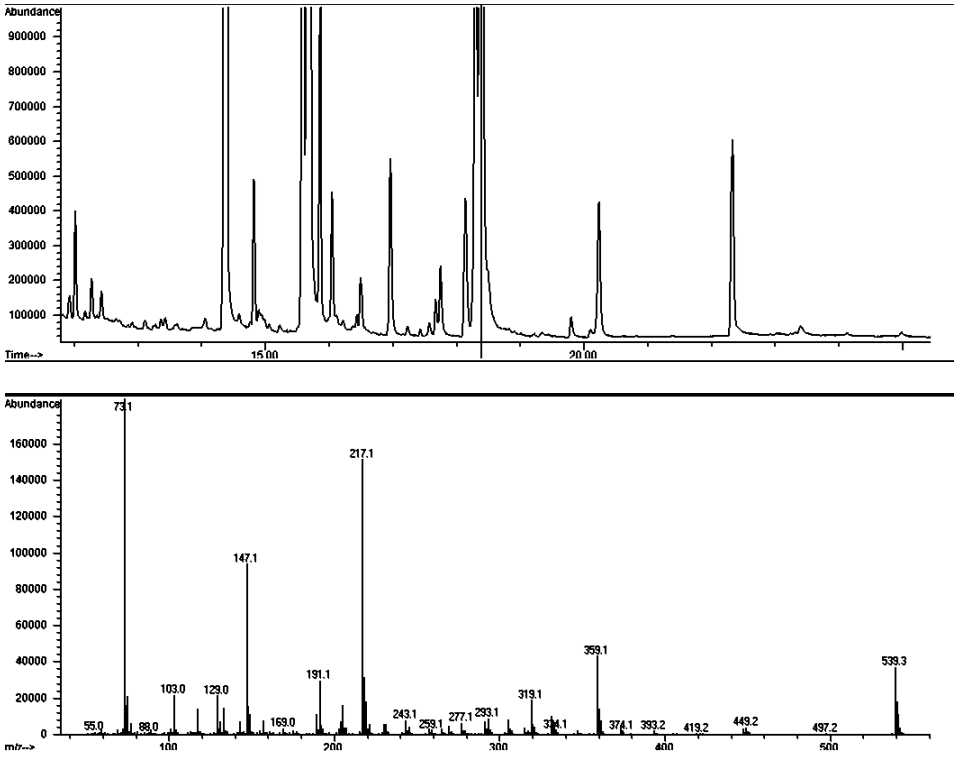

Fig. 3.34. The chromatogram of the TMS derivatives of the dephosphorylated reaction product with **ribose-5-phosphate** as acceptor substrate and **fructose-6-phosphate** as donor (upper part) and the mass spectrum of the TMS derivative of the sedoheptulose candidate (lower part). The TMS derivative of the internal standard xylitol is labeled by a triangle and that of the sedoheptulose candidate is labeled by a vertical line. The reaction condition is the same as described in Fig. 3.31.

3.18 Attempts to clone phosphatase genes

3.18.1 Design of degenerate primers and PCR reactions

The alignment of sugar phosphatase genes from *A. thaliana* (Fig. 4.1) showed that there is a conserved domain that could be found in the genes of fructose-1,6-bisphosphatase, seduheptulose-1,7-bisphosphatase, galactose-1-phosphatase and inositol monophosphatase. Thus it is reasonable to hypothesize that the phosphatase related to D-g-D-i-oct phosphate might also contain this domain. In order to primarily judge whether there are *C. plantagineum* genes containing this domain, the conserved domain was used for a blast in the trasnscriptome of *C. plantagineum*. Results showed that eight contigs were found which have this conserved domain. The retrieved data of these eight contigs suggested that they were all homologues of fructose-1,6-disphosphatase (FBPase) (Table 4.1). This indicates that the conserved domain could be contained in the genes of *C. plantagineum*. So two degenerate primers were designed according

to the sequence of the conserved domain (Table 4.2) and were used with the M13 primers from the vector pbluescript sk- in the PCRs with the *C. plantagineum* cDNA library as template. The products of the PCR reactions that use the SPP001de primer and the M13 reverse primer were named "X1" and that using the SPP002de primer and the M13 forward primer were named "X2" (Fig. 4.2).

Fig. 4.1. Alignment of monosaccharide phosphatase gene sequences from *A. thaliana*. The conserved domain is labeled by a rectangle.

Table 4.1 The contigs of *C. plantagineum* transcriptome containing identified conserved domain

Sequences producing significant alignments	Score (Bits)	E value
contig04025#length=612	31.2	0.002
contig26150#length=601	30.8	0.003
contig02151#length=1310	30.8	0.004
contig06965#length=590	29.3	0.010
contig00164#length=250	26.9	0.022
contig20215#length=594	25.4	0.23
contig24573#length=513	23.5	0.86

Table 4.2 Primers used in PCRs for cloning phosphatase gene sequences with regard to D-g-D-i-oct metabolism.

primers	Sequence 5'-3'
SPP001de	KCTNGGYAGNTNNCCYAG
SPP002de	CANRAGCTRGGNNANCTRGG
M13 forward	TGTAAAACGACGGCCAGT
M13 reverse	CAGGAAACAGCTATGAACC

R: A, G; Y: C, T; M: A, C; K: G, T; S: C, G; W: A, T; H: A, C, T; B: C, G, T; V: A, C, G; D: A, G, T; N: A, C, G, T;

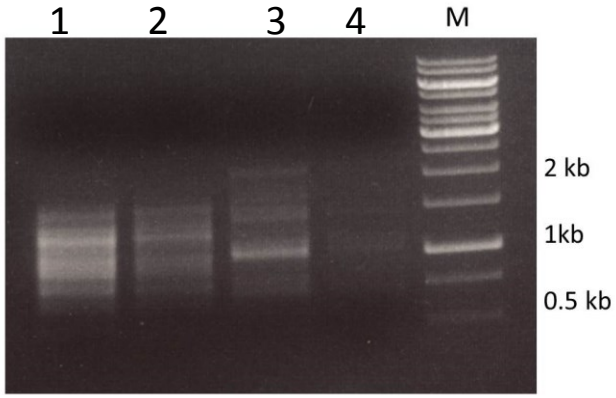

Fig. 4.2. Electrophoresis of X1 (lane 1 and lane 2) and X2 (lane 3 and lane 4). Lane 1 and lane 3 were loaded with 10 μL, lane 2 and lane 4 were loaded with 5 μL.

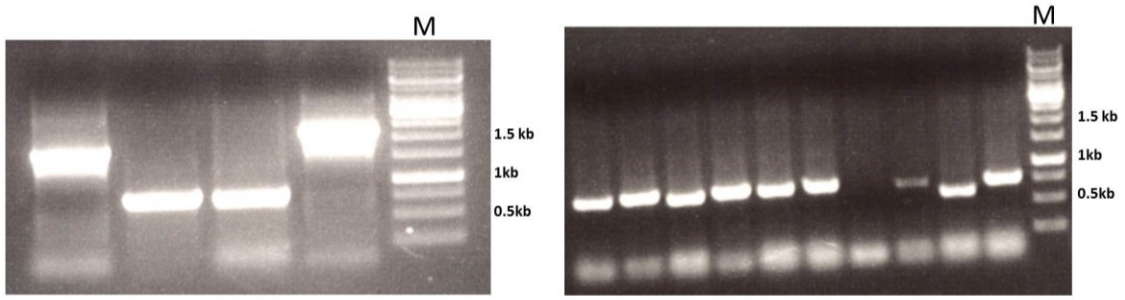

Fig. 4.3. Electrophoresis of the products of colony PCR reactions for selecting the positive transformants of pjet1.2 clones containing X1 inserts.

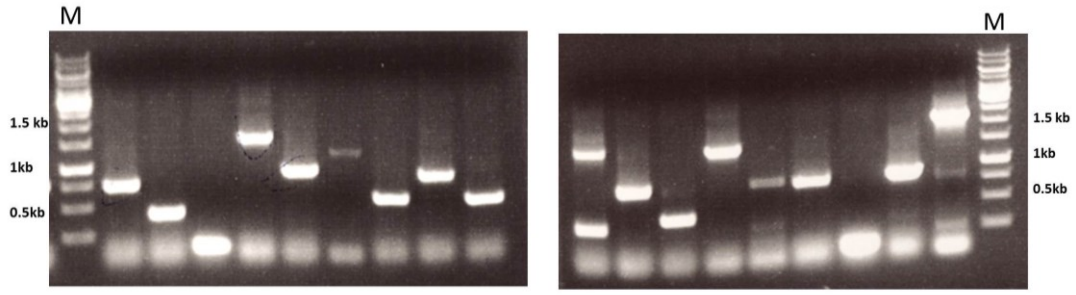

Fig. 4.4. Electrophoresis of the products of colony PCR reactions for selecting positive transformants of pjet1.2 clones containing X2 inserts.

3.18.2 Sequencing of PCR products

Table 4.3 Information of fragments obtained from PCR reactions using degenerate primers

Name	conserved domains detected in blast analysis	The gene which gives highest homologye
X1a	DUF179 super family	uncharacterized protein LOC100261075 [*Vitis vinifera*]
X1b	Cyclophilin superfamily	*Theobroma cacao* Peptidyl-prolyl cis-trans isomerase / cyclophilin-40 (CYP40) / rotamase isoform 9 (TCM_000565)
X1c	Cyclophilin superfamily	Peptidyl-prolyl cis-trans isomerase / cyclophilin-40 (CYP40) / rotamase isoform 1 [*Theobroma cacao*]
X1d	Cyclophilin superfamily	PREDICTED: peptidyl-prolyl cis-trans isomerase CYP40 isoform X2 [*Sesamum indicum*]
X2a	PLN02758	PREDICTED: probable 2-oxoglutarate-dependent dioxygenase AOP1 [*Sesamum indicum*]
X2b	MFS superfamily	PREDICTED: sodium-dependent phosphate transport protein 1, chloroplastic [*Sesamum indicum*]
X2c	SLC5-6-like_sbd superfamily	PREDICTED: metal transporter Nramp3 [*Sesamum indicum*]

The PCR products were successfully ligated into pJET1.2 vector. The construct containing amplified fragments were transformed into *E. coli* DH10B cells (Fig.4.3 and Fig. 4.4). The plasmid DNAs were isolated and the inserts were sequenced. The sequencing results showed that 6 different gene fragments were obtained. The sequences are shown in the supplementary data. Their main information is shown in table 4.3. Though the degenerate primers were feasible in PCRs, the sequencing results did not provide information on possible phosphatase candidate transcripts.

3.19 Influence of phosphate on D-g-D-i-oct accumulation in *C. plantagineum*

Considering that D-g-D-i-oct-8-phosphate is synthesized in the exchange reaction and free D-g-D-i-oct accumulated in leaves of *C. plantagineum*, it is reasonable to assume that there must be a process of dephosphorylation of D-g-D-i-oct-8-phosphate to form D-g-D-i-oct and release phosphorus. Although the enzyme catalyzing this reaction is unknown, we examined the influence of Pi on this reaction. *C. plantagineum* seedlings grown on solid MS medium were transferred to fresh MS medium or MS medium lacking phosphate. Results showed that despite the treatment, the levels of D-g-D-i-oct and sucrose were far higher than those of fructose and glucose. The concentration of D-g-D-i-oct increased in tissues of *C. plantagineum* lacking Pi for 7 days (Fig. 4.5). Although it also increased in the control, the difference was not significant. In contrast, sucrose, as the second most abundant sugar in *C. plantagineum*, increased rapidly and then declined towards the initial level; while in control plants sucrose continuously increased due to the sufficient sucrose supply from fresh medium. Therefore, it is concluded that when sucrose acts as carbon source, phosphate might retard D-g-D-i-oct accumulation and the take-up of sucrose. The phenomenon that the sucrose level of *C. plantagineum* lacking Pi declined three days later could be explained by the rearrangement of carbon metabolism in response to Pi deprivation.

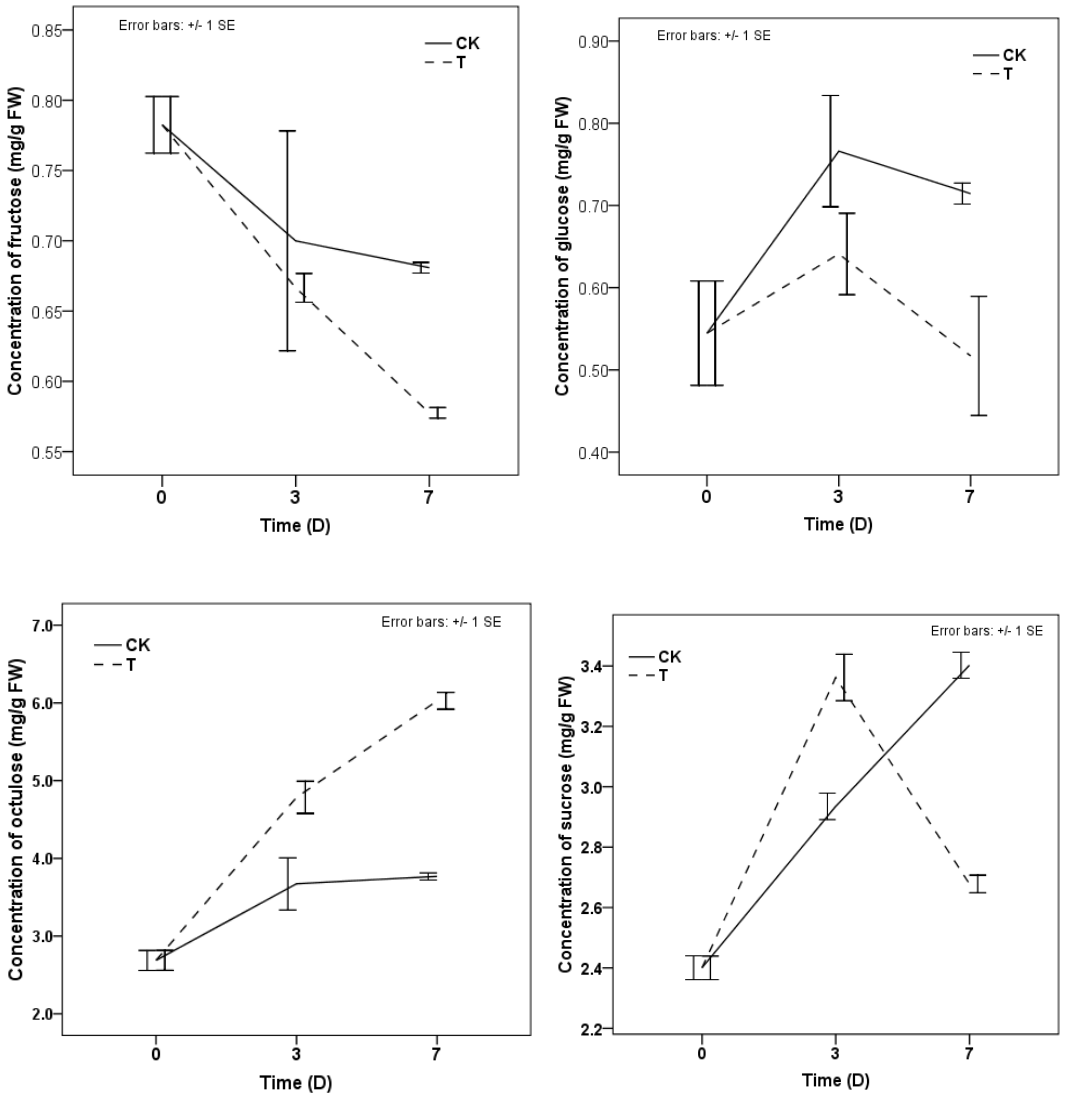

Fig. 4.5. Concentrations of the main sugars in leaves of *C. plantagineum* transferred to fresh MS medium (CK) or phosphate free MS medium (T).

The result of the phosphate assay (Fig. 4.6) showed that the cellular phosphate levels would decline for both the control and phosphate-deprivation treatment and there was no significant difference between them, because the plant seedlings were transferred to fresh medium and the absorption ability of roots needed to recover. Seven days after phosphate deprivation, the phosphate levels of plants were significantly lower than those of the control. This demonstrated that phosphate deprivation could reduce the level of phosphate in cells.

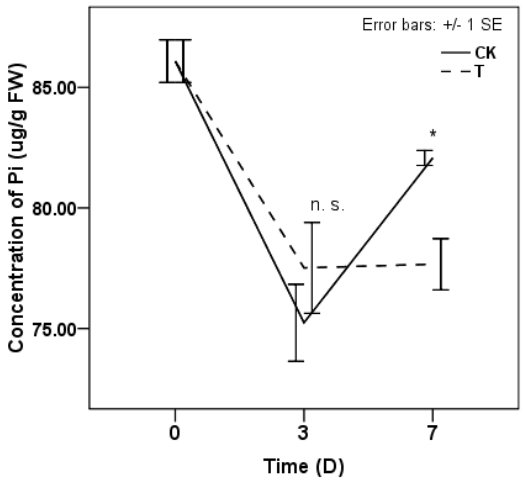

Fig. 4.6. Cellular phosphate levels in in leaves of *C. plantagineum* transferred to fresh MS medium (CK) or phosphate free MS medium (T)

Which influence would the excessive phosphate have on the sugar metabolism in *C. plantagineum*? This question was answered by experiments supplying exogenous phosphate to roots and leaves. After supplying10 mM Pi to roots of *C. plantagineum* plants, it was observed that the levels of D-g-D-i-oct increased continuously (Fig 4.7). When 10 mM Pi was sprayed on leaves of *C. plantagineum* plants (3 times per day), the D-g-D-i-oct level declined 4 days later and rose to the initial level 8 days later (Fig. 4.8). Although the sucrose level of plants treated with additional Pi to roots increased 4 days later and the sucrose level of plants treated by spraying Pi on leaves increased in 8 days after treatment, the sucrose levels were always tiny relative to D-g-D-i-oct.

C. plantagineum plants rely on photosynthesis as energy source. Pi taken up by roots is beneficial for improving photosynthesis, thereby increasing the D-g-D-i-oct level. By analyzing the cellular phosphate content, it is found that the cellular phosphate contents were not changed in leaves though the roots were supplied with phosphate (Fig. 4.9). Compared with phosphate treatment on roots, the foliage application of phosphate significantly increased the levels of cellular phosphate in leaves (Fig. 4.10). While a considerable amount of Pi was present in leaves, the D-g-D-i-oct level decreased rapidly and then recovered to the initial level before the leaves were treated with Pi. These results revealed an adaptive response to the Pi status in sugar metabolism of *C. plantagineum*. This indicated that there might be a phosphatase that is activated by a lack of Pi

and attenuated by Pi excess. It appears that the D-g-D-i-oct level is also influenced by the Pi status.

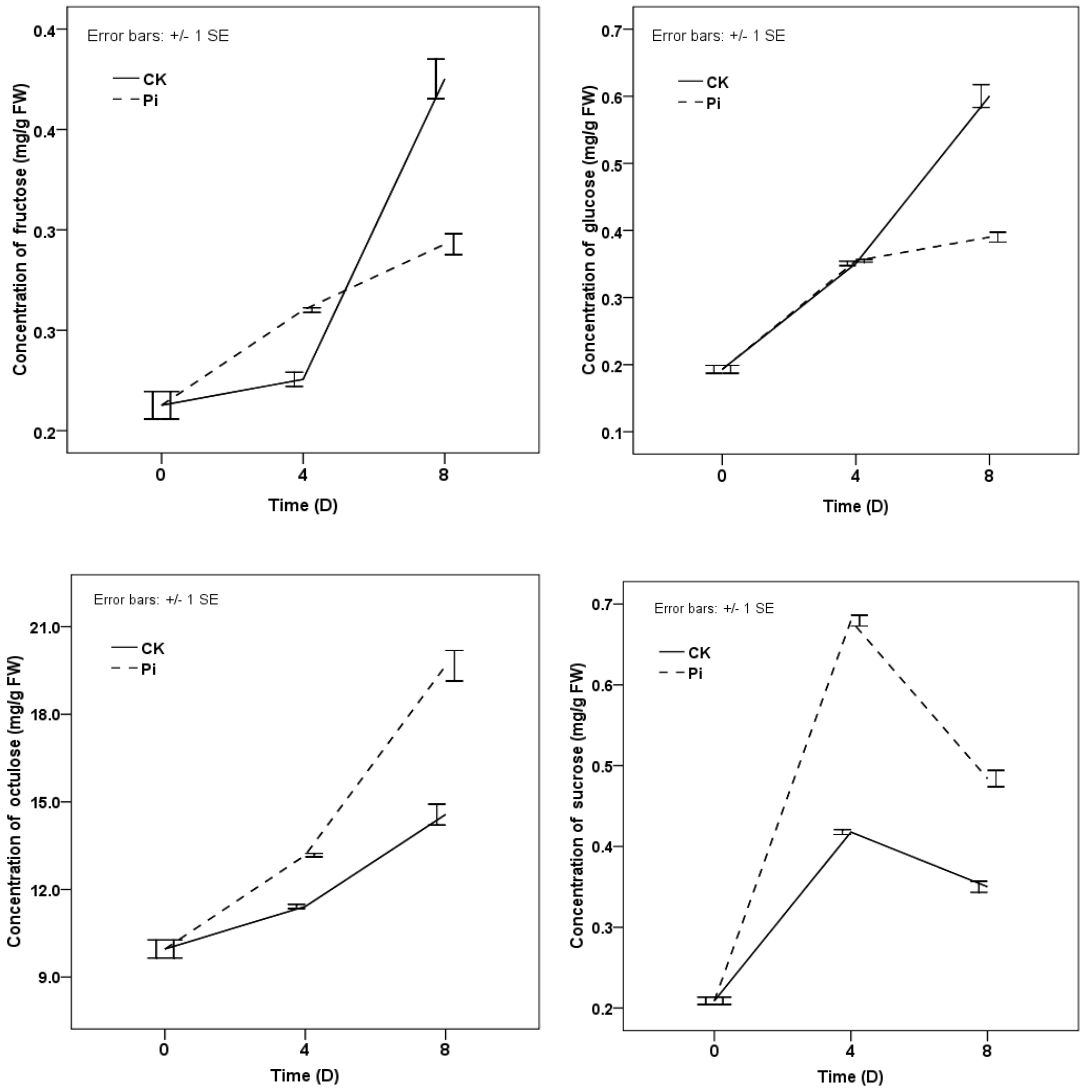

Fig. 4.7. Concentrations of the sugars in leaves treated with 10 mM sodium phosphate supplied in hydroponic solution (Pi) and normal nutrient supply (CK). *C. plantagineum* plants were supplied with nutrient solution once a week and irrigated with wate or 10 mM sodium phosphate three times per week.

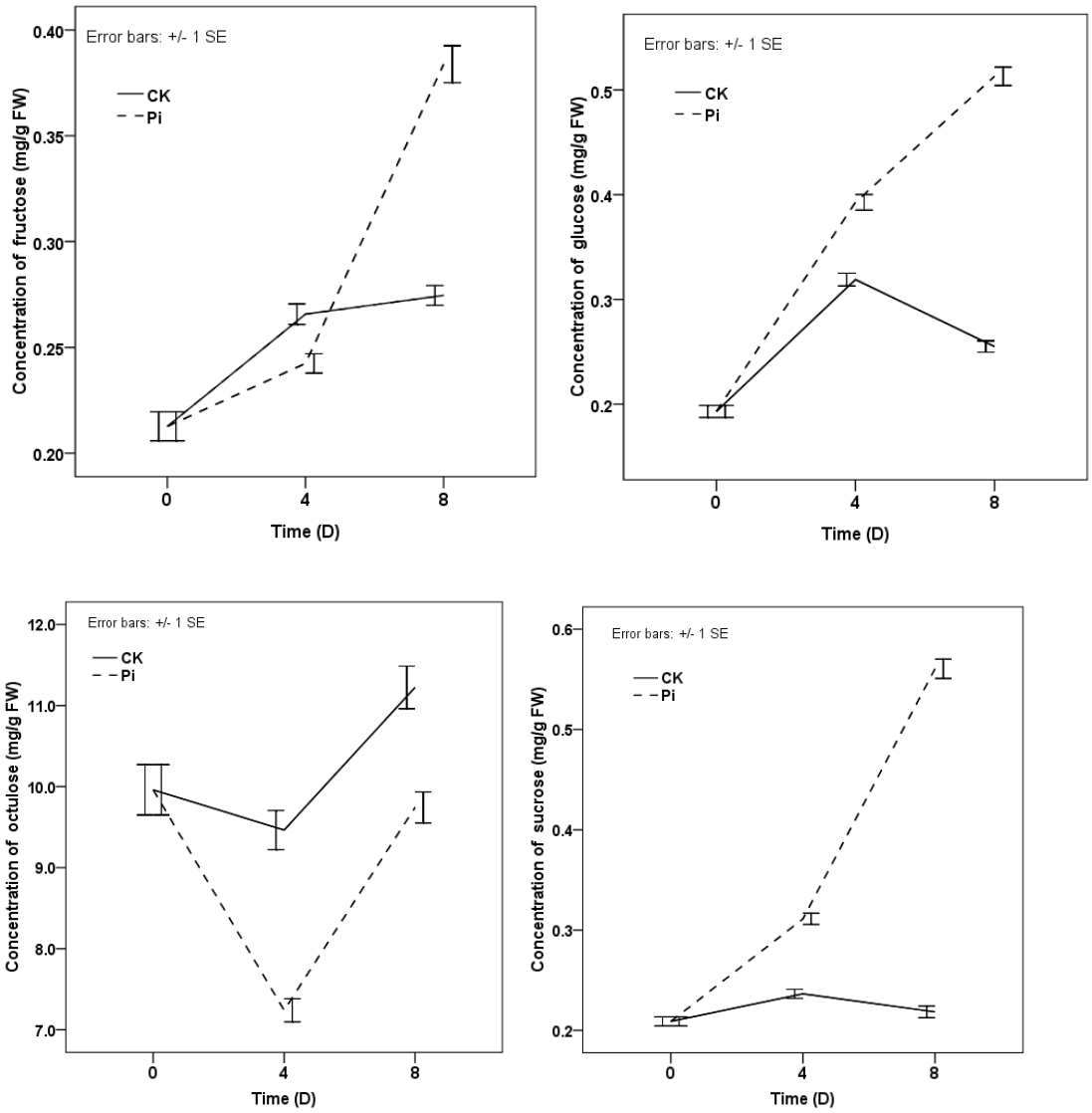

Fig. 4.8. Concentrations of the main sugars in leaves treated with 10 mM sodium phosphate (Pi) and water (CK). *C. plantagineum* plants were supplied with nutrient solution once a week and irrigated with water once a week. The leaves of *C. plantagineum* were sprayed with water or 10 mM sodium phosphate three times per day.

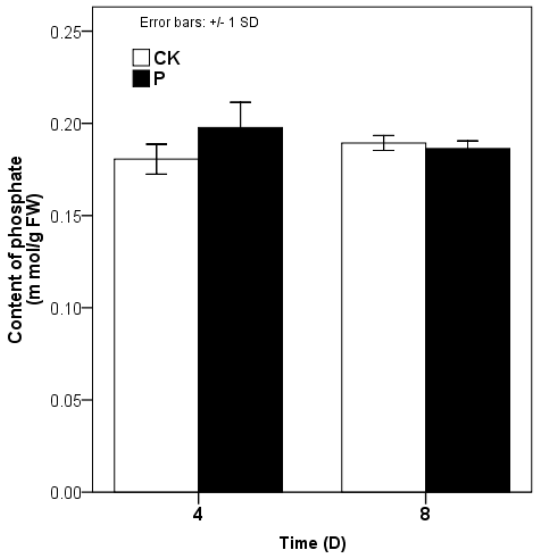

Fig. 4.9. Cellular phosphate levels in leaves treated with 10 mM sodium phosphate supplied in hydroponic solution (P) and normal nutrient supply (CK). *C. plantagineum* plants were supplied with nutrient solution once a week and irrigated with wate or 10 mM sodium phosphate three times per week.

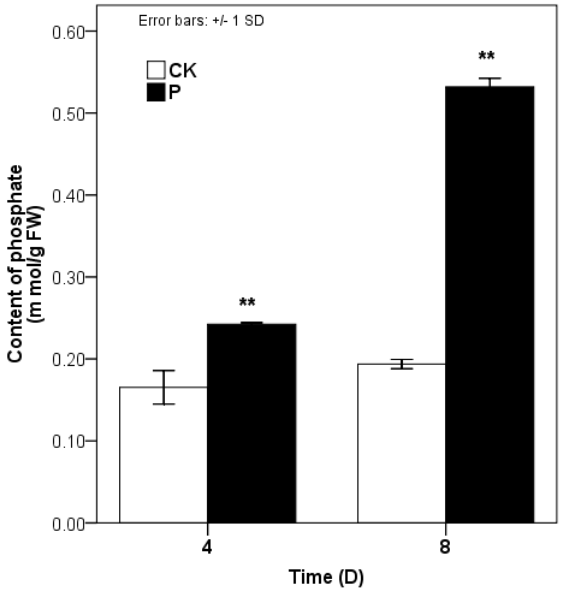

Fig. 4.10. Cellular phosphate levels in leaves treated with 10 mM sodium phosphate (Pi) and water (CK). *C. plantagineum* plants were supplied with nutrient solution once a week and irrigated with water once a week. The leaves of *C. plantagineum* were sprayed with water or 10 mM sodium phosphate three times per day.

Chapter 4 Discussion and conclusions

4.1 Discussion

Desiccation tolerance and senescence

As the main energy source carbohydrates affect plant development strongly. Experimental results showed that there are significant differences of the carbohydrate status between old and young plants of *C. plantagineum*. Sufficient carbohydrates are the preconditions for desiccation tolerance but are not sufficient to ensure desiccation tolerance. This is confirmed by the performance of outer leaves of old plants that possessed D-g-D-i-oct at the same level as inner leaves of old plants, but would not survive desiccation. Martinelli *et al.* (2007) also showed that older leaves of the resurrection plant *Sporobolus stapfianus* were desiccation-sensitive whereas younger leaves were desiccation-tolerant. Most leaves of the resurrection grass *Eragrostis nindensis* are tolerant to desiccation, but the oldest outermost leaf on a tiller is not tolerant to desiccation (Vander Willigen *et al.*, 2003). Starvation (or dark treatment) leads directly to carbohydrate deficiency in plants (Yu, 1999) and can be used to artificially induce senescence (Buchanan-Wollaston *et al.*, 2005). The starvation-induced senescence results in the loss of plant desiccation tolerance in this study. Although the mechanisms underlying the loss of desiccation tolerance are still unknown (Griffiths *et al.*, 2014), it could be speculated that desiccation tolerance is regulated by senescence. Desiccation tolerance involves the protection of chloroplasts, membranes and macromolecules (Dinakar and Bartels, 2013; Gechev *et al.*, 2012). In contrast, senescence is an active degenerative process that begins with chloroplast dismantling followed by degradation of macromolecules such as chlorophyll, proteins, lipids, and RNA (Besseau *et al.*, 2012). Senescence remobilizes nutrients from senescing leaves to reproductive and developing structures and is therefore of pivotal importance for overall plant development, while desiccation tolerance only allows plants to survive periods of extreme water deficiency.

Besides the differences in carbohydrates and morphological performance (the old outer leaves of *C. plantagineum* plants will naturally die), there are differences in gene expression levels between senescent and vigorous plants. The expression of SRG1, SRG2, SRG3 and SRG4 are all induced by dehydration (Rodriguez *et al.*, 2010); they show differential expression patterns in

old and young plants. The SnRK (Rolland *et al.*, 2006) and the HXK (Dai *et al.*, 1999; Xiao *et al.*, 2000) of Arabidopsis participate in the regulation of a range of processes regarding signaling and gene expressions. As a typical member of late embryogenesis abundant proteins (LEAs), *CDeT11-24* is involved in desiccation tolerance (Petersen *et al.*, 2012), it was expressed higher in outer leaves than in inner leaves and higher in young plants than in old plants. Compared to the carbohydrate status, gene expressions reflected the influence of senescence on desiccation tolerance. The differences of the gene expression programs and carbohydrate status indicate that in the development of organs or plants, different preparation are adopted for possible dehydration stress. In this context, relative to desiccation tolerance, leaf senescence is a strategy for resurrection plants to optimize the overall use of energy and resources.

Sucrose is an important metabolite during desiccation tolerance in plants (Bianchi *et al.*, 1991; Drennan *et al.*, 1993; Müller *et al.*, 1997). Does the rate of sucrose formation reflect on the ability of plants to survive desiccation? In this study the sucrose accumulating rate of desiccation-tolerant inner leaves in young plants was the same as that of desiccation-sensitive outer leaves in starved plants. This means that sucrose synthesis does not correlate with the ability of plant to survive desiccation. Cooper and Farrant (2002) found that sucrose substantially accumulated in *Craterostigma wilmsii* only during the late stages of dehydration (below 25% RWC). But this could not explain why the sucrose accumulating rates are not correlated with D-g-D-i-oct levels. Sucrose synthesis in the early stage of dehydration might only act as sugar signaling. Another possible explanation is that sucrose synthesis is rapidly regulated by water stress before senescence-induced nutrient distribution and leaf death.

D-g-D-i-oct metabolism

D-g-D-i-oct and sucrose act as the main sugars in hydrated and dehydrated conditions, respectively. To explore the relationship between them, leaf tissues were supplied with excess sucrose in hydrated conditions. Results showed that relative to glucose and fructose, D-g-D-i-oct did not accumulate to high levels when *C. plantagineum* plants are supplied with exogenous sucrose. In contrast, in the rehydration of dried *C. plantagineum* plants, all sucrose is nearly converted to D-g-D-i-oct with little fructose and glucose remaining in the leaves (Bianchi *et al.*, 1991). This suggests that the reversible conversion between D-g-D-i-oct and sucrose is regulated

by a mechanism that is related to the water status of the plant. Experiments revealed that the formation of D-g-D-i-oct in leaf tissues supplied with exogenous sucrose was enhanced by light, suggesting that the pathways of D-g-D-i-oct metabolism might interact with photosynthesis or the enzymes catalyzing the formation of D-g-D-i-oct are light-regulated. Previous studies also showed that light plays an important role in resurrection plants regarding gene expression (Bartels *et al.*, 1992) and sucrose accumulation (Farrant *et al.*, 2003). Leaves of *Craterostigma wilmsii* dehydrated in the dark accumulated only half the amount of sucrose compared to those in the light, indicating that photosynthesis, and/or a light-regulated gene expression is necessary for sucrose accumulation during dehydration (Farrant *et al.*, 2003).

Paraquat accepts electrons from photosystem I and transfers them to molecular oxygen, producing reactive oxygen species (Bus and Gibson, 1984). In our study, the level of D-g-D-i-oct is strongly reduced in the presence of paraquat without exogenous sucrose supply and this process was enhanced by light. This shows that D-g-D-i-oct was consumed to cope with ROS produced by paraquat. When leaf tissues were supplied with sucrose in the absence of paraquat, the levels of D-g-D-i-oct increased. With the supply of sucrose and the presence of paraquat, sucrose levels did not change in the dark or in the light, while the D-g-D-i-oct level declined in the presence of light. In the experiments the exogenous sucrose level was excessive compared to the sucrose level in leaf tissue of *C. plantagineum*. Thus it is proposed that D-g-D-i-oct is produced from exogenous sucrose and would be consumed by the ROS produced by paraquat. This also suggests that it is important to maintain a certain amount of D-g-D-i-oct for *C. plantagineum* plants to deal with oxidative stress.

Many studies showed that glucose, fructose and sucrose are important regulators in sugar sensing and signaling in plants (Rolland *et al.*, 2006; Smeekens and Hellmann, 2014) and sucrose is fundamental for desiccation tolerance (Dinakar and Bartels, 2013; Vicré *et al.*, 2004). In this context, the accumulation of D-g-D-i-oct to a high amount might have less effect on primary carbon metabolism (e.g. photosynthesis) and related processes and therefore accumulation of high levels of D-g-D-i-oct may have an advantage during evolution.

Localization and physiological function of D-g-D-i-oct

This study supports circadian changes in D-g-D-i-oct accumulation as described by Norwood *et al.* (2003). D-g-D-i-oct was the dominant sugar in leaf exudate by phloem exudate analysis. This indicates that *C. plantagineum* leaves transport D-g-D-i-oct to roots as energy supply. Most plants transport sucrose, but some also transport raffinose and stachyose and/or sugar alcohols (Turgeon and Wolf, 2009). However, some studies also proposed sedoheptulose as sugar transport form (Ceusters *et al.*, 2013; Liu *et al.*, 2002). Therefore, D-g-D-i-oct is also a candidate for a transport form of sugars in plants.

Sugars are often seen as energy resource and signaling molecules in plant cells (Eveland and Jackson, 2012). In the present study we compared D-g-D-i-oct levels in isolated chloroplasts and intact leaf tissues, which suggests that D-g-D-i-oct is localized in the cytosol (probably in vacuole that occupies >95% of the cell volume). Many studies showed that glucose, fructose and sucrose are important regulators in sugar sensing and signaling in plants (Rolland et al. 2006; Smeekens and Hellmann 2014) and sucrose is fundamental for desiccation tolerance (Hoekstra et al. 1997; Vicré et al. 2004; Peters et al. 2007). In this context, the accumulation of D-g-D-i-oct to a high amount might have less effect on primary carbon metabolism (e.g. photosynthesis) and related processes and therefore accumulation of high levels of D-g-D-i-oct may have an advantage during evolution. Increasing evidence suggests that sugar-(like) molecules counteract oxidative stress by acting as genuine ROS scavengers (Peshev *et al.*, 2013; Van den Ende and Valluru, 2009). Our analysis suggested that D-g-D-i-oct has stronger hydroxyl radical (OH) scavenging ability than sucrose. Previous studies showed that sucrose is a more efficient scavenger than glucose and fructose (Nishizawa *et al.*, 2008; Peshev *et al.*, 2013). Relative to sucrose, the antioxidant advantage of D-g-D-i-oct might explain its high accumulation in *C. plantagineum* and *L. brevidens* in normal condition from another perspective.

Differentiation of *C. plantagineum* transketolases in evolution

As an important component of the photosynthesis reaction and the pentose phosphate pathway, the evolution of transketolase might reflect various strategies in sugar metabolism of organisms in response to environment. An alignment of spinach chloroplast transketolase with homologous sequences from eubacterial and eukaryotic sources showed that plant transketolases have special characteristic and occupy one branch that is separated with eubacterial, fungal and animal

transketolase from in the phylogenetic tree (Flechner *et al.*, 1996). Phylogeny analysis of transketolase genes from about 40 angiosperm plant species demonstrates that TKT7 and TKT10 in *C. plantagineum* and their homologs from *L. brevidens* and *L. subracemosa* have diverged from other transketolase genes of many desiccation sensitive species in the phylogenetic tree. The sequence analysis showed that the sequences of *C. plantagineum* TKT7 and TKT10 and their homologous genes (e.g. con 8 lb from *L brevidens* and con 3 ls from *L. subracemosa*) lack recognizable transit peptides that transits the transketolase to the chloroplast. This may explain the specificity of *C. plantagineum* TKT7 and TKT10 and their homologous genes from *L brevidens* and *L. subracemosa,* and may be related to the fact that they encode enzymes related to the D-g-D-i-oct metabolism in these plants. It is interesting that the D-g-D-i-oct mono- or diphosphate were observed in spinach and they were proposed to be synthesized by transketolase, but the alignment of genes showed that the spinach transketolase gene was closer to TKT3 than TKT7 and TKT10 in the phylogenetic tree. Does this suggest that tkt3 is involved in D-g-D-i-oct synthesis?

Differentiation of *C. plantagineum* transketolases in functions

The results of D-g-D-i-oct localization showed that D-g-D-i-oct accumulates in the cytosol. In addition, the subcellular study of *C. plantagineum* transketolase (Willige *et al.*, 2009) found that tkt3 was localized in chloroplasts and tkt7 and tkt10 in the cytosol and transketolase purified from the chloroplastic fraction did not lead to the synthesis of D-g-D-i-oct whereas the cytoplasmic transketolase fraction from the rehydrated leaves resulted in D-g-D-i-oct synthesis. Thus it is reasonable to hypothesize that the reaction catalyzed by tkt7 and tkt10 is likely to be involved in the D-g-D-i-oct biosynthesis in *C. plantagineum*. However, the transketolases purified from plants are still a mixture of proteins, it can not be excluded that other proteins except transketolase participate in the reaction. Besides, it is still unknown whether tkt7 and tkt10 have the same functions in carbon metabolism in *C. plantagineum*.

In this study, transketolases were extracted from leaves of *C. plantagineum* plant and were verified by Western blot. The enzymatic reaction reported by Willige *et al.* (2009) was repeated: D-g-D-i-oct-8-phosphate was synthesized with hydroxypyruvate and glucose-6-phosphate as substrates. However, it is intriguing that D-g-D-i-oct-8-phosphate could also be synthesized when

fructose-6-phosphate and glucose-6-phosphate were used as substrates. This indicates that the exchange reaction proposed by Williams and MacLeod (2006) exists in *C. plantagineum*. When hydroxypyruvate and ribose-5-phospahte were used as substrates sedoheptulose-7-phospahte was synthesized. Therefore, it could be suggested that hydroxypyruvate plays a role of providing two-carbon ketol group that would be transferred to the donor acceptor. In enzymatic reactions, sedoheptulose-7-phospahte was synthesized in the reaction with fructose-6-phosphate and ribose-5-phosphate as substrates. This showed that fructose-6-phosphate could also exert similar function as hydroxypyruvate. It is more feasible for plants to synthesize D-g-D-i-oct-8-phospahte with glucose-6-phospahte and fructose-6-phosphate as substrates, since hydroxypyruvate is the metabolite involved in the photorespiration pathway of carbon (Givan and Kleczkowski, 1992) that is mainly localized in chloroplasts, peroxisomes and mitochondria while D-g-D-i-oct is synthesized in the cytosol.

Although Willige *et al.* (2009) reported that they used the transketolase purified from fully hydrated, untreated plants and from 28-h rehydrated plants, only the cytoplasmic transketolase fraction from the rehydrated leaves resulted in D-g-D-i-oct synthesis. Expression analysis of transketolase isoforms showed that tkt3 is constitutively expressed in leaves and roots, while tkt7 and tkt10 are upregulated in leaves during rehydration of the desiccated plant (Bernacchia *et al.*, 1995). These results could not explain the D-g-D-i-oct accumulation in normal growth condition. In our study, transketolase extracted from hydrated plant leaves was also capable of catalyzing the synthesis of D-g-D-i-oct-8-phosphate using glucose-6-phospahte and fructose-6-phosphate as substrates. This could be easily understood since D-g-D-i-oct is accumulated to high amount in hydrated conditions and the relevant enzymes of the synthesis should also be activated in hydrated conditions.

In order to distinguish the possible functions of tkt3, tkt7 and tkt10, the recombinant tkt3, tkt7 and tkt10 were purified and used in the enzymatic reactions. Our results showed that tkt3 catalyzed the transfer of a two-carbon ketol group from hydroxypyruvate or fructose-6-phosphate to ribose-5-phosphate to form sedoheptulose-7-phosphate. Besides catalyzing the same transfer reaction, tkt7 and tkt10 also catalyze the formation of D-g-D-i-oct-8-phosphate using glucose-6-phosphate as acceptor and hydroxypyruvate/fructose-6-phosphate as donor. This confirms again that transketolase is involved in D-g-D-i-oct synthesis and also means that the exchange reaction

is implemented in *C. plantagineum* like in spinach Williams and MacLeod (2006). With the consideration that tkt3 is localized in chloroplasts while tkt7 and tkt10 in the cytoplasm (Willige *et al.*, 2009) and transketolase might play a novel role in the supplemented Calvin cycle (Flanigan *et al.*, 2006), it is reasonable to suggest that tkt3 is only involved in carbon reactions in photosynthesis and the pentose phosphate pathway, while tkt7 and tkt10 are responsible for the accumulation of D-g-D-i-oct in *C. plantagineum*. Certainly, tkt7 and tkt10 could also participate in the pentose phosphate pathway, as both these transketolases can accept various substrates (Krüger and von Schaewen, 2003; Williams *et al.*, 1987), which is also shown by our study. However, we are still left with the question: How are three different transketolase isoforms regulated and how do they cooperate in carbon reactions in *C. plantagineum*?

An inhibitor of *C. plantagineum* transketolases

To further characterize *C. plantagineum* transketolases, oxythiamine, an irreversible inhibitor of transketolase, was used in a series of experiments. During the rehydration of dehydrated leaves, oxythiamine lead to the reduced level of D-g-D-i-oct in rehydrated leaves. But it is hard to evaluate whether the activity of transketolase was inhibited by oxythiamine, because there are several enyzmes that are thiamine diphosphate dependent and may be inhibited by oxythiamine. The activity assays suggested that the activity of transketolase extracted from *C. plantagineum* leaves could be inhibited by oxythiamine and the inhibition effect was enhanced with higher amounts of oxythiamine present in the reaction system. The analysis of the products in reaction with the presence of the recombinant transketolase 7 showed that the activity of the recombinant transketolase 7 was also inhibited by oxythiamine. Oxythiamine was reported in the inhibition of the growth of *Saccharomyces cerevisiae* (Czerniecki *et al.*, 2003), the proliferation of tumor cells by inhibiting the non-oxidative synthesis of ribose (Boros *et al.*, 1997) and altering dynamics of protein signals (Wang *et al.*, 2013). This is the first time that the inhibition of oxythiamine was observed for plant transketolases.

The universality of D-g-D-i-oct synthesis

Previous studies showed that D-g-D-i-oct mono or diphosphate could be synthesized in rat liver (Paoletti *et al.*, 1979), yeast (Clasquin *et al.*, 2011) and spinach Williams and MacLeod (2006). The results of enzymatic assays using *E. coli* transketolase A22 showed that the transketolase of

E. coli could also catalyze D-g-D-i-oct-8-phosphate with hydroxypyruvate or fructose-6-phosphate as donor substrate and glucose-6-phospahte as acceptor substrate. This indicates that eukaryote could also have the ability to synthesize D-g-D-i-oct. Research have revealed that *E. coli* is capable of synthesizing an eight-carbon sugar, such as 3-Deoxy-D-manno-octulosonate-8-phosphate synthesized by condensation of 2-phosphoenolpyruvate (PEP) and d-arabinose-5-phosphate (Wagner *et al.*, 2000). However, whether the synthesis reaction of D-g-D-i-oct-8-phosphate has physiological meaning in *E. coli* should be explored in future.

The influence of D-g-D-i-oct synthesis on phosphorus homeostasis in *C. plantagineum*

D-g-D-i-oct mono or diphosphate is only an intermediate in the pentose phosphate pathway. The rare monosaccharide D-g-D-i-oct accumulates to high amounts in *C. plantagineum*. Thus a specific phosphatase is essential for the hydrolysis of D-g-D-i-oct-8-phosphate to produce D-g-D-i-oct and release phosphate. Even though we did not identify this phosphatase, experiments with regard to the influence of phosphorus on D-g-D-i-oct level in *C. plantagineum* demonstrated that the accumulation of D-g-D-i-oct was influenced by phosphate. Phosphate deprivation leaded to lower level of cellular phosphate but leaded to higher level of D-g-D-i-oct in *C. plantagineum* plants. In addition the foliage treatment with phosphate could reduce the level of D-g-D-i-oct in *C. plantagineum* leaves. This suggested the existence of a specific phosphatase that is activated by a lack of phosphorus and inhibited by excess phosphorus. Similarly, Ceusters *et al.* (2013) reported a sedoheptulose-7-phosphate phosphatase that produces sedoheptulose from sedoheptulose-7-phosphate in the Crassulacean acid metabolism (CAM) plants *Kalanchoe pinnata* and *Sedum spectabile* that can accumulate high amount of free sedoheptulose. The activity of sedoheptulose-7-phosphate phosphatase is attenuated by ADP and inorganic phosphate. The study with *A. thaliana* (Jost *et al.*, 2015; Müller *et al.*, 2007) also showed that phosphate starvation would lead to lower levels of cellular phosphate and total phosphate in plants. Leaves of phosphate-starved plants had a higher level of sugars (3-fold) than phosphate-supplied plants. Moreover, sucrose supply would lead to the reduction of cellular phosphate level. This demonstrated again that phosphate could affect the activity of sugar phosphate phosphatase in plants.

It is well known that phosphorus is an essential element for plant growth and plays an important role in many processes, including energy generation, nucleic acid synthesis, photosynthesis, glycolysis, respiration, membrane synthesis and stability, enzyme activation/inactivation, redox reactions, signaling, carbohydrate metabolism and nitrogen fixation (Vance *et al.*, 2003). Ceusters *et al.* (2013) proposed that the formation of sedoheptulose is not only beneficial with regard to carbon allocation under elevated CO_2 conditions but also contributes to Pi homeostasis as CAM plants generally utilize more ATP and as such more Pi to convert carbon into sugars during photosynthesis. Thus plants are particularly vulnerable to Pi imbalances. In a similar way we suggest that D-g-D-i-oct could also play a role in Pi homeostasis. In fact, most resurrection plant species natively occur on rock outcrops and grow in shallow and sandy soils (Gaff, 1977; Porembski and Barthlott, 2000; Sherwin and Farrant, 1995). Therefore phosphorus should be an important resource for survival and it is hardly surprising that plants such as *C. plantagineum* evolved specific mechanisms to adapt phosphorus deficiency. Availability of phosphorus is critical for *C. plantagineum*, because abundant stress proteins, essential for desiccation tolerance are often phosphorylated (Röhrig *et al.*, 2006). The remodeling of membranes during dehydration and rehydration in *C. plantagineum* may also require phosphorus (Gasulla *et al.*, 2013); This emphasizes again the importance of phosphorus for *C. plantagineum*. Compared to sucrose that is also synthesized in *C. plantagineum*, D-g-D-i-oct is more efficient in energy utilization and phosphorus with the aid of the exchange reaction, whereas the synthesis of sucrose entails UTP assimilation and other metabolic pathways regarding sugar phosphate (Taiz and Zeiger, 2010).

4.2 Conclusions

From the results, it is concluded that desiccation tolerance is regulated by senescence and this reflects the strategy of resurrection plants to adapt to a complex environment. The differences in expression patterns of senescence-related genes and carbohydrate status between senescent and vigorous *C. plantagineum* plants indicate that resurrection plants or their organs will be prepared in different ways for dehydration according to developmental stage. By analyzing the levels of sucrose, it is found that sucrose synthesis is more inclined to be regulated by water stress than by senescence in *C. plantagineum*. Light is an important factor for D-g-D-i-oct synthesis. The D-g-D-i-oct level is strictly controlled in *C. plantagienum* and D-g-D-i-oct was consumed to defend ROS species produced by paraquat. D-g-D-i-oct is localized in the cytosol and could be exported

from leaves. Relative to common sugars accumulating in *C. plantagineum* leaves, the substantial accumulation of D-g-D-i-oct may suggest that D-g-D-i-oct is not primarily be a sensing molecule but has some "structural" role. The excellent hydroxyl scavenging ability of D-g-D-i-oct implies that D-g-D-i-oct may be important for ROS scavenging, which could further explain the substantial accumulation.

Our study suggests that the three isoforms of *C. plantagineum* transketolase may exert different functions. The tkt3 plays a role in the photosynthesis and the pentose phosphate pathway. The tkt7 and tkt10 isoforms of transketolase that show distinct specificity in function and evolution catalyze the formation of D-g-D-i-oct-8-phosphate using glucose-6-phosphate and fructose-6-phosphate as substrates. The activity of transketolase was inhibited by the analogue of thiamine diphosphate, oxythiamine. The transketolase A22 of *E. coli* K12 could achieve the same reactions as tkt7and tkt10. This may indicate that the D-g-D-i-oct and its metabolism might exist in organisms more commonly than they are known. Although the phosphatase that hydrolyzes D-g-D-i-oct phosphate to produce D-g-D-i-oct could not be identified and characterized so far, the influence of phosphate on D-g-D-i-oct metabolism indicate that the phosphatase exists and is activated by a lack of phosphate and attenuated by an excess of phosphate.

References

Bar-Peled M, O'Neill MA. 2011. Plant nucleotide sugar formation, interconversion, and salvage by sugar recycling. Annual Review of Plant Biology 62, 127-155.

Bartels D, Hanke C, Schneider K, Michel D, Salamini F. 1992. A desiccation-related Elip-like gene from the resurrection plant *Craterostigma plantagineum* is regulated by light and ABA. The EMBO Journal 11, 2771-2778.

Bartels D, Salamini F. 2001. Desiccation Tolerance in the Resurrection Plant *Craterostigma plantagineum*. A Contribution to the Study of Drought Tolerance at the Molecular Level. Plant Physiology 127, 1346-1353.

Bartels D, Schneider K, Terstappen G, Piatkowski D, Salamini F. 1990. Molecular cloning of abscisic acid-modulated genes which are induced during desiccation of the resurrection plant *Craterostigma plantagineum*. Planta 181, 27-34.

Bernacchia G, Schwall G, Lottspeich F, Salamini F, Bartels D. 1995. The transketolase gene family of the resurrection plant *Craterostigma Plantagineum*: differential expression during the rehydration phase. The EMBO Journal 14, 610-618.

Besseau S, Li J, Palva ET. 2012. WRKY54 and WRKY70 co-operate as negative regulators of leaf senescence in *Arabidopsis thaliana*. Journal of Experimental Botany 63, 2667-2679.

Bianchi G, Gamba A, Murelli C, Salamini F, Bartels D. 1991. Novel carbohydrate metabolism in the resurrection plant *Craterostigma plantagineum*. The Plant Journal 1, 355-359.

Bockel C, Salamini F, Bartels D. 1998. Isolation and characterization of genes expressed during early events of the dehydration process in the resurrection plant *Craterostigma plantagineum*. Journal of Plant Physiology 152, 158-166.

Bolouri-Moghaddam MR, Le Roy K, Xiang L, Rolland F, Van den Ende W. 2010. Sugar signalling and antioxidant network connections in plant cells. FEBS Journal 277, 2022-2037.

Boros LG, Puigjaner J, Cascante M, Lee W-NP, Brandes JL, Bassilian S, Yusuf FI, Williams RD, Muscarella P, Melvin WS. 1997. Oxythiamine and dehydroepiandrosterone inhibit the nonoxidative synthesis of ribose and tumor cell proliferation. Cancer Research 57, 4242-4248.

Buchanan-Wollaston V, Page T, Harrison E, Breeze E, Lim PO, Nam HG, Lin J-F, Wu S-H, Swidzinski J, Ishizaki K, Leaver CJ. 2005. Comparative transcriptome analysis reveals significant differences in gene expression and signalling pathways between developmental and dark/starvation-induced senescence in Arabidopsis. The Plant Journal 42, 567-585.

Bunik VI, Tylicki A, Lukashev NV. 2013. Thiamin diphosphate ‐ dependent enzymes: from enzymology to metabolic regulation, drug design and disease models. FEBS Journal 280, 6412-6442.

Bus JS, Gibson JE. 1984. Paraquat: model for oxidant-initiated toxicity. Environmental Health Perspectives 55, 37-46.

Ceusters J, Godts C, Peshev D, Vergauwen R, Dyubankova N, Lescrinier E, De Proft MP, Van den Ende W. 2013. Sedoheptulose accumulation under CO_2 enrichment in leaves of *Kalanchoe pinnata*: a novel mechanism to enhance C and P homeostasis? Journal of Experimental Botany 64, 1497-1507.

Charlson AJ, Richtmyer NK. 1960. The Isolation of an Octulose and an Octitol from Natural Sources - D-Glycero-D-Manno-Octulose and D-Erythro-D-Galacto-Octitol from the Avocado and D-Glycero-D-Manno-Octulose from Sedum Species. Journal of the American Chemical Society 82, 3428-3434.

Clasquin MF, Melamud E, Singer A, Gooding JR, Xu XH, Dong AP, Cui H, Campagna SR, Savchenko A, Yakunin AF, Rabinowitz JD, Caudy AA. 2011. Riboneogenesis in Yeast. Cell 145, 969-980.

Cooper K, Farrant JM. 2002. Recovery of the resurrection plant *Craterostigma wilmsii* from desiccation: protection versus repair. Journal of Experimental Botany 53, 1805-1813.

Couée I, Sulmon C, Gouesbet G, El Amrani A. 2006. Involvement of soluble sugars in reactive oxygen species balance and responses to oxidative stress in plants. Journal of Experimental Botany 57, 449-459.

Czerniecki J, Dobrzyń P, Strumiło S. 2003. Effect of oxythiamin on growth rate, survival ability and pyruvate decarboxylase activity in *Saccharomyces cerevisiae*. Journal of Basic Microbiology 43, 522-529.

Dai N, Schaffer A, Petreikov M, Shahak Y, Giller Y, Ratner K, Levine A, Granot D. 1999. Overexpression of Arabidopsis hexokinase in tomato plants inhibits growth, reduces photosynthesis, and induces rapid senescence. The Plant Cell 11, 1253-1266.

Devi R, Munjral N, Gupta AK, Kaur N. 2007. Cadmium induced changes in carbohydrate status and enzymes of carbohydrate metabolism, glycolysis and pentose phosphate pathway in pea. Environmental and Experimental Botany 61, 167-174.

Dinakar C, Bartels D. 2013. Desiccation tolerance in resurrection plants: new insights from transcriptome, proteome and metabolome analysis. Frontiers in Plant Science 4, 1-14.

dos Santos R, Vergauwen R, Pacolet P, Lescrinier E, Van den Ende W. 2013. Manninotriose is a major carbohydrate in red deadnettle (*Lamium purpureum*, Lamiaceae). Annals of Botany 111, 385-393.

Drennan PM, Smith MT, Goldsworthy D, van Staden J. 1993. The occurrence of trehalose in the leaves of the desiccation-tolerant angiosperm *Myrothamnus flabellifolius* welw. Journal of Plant Physiology 142, 493-496.

Dubois M, Gilles K, Hamilton JK, Rebers PA, Smith F. 1951. A colorimetric method for the determination of sugars. Nature 168, 167.

Duewel HS, Sheflyan GY, Woodard RW. 1999. Functional and biochemical characterization of a recombinant 3-deoxy-D-manno-octulosonic acid 8-phosphate synthase from the hyperthermophilic bacterium *Aquifex aeolicus*. Biochemical and Biophysical Research Communications 263, 346-351.

Duff SM, Sarath G, Plaxton WC. 1994. The role of acid phosphatases in plant phosphorus metabolism. Physiologia Plantarum 90, 791-800.

Elsayed AI, Rafudeen MS, Golldack D. 2014. Physiological aspects of raffinose family oligosaccharides in plants: protection against abiotic stress. Plant Biology 16, 1-8.

Eveland AL, Jackson DP. 2012. Sugars, signalling, and plant development. Journal of Experimental Botany 63, 3367-3377.

Farrant JM, Vander Willigen C, Loffell DA, Bartsch S, Whittaker A. 2003. An investigation into the role of light during desiccation of three angiosperm resurrection plants. Plant Cell & Environment 26, 1275-1286.

Fernandez O, Béthencourt L, Quero A, Sangwan RS, Clément C. 2010. Trehalose and plant stress responses: friend or foe? Trends in Plant Science 15, 409-417.

Flanigan IL, MacLeod JK, Williams JF. 2006. A re-investigation of the path of carbon in photosynthesis utilizing GC/MS methodology. Unequivocal verification of the participation of octulose phosphates in the pathway. Photosynthesis Research 90, 149-159.

Flechner A, Dressen U, Westhoff P, Henze K, Schnarrenberger C, Martin W. 1996. Molecular characterization of transketolase (EC 2.2.1.1) active in the Calvin cycle of spinach chloroplasts. Plant Molecular Biology 32, 475-484.

Flitsch SL, Ulijn RV. 2003. Sugars tied to the spot. Nature 421, 219-220.

Gaff D. 1977. Desiccation tolerant vascular plants of Southern Africa. Oecologia 31, 95-109.

Gaff D, Loveys B. 1984. Abscisic acid content and effects during dehydration of detached leaves of desiccation tolerant plants. Journal of Experimental Botany 35, 1350-1358.

Gasulla F, Vom Dorp K, Dombrink I, Zahringer U, Gisch N, Dormann P, Bartels D. 2013. The role of lipid metabolism in the acquisition of desiccation tolerance in *Craterostigma plantagineum*: a comparative approach. The Plant Journal 75, 726-741.

Gechev T, Dinakar C, Benina M, Toneva V, Bartels D. 2012. Molecular mechanisms of desiccation tolerance in resurrection plants. Cellular and Molecular Life Sciences 69, 3175-3186.

Giarola V, Challabathula D, Bartels D. 2015. Quantification of expression of dehydrin isoforms in the desiccation tolerant plant *Craterostigma plantagineum* using specifically designed reference genes. Plant Science 236, 103-115.

Gillaspy GE, Keddie JS, Oda K, Gruissem W. 1995. Plant inositol monophosphatase is a lithium-sensitive enzyme encoded by a multigene family. The Plant Cell 7, 2175-2185.

Givan CV, Kleczkowski LA. 1992. The enzymic reduction of glyoxylate and hydroxypyruvate in leaves of higher plants. Plant Physiology 100, 552-556.

Griffiths CA, Gaff DF, Neale AD. 2014. Drying without senescence in resurrection plants. Frontiers in Plant Science 5, 1-18.

Groisillier A, Shao Z, Michel G, Goulitquer S, Bonin P, Krahulec S, Nidetzky B, Duan D, Boyen C, Tonon T. 2014. Mannitol metabolism in brown algae involves a new phosphatase family. Journal of Experimental Botany 65, 559-570.

Haustveit G, Mccomb EA, Rendig VV. 1975a. Biosynthesis of D- and L-Glycero-L-Galacto-Octulose from Pentoses and Hexoses. Carbohydrate Research 39, 125-129.

Haustveit G, Mccomb EA, Rendig VV. 1975b. Biosynthesis of D-Glycero-D-Altro-Octulose from D-Ribose and D-Allose. Carbohydrate Research 41, 363-365.

Ho C-L, Noji M, Saito K. 1999. Plastidic pathway of serine biosynthesis molecular cloning and expression of 3-phosphoserine phosphatase from *Arabidopsis thaliana*. Journal of Biological Chemistry 274, 11007-11012.

Hoekstra FA, Wolkers WF, Buitink J, Golovina EA, Crowe JH, Crowe LM. 1997. Membrane stabilization in the dry state. Comparative Biochemistry and Physiology Part A: Physiology 117, 335-341.

Huber SC, Huber JL. 1996. Role and regulation of sucrose-phosphate synthase in higher plants. Annual Review of Plant Physiology and Plant Molecular Biology 47, 431-444.

Ingram J, Chandler JW, Gallagher L, Salamini F, Bartels D. 1997. Analysis of cDNA clones encoding sucrose-phosphate synthase in relation to sugar interconversions associated with dehydration in the resurrection plant *Craterostigma plantagineum* Hochst. Plant Physiology 115, 113-121.

Janeček Š, Lanta V, Klimešová J, Doležal J. 2011. Effect of abandonment and plant classification on carbohydrate reserves of meadow plants. Plant Biology 13, 243-251.

Jost R, Pharmawati M, Lapis-Gaza HR, Rossig C, Berkowitz O, Lambers H, Finnegan PM. 2015. Differentiating phosphate-dependent and phosphate-independent systemic phosphate-starvation response networks in *Arabidopsis thaliana* through the application of phosphite. Journal of Experimental Botany doi:10.1093/jxb/erv025.

Kötting O, Kossmann J, Zeeman SC, Lloyd JR. 2010. Regulation of starch metabolism: the age of enlightenment? Current Opinion in Plant Biology 13, 320-328.

Kano A, Fukumoto T, Ohtani K, Yoshihara A, Ohara T, Tajima S, Izumori K, Tanaka K, Ohkouchi T, Ishida Y, Nishizawa Y, Ichimura K, Tada Y, Gomi K, Akimitsu K. 2013. The rare sugar D-allose acts as a triggering molecule of rice defence via ROS generation. Journal of Experimental Botany 64, 4939-4951.

Keunen E, Peshev D, Vangronsveld J, Van den Ende W, Cuypers A. 2013. Plant sugars are crucial players in the oxidative challenge during abiotic stress: extending the traditional concept. Plant Cell & Environment 36, 1242-1255.

Kingstonsmith AH, Major I, Parry MAJ, Keys AJ. 1992. Purification and properties of a phosphatase in French bean (*Phaseolus vulgaris* l) leaves that hydrolyzes 2'-carboxy-d-arabinitol 1-phosphate. Biochemical Journal 287, 821-825.

Kleines M, Elster RC, Rodrigo MJ, Blervacq AS, Salamini F, Bartels D. 1999. Isolation and expression analysis of two stress-responsive sucrose-synthase genes from the resurrection plant *Craterostigma plantagineum* (Hochst.). Planta 209, 13-24.

Krüger NJ, von Schaewen A. 2003. The oxidative pentose phosphate pathway: structure and organisation. Current Opinion in Plant Biology 6, 236-246.

Kutzer M. 2004. Untersuchung zum Zuckerstoffwechsel der Wiederauferstehungspflanze Craterostigma plantagineum und einiger Lindernia-Arten, Ph. D. Thesis, University of Bonn, Germany.

Laing WA, Bulley S, Wright M, Cooney J, Jensen D, Barraclough D, MacRae E. 2004. A highly specific L-galactose-1-phosphate phosphatase on the path to ascorbate biosynthesis. Proceedings of the National Academy of Sciences 101, 16976-16981.

Lastdrager J, Hanson J, Smeekens S. 2014. Sugar signals and the control of plant growth and development. Journal of Experimental Botany 65, 799-807.

Lee J. 2015. Sorbitol, Rubus fruit, and misconception. Food Chemistry 166, 616-622.

Lemoine R, La Camera S, Atanassova R, Dédaldéchamp F, Allario T, Pourtau N, Bonnemain J-L, Laloi M, Coutos-Thévenot P, Maurousset L. 2013. Source-to-sink transport of sugar and regulation by environmental factors. Frontiers in Plant Science 4, 1-21.

Liu X, Sievert J, Arpaia ML, Madore MA. 2002. Postulated physiological roles of the seven-carbon sugars, mannoheptulose, and perseitol in avocado. Journal of the American Society for Horticultural Science 127, 108-114.

Loescher WH. 1987. Physiology and metabolism of sugar alcohols in higher plants. Physiologia Plantarum 70, 553-557.

Lunn JE, Ashton AR, Hatch MD, Heldt HW. 2000. Purification, molecular cloning, and sequence analysis of sucrose-6F-phosphate phosphohydrolase from plants. Proceedings of the National Academy of Sciences 97, 12914-12919.

Müller J, Sprenger N, Bortlik K, Boller T, Wiemken A. 1997. Desiccation increases sucrose levels in Ramonda and Haberlea, two genera of resurrection plants in the Gesneriaceae. Physiologia Plantarum 100, 153-158.

Müller R, Morant M, Jarmer H, Nilsson L, Nielsen TH. 2007. Genome-wide analysis of the Arabidopsis leaf transcriptome reveals interaction of phosphate and sugar Metabolism. Plant Physiology 143, 156-171.

Mäki-Arvela Pi, Salmi T, Holmbom B, Willför S, Murzin DY. 2011. Synthesis of sugars by hydrolysis of hemicelluloses-a review. Chemical reviews 111, 5638-5666.

Mamedov TG, Suzuki K, Miura K, Kucho K-i, Fukuzawa H. 2001. Characteristics and sequence of phosphoglycolate phosphatase from a eukaryotic green alga *Chlamydomonas reinhardtii*. Journal of Biological Chemistry 276, 45573-45579.

Martinelli T, Whittaker A, Bochicchio A, Vazzana C, Suzuki A, Masclaux-Daubresse C. 2007. Amino acid pattern and glutamate metabolism during dehydration stress in the 'resurrection' plant *Sporobolus stapfianus*: a comparison between desiccation-sensitive and desiccation-tolerant leaves. Journal of Experimental Botany 58, 3037-3046.

Milo R, Last RL. 2012. Achieving diversity in the face of constraints: lessons from metabolism. Science 336, 1663-1667.

Mittler R. 2002. Oxidative stress, antioxidants and stress tolerance. Trends in Plant Science 9, 405-410.

Moghaddam MRB, Van den Ende W. 2012. Sugars and plant innate immunity. Journal of Experimental Botany, doi:10.1093/jxb/ers129.

Moore JP, Le NT, Brandt WF, Driouich A, Farrant JM. 2009. Towards a systems-based understanding of plant desiccation tolerance. Trends in Plant Science 14, 110-117.

Nishizawa A, Yabuta Y, Shigeoka S. 2008. Galactinol and raffinose constitute a novel function to protect plants from oxidative damage. Plant Physiology 147, 1251-1263.

Norwood M, Toldi O, Richter A, Scott P. 2003. Investigation into the ability of roots of the poikilohydric plant *Craterostigma plantagineum* to survive dehydration stress. Journal of Experimental Botany 54, 2313-2321.

Norwood M, Truesdale MR, Richter A, Scott P. 2000. Photosynthetic carbohydrate metabolism in the resurrection plant *Craterostigma plantagineum*. Journal of Experimental Botany 51, 159-165.

Ohdan T, Francisco PB, Sawada T, Hirose T, Terao T, Satoh H, Nakamura Y. 2005. Expression profiling of genes involved in starch synthesis in sink and source organs of rice. Journal of Experimental Botany 56, 3229-3244.

Pampurova S, Van Dijck P. 2014. The desiccation tolerant secrets of *Selaginella lepidophylla*: What we have learned so far? Plant Physiology and Biochemistry 80, 285-290.

Paoletti F, Williams JF, Horecker BL. 1979b. Synthesis and cleavage of octulose bisphosphates with liver and muscle aldolases. Archives of Biochemistry and Biophysics 198, 614-619.

Paul MJ, Primavesi LF, Jhurreea D, Zhang Y. 2008. Trehalose metabolism and signaling. Annu. Rev. Plant Biol. 59, 417-441.

Pauly M, Gille S, Liu L, Mansoori N, de Souza A, Schultink A, Xiong G. 2013. Hemicellulose biosynthesis. Planta 238, 627-642.

Pego JV, Kortstee AJ, Huijser C, Smeekens SC. 2000. Photosynthesis, sugars and the regulation of gene expression. Journal of Experimental Botany 51, 407-416.

Penney C. 1976. A simple micro-assay for inorganic phosphate. Analytical Biochemistry 75, 201-210.

Peshev D, Vergauwen R, Moglia A, Hideg E, Van den Ende W. 2013. Towards understanding vacuolar antioxidant mechanisms: a role for fructans? Journal of Experimental Botany 64, 1025-1038.

Peterbauer T, Lahuta LB, Blöchl A, Mucha J, Jones DA, Hedley CL, Gòrecki RJ, Richter A. 2001. Analysis of the raffinose family oligosaccharide pathway in pea seeds with contrasting carbohydrate composition. Plant Physiology 127, 1764-1772.

Peters S, Mundree SG, Thomson JA, Farrant JM, Keller F. 2007. Protection mechanisms in the resurrection plant Xerophyta viscosa (Baker): both sucrose and raffinose family oligosaccharides (RFOs) accumulate in leaves in response to water deficit. Journal of Experimental Botany 58, 1947-1956.

Petersen J, Eriksson SK, Harryson P, Pierog S, Colby T, Bartels D, Röhrig H. 2012. The lysine-rich motif of intrinsically disordered stress protein CDeT11-24 from *Craterostigma plantagineum* is responsible for phosphatidic acid binding and protection of enzymes from damaging effects caused by desiccation. Journal of Experimental Botany 63, 4919-4929.

Poirier Y, Thoma S, Somerville C, Schiefelbein J. 1991. A mutant of Arabidopsis deficient in xylem loading of phosphate. Plant Physiology 97, 1087-1093.

Porembski S, Barthlott W. 2000. Granitic and gneissic outcrops (inselbergs) as centers of diversity for desiccation-tolerant vascular plants. Plant Ecology 151, 19-28.

Röhrig H, Schmidt J, Colby T, Brautigam A, Hufnagel P, Bartels D. 2006. Desiccation of the resurrection plant Craterostigma plantagineum induces dynamic changes in protein phosphorylation. Plant Cell & Environment 29, 1606-1617.

Racker E, Haba GDL, Leder I. 1953. Thiamine pyrophosphate, a coenzyme of transketolase. Journal of the American Chemical Society 75, 1010-1011.

Ray PH, Benedict CD. 1980. Purification and characterization of a specific 3-deoxy-D-manno-octulosonate 8-phosphate phosphatase from Escherichia coli B. Journal of Bacteriology 142, 60-68.

Robyt JF. 1998. Polysaccharides I. Essentials of Carbohydrate Chemistry: Springer, 157-227.

Rodriguez MCS, Edsgärd D, Hussain SS, Alquezar D, Rasmussen M, Gilbert T, Nielsen BH, Bartels D, Mundy J. 2010. Transcriptomes of the desiccation-tolerant resurrection plant *Craterostigma plantagineum*. The Plant Journal 63, 212-228.

Rolland F, Baena-Gonzalez E, Sheen J. 2006. Sugar sensing and signaling in plants: conserved and novel mechanisms. Annual Review of Plant Biology 57, 675-709.

Rowan B, Bendich A. 2011. Isolation, Quantification, and Analysis of Chloroplast DNA. In: Jarvis RP, ed. Chloroplast Research in Arabidopsis, Humana Press, 151-170.

Rumpho ME, Edwards GE, Loescher WH. 1983. A pathway for photosynthetic carbon flow to mannitol in celery leaves activity and localization of key enzymes. Plant Physiology 73, 869-873.

Salerno GL, Curatti L. 2003. Origin of sucrose metabolism in higher plants: when, how and why? Trends in Plant Science 8, 63-69.

Sambrook J, Russell DW, Irwin N. 2001. Molecular cloning: a laboratory manual. Cold Spring Harbor, NY: Cold Spring Harbor Laboratory Press, 163-170.

Sasaki E, Lin C-I, Lin K-Y, Liu H-w. 2012. Construction of the octose 8-phosphate intermediate in lincomycin A biosynthesis: characterization of the reactions catalyzed by LmbR and LmbN. Journal of the American Chemical Society 134, 17432-17435.

Schenk G, Guddat LW, Ge Y, Carrington LE, Hume DA, Hamilton S, de Jersey J. 2000. Identification of mammalian-like purple acid phosphatases in a wide range of plants. Gene 250, 117-125.

Sherwin H, Farrant J. 1995. Surviving desiccation. Veld and Flora, 119-121.

Smeekens S, Hellmann HA. 2014. Sugar sensing and signaling in plants. Frontiers in Plant Science 5,1-2.

Smeekens S, Ma J, Hanson J, Rolland F. 2010. Sugar signals and molecular networks controlling plant growth. Current Opinion in Plant Biology 13, 273-278.

Smith AM, Zeeman SC. 2006. Quantification of starch in plant tissues. Nature Protocols 1, 1342-1345.

Somerville C. 2006. Cellulose Synthesis in Higher Plants. Annual Review of Cell and Developmental Biology 22, 53-78.

Stincone A, Prigione A, Cramer T, Wamelink MMC, Campbell K, Cheung E, Olin-Sandoval V, Grüning N-M, Krüger A, Tauqeer Alam M, Keller MA, Breitenbach M, Brindle KM, Rabinowitz JD, Ralser M. 2015. The return of metabolism: biochemistry and physiology of the pentose phosphate pathway. Biological Reviews 90, 927-963.

Stitt M, Zeeman SC. 2012. Starch turnover: pathways, regulation and role in growth. Current Opinion in Plant Biology 15, 282-292.

Stoop JM, Williamson JD, Pharr DM. 1996. Mannitol metabolism in plants: a method for coping with stress. Trends in Plant Science 1, 139-144.

Sturm A. 1999. Invertases. Primary structures, functions, and roles in plant development and sucrose partitioning. Plant Physiology 121, 1-8.

Taiz L, Zeiger E. 2010. Plant physiology. Sunderland, MA: Sinauer Associates, 145-170.

Turgeon R, Wolf S. 2009. Phloem transport: cellular pathways and molecular trafficking. Annual Review of Plant Biology 60, 207-221.

Turner NJ. 2000. Applications of transketolases in organic synthesis. Current Opinion in Biotechnology 11, 527-531.

Valenzuela-Avendaño JP, Mota IAE, Uc GL, Perera RS, Valenzuela-Soto EM, Aguilar JJZ. 2005. Use of a simple method to isolate intact RNA from partially hydrated *Selaginella lepidophylla* plants. Plant Molecular Biology Reporter 23, 199-200.

van den Dries N, Facchinelli F, Giarola V, Phillips JR, Bartels D. 2011. Comparative analysis of LEA-like 11-24 gene expression and regulation in related plant species within the Linderniaceae that differ in desiccation tolerance. New Phytologist 190, 75-88.

Van den Ende W, Valluru R. 2009. Sucrose, sucrosyl oligosaccharides, and oxidative stress: scavenging and salvaging? Journal of Experimental Botany 60, 9-18.

Vance CP, Uhde‐Stone C, Allan DL. 2003. Phosphorus acquisition and use: critical adaptations by plants for securing a nonrenewable resource. New Phytologist 157, 423-447.

Vander Willigen C, Pammenter NW, Jaffer MA, Mundree SG, Farrant JM. 2003. An ultrastructural study using anhydrous fixation of Eragrostis nindensis, a resurrection grass with both desiccation-tolerant and-sensitive tissues. Functional Plant Biology 30, 281-290.

Vicré M, Farrant JM, Driouich A. 2004. Insights into the cellular mechanisms of desiccation tolerance among angiosperm resurrection plant species. Plant Cell & Environment 27, 1329-1340.

Villafranca JJ, Axelrod B. 1971. Heptulose synthesis from nonphosphorylated aldoses and ketoses by spinach transketolase. Journal of Biological Chemistry 246, 3126-3131.

Vogel G, Aeschbacher RA, Müller J, Boller T, Wiemken A. 1998. Trehalose‐6‐phosphate phosphatases from Arabidopsis thaliana: identification by functional complementation of the yeast tps2 mutant. The Plant Journal 13, 673-683.

Wagner T, Kretsinger RH, Bauerle R, Tolbert WD. 2000. 3-Deoxy-D-manno-octulosonate-8-phosphate synthase from *Escherichia coli.* Model of binding of phosphoenolpyruvate and D-arabinose-5-phosphate. Journal of Molecular Biology 301, 233-238.

Wang J, Zhang X, Ma D, Lee WN, Xiao J, Zhao Y, Go VL, Wang Q, Yen Y, Recker R, Xiao GG. 2013. Inhibition of transketolase by oxythiamine altered dynamics of protein signals in pancreatic cancer cells. Experimental Hematology & Oncology 2, 1-14.

Williams JF, Arora KK, Longenecker JP. 1987. The pentose pathway: A random harvest: Impediments which oppose acceptance of the classical (F-type) pentose cycle for liver, some neoplasms and photosynthetic tissue. The case for the L-type pentose pathway. International Journal of Biochemistry 19, 749-817.

Williams JF, Blackmore PF, Clark MG. 1978. New reaction sequences for the non-oxidative pentose phosphate pathway. Biochemical Journal 176, 257-282.

Williams JF, MacLeod JK. 2006. The metabolic significance of octulose phosphates in the photosynthetic carbon reduction cycle in spinach. Photosynthesis Research 90, 125-148.

Willige BC, Kutzer M, Tebartz F, Bartels D. 2009. Subcellular localization and enzymatic properties of differentially expressed transketolase genes isolated from the desiccation tolerant resurrection plant *Craterostigma plantagineum*. Planta 229, 659-666.

Wingenter K, Schulz A, Wormit A, Wic S, Trentmann O, Hoermiller, II, Heyer AG, Marten I, Hedrich R, Neuhaus HE. 2010. Increased activity of the vacuolar monosaccharide transporter TMT1 alters cellular sugar partitioning, sugar signaling, and seed yield in Arabidopsis. Plant Physiology 154, 665-677.

Winter H, Huber SC. 2000. Regulation of Sucrose Metabolism in Higher Plants: Localization and regulation of Activity of Key Enzymes. Critical Reviews in Plant Sciences 19, 31-67.

Wood AJ, Jenks MA. 2007. Plant Desiccation Tolerance: Diversity, Distribution, and Real-World Applications. In Jenks MA, Wood AJ, eds. Plant desiccation tolerance: Oxford, UK: 3-8.

Wu J, Patel M, Sundaram A, Woodard R. 2004. Functional and biochemical characterization of a recombinant Arabidopsis thaliana 3-deoxy-D-manno-octulosonate 8-phosphate synthase. Biochemical Journal 381, 185-193.

Wu Q, Cho JG, Lee DS, Lee DY, Song NY, Kim YC, Lee KT, Chung HG, Choi MS, Jeong TS, Ahn EM, Kim GS, Baek NI. 2013. Carbohydrate derivatives from the roots of Brassica rapa ssp campestris and their effects on ROS production and glutamate- induced cell death in HT-22 cells. Carbohydrate Research 372, 9-14.

Xiao W, Sheen J, Jang J-C. 2000. The role of hexokinase in plant sugar signal transduction and growth and development. Plant Molecular Biology 44, 451-461.

Yu S-M. 1999. Cellular and genetic responses of plants to sugar starvation. Plant Physiology 121, 687-693.

Yuan X-H, Anderson LE. 1987. Changing activity of glucose-6-phosphate dehydrogenase from pea chloroplasts during photosynthetic induction. Plant Physiology 85, 598-600.

Zhang Z, Liao H, Lucas WJ. 2014. Molecular mechanisms underlying phosphate sensing, signaling, and adaptation in plants. Journal of Integrative Plant Biology 56, 192-220.

Zhou ML, Zhang Q, Zhou M, Sun ZM, Zhu XM, Shao JR, Tang YX, Wu YM. 2012. Genome-wide identification of genes involved in raffinose metabolism in Maize. Glycobiology 22, 1775-1785.

Zhou R, Cheng L, Wayne R. 2003. Purification and characterization of sorbitol-6-phosphate phosphatase from apple leaves. Plant Science 165, 227-232.

Supplementary data

Table S1 Genes related to starch metabolism in *C. plantagineum*

Assembly UniProt ID	Description
Q45TX6	Starch branching enzyme I OS=Malus domestica
Q41058	Starch branching enzyme I OS=Pisum sativum
Q43846	Soluble starch synthase 3, chloroplastic/amyloplastic OS=Solanum tuberosum
B2ZGN0	Starch synthase VI OS=Vitis vinifera
B2M0R3	Starch-granule-bound R1 protein OS=Solanum tuberosum
O82627	Granule-bound starch synthase 1, chloroplastic/amyloplastic OS=Antirrhinum majus
Q18PQ6	Starch branching enzyme I OS=Ipomoea batatas
P93568	Soluble starch synthase 1, chloroplastic/amyloplastic OS=Solanum tuberosum
B9S156	Starch synthase, putative OS=Ricinus communis
Q1L5W1	Starch synthase isoform 3 (Fragment) OS=Nicotiana langsdorffii x Nicotiana sanderae
P23509	Glucose-1-phosphate adenylyltransferase small subunit, chloroplastic/amyloplastic OS=Solanum tuberosum
B2ZGM8	Starch synthase V OS=Vitis vinifera
B9H112	Predicted protein OS=Populus trichocarpa
Q9XGA9	Starch branching enzyme II (Fragment) OS=Solanum tuberosum
B2ZGM7	Starch synthase V OS=Solanum tuberosum
Q9XGC0	Starch synthase isoform SS III OS=Vigna unguiculata
B9R8M9	Starch branching enzyme II, putative OS=Ricinus communis
Q9LTP8	Starch-branching enzyme-like protein OS=Arabidopsis thaliana
B9S2B5	Alpha-amylase, putative OS=Ricinus communis
B9HSW9	Predicted protein (Fragment) OS=Populus trichocarpa
Q9AT14	Beta-amylase OS=Castanea crenata
B9MXU8	Predicted protein OS=Populus trichocarpa
Q0JJV2	Putative uncharacterized protein OS=Oryza sativa subsp. japonica
B9RDR8	Beta-amylase, putative OS=Ricinus communis
A7PXL0	Beta-amylase OS=Vitis vinifera
B9HMN6	Predicted protein (Fragment) OS=Populus trichocarpa
P53535	Alpha-1,4 glucan phosphorylase L-2 isozyme, chloroplastic/amyloplastic OS=Solanum tuberosum
O65258	F6N23.1 protein OS=Arabidopsis thaliana
A7NW88	Chromosome chr5 scaffold_2, whole genome shotgun sequence OS=Vitis vinifera
Q5ZFR9	Alpha-amylase OS=Plantago major
A7QU41	Chromosome chr2 scaffold_176, whole genome shotgun sequence OS=Vitis vinifera
B9RWS7	Beta-amylase, putative OS=Ricinus communis

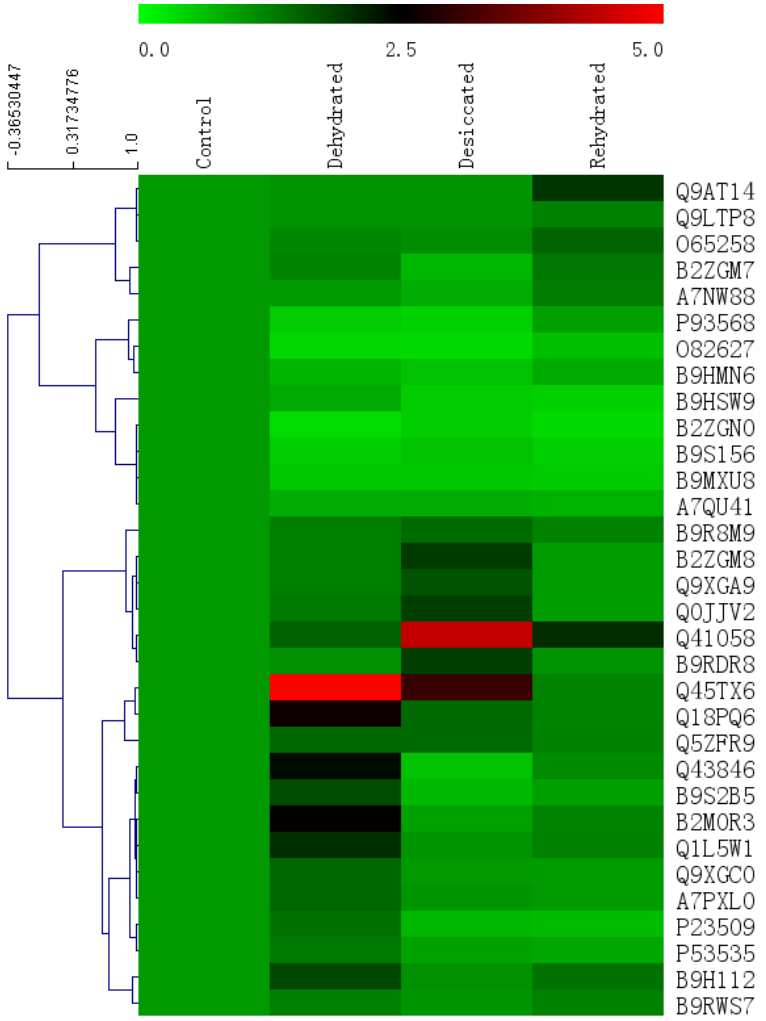

Fig. S1. The heatmap of gene expression profiles regarding starch metabolism in *C. plantagineum.* The description of the genes is given in table S1. The details of plant treatments are given in chapter 2.

The sequence of transaldolase 1 fragment was obtained from contig27562 in the transcriptome of *C.plantagineum*. The sequence underlined encodes the fragment used in this study.

AAGGTGCTCCAAGGGCGATGGTAATGGAAGCAGTGGCGGGAGAACGACGCTTCACGATCTTTACGAGAAA
GAAGGTCAAAGCCCATGGTACGACAATCTGTGTCGTCCCGTCACGGATCTCATTCCGCTCATTGAACGTG
GAGTTCGAGGAGTGACCAGCAATCCTGCGATTTTCCAAAAGGGGATATCTACCTCAAATGCATACAATGA
TCAGTTCAAGGAACTTGTCCAATCTGGAAAAGACATTGAAAGTGCTTACTGGGAACTTGTGATTAAGGAT
ATTCAAGATGCATGCAAACTCTTCGAGCCAATCTATGATCAAACAGATGGAGGCGACGGATACGTCTCCG
TCGAAGTTTCGCCTAAACTCGCTGATGACACCGAGAACACCATTGAAGCTGCAAAATGGCTTCACCAGAG
GGTTGATCGCTCTAATGTATATATTAAGATTCCTGCTACTGCTCCATGCATCCCGTCAATCAAGGAAGTC
ATTGCAAAAGGAATAAGTGTGAATGTCACGCTTATATTCTCTCTTGCTAGATATGAAGATGTGATTGATG
CATACCTCGATGGTCTCGAGAAATCTGGGCTCGATGATCTGTCCCGAGTCACGAGCGTTGCATCTTTCTT
TGTTAGCCGGGTGGATACCCTTGTCGACAAGATGCTTGAGAAGATTGGAACGCCTGAAGCCCTTGATCTT
CGCGGAAAAGCTGCAGTTGCTCAAGCAGCGCTGGCTTTTCAGCTCTACCAGCGGAAATTCTCAGGCCCAA
GATGGGAAGCTCTTGTGAAGAAAGGAGCCAAGAAGCAAAGACTCCTCTGGGCCTCAACTAGCGTCAAGAA

TCCAGCTTATCCTGACACACTCTATGTGGCTCCTCTTATTGGACCTGAGACGGTCTCCACCATGCCTGAT
CAAGCACTTGAAGCATTCATAGACCATGGCTCTGTTGGAAGAACGATAGACTCTAACGTCTCAGAAGCCG
AAGGCATTTACAGTGCTCTTGAGAAGCTTGGCATTGATTGGGGCTATGTGGGCACCCAGCTCGAGGTGGA
AGGAGTCGACTCCTTCAAGAAGAGCTTCGACAGCTTGCTGGATAGCCTTCAAGAGAAGGCAAACTCTCTC
AAACTAGTTAGCCTGTAAGAATGGAACTTGTTCGGTTGCTTTGATAATAAAGAGAGG

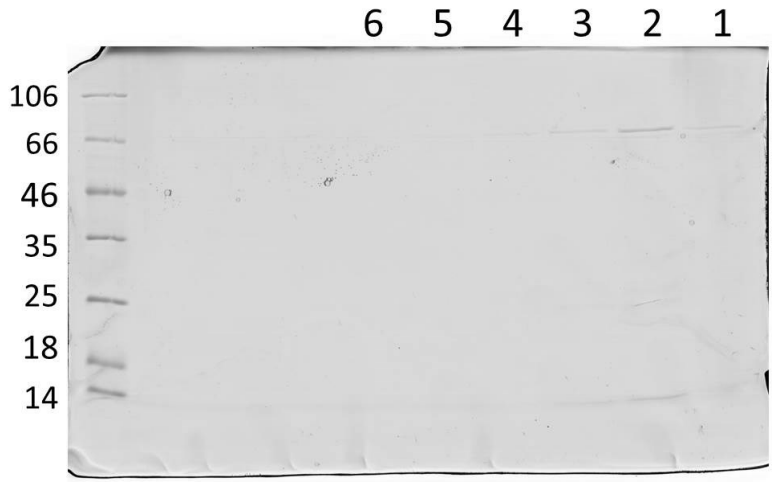

Fig. S2. SDS-PAGE of the protein purified from *E. coli* cells transformed with empty pET28a+ vector From right to left the lanes represent the protein size markers and the eluted fractions 1 to 6. The protein size markers are given in kDa.

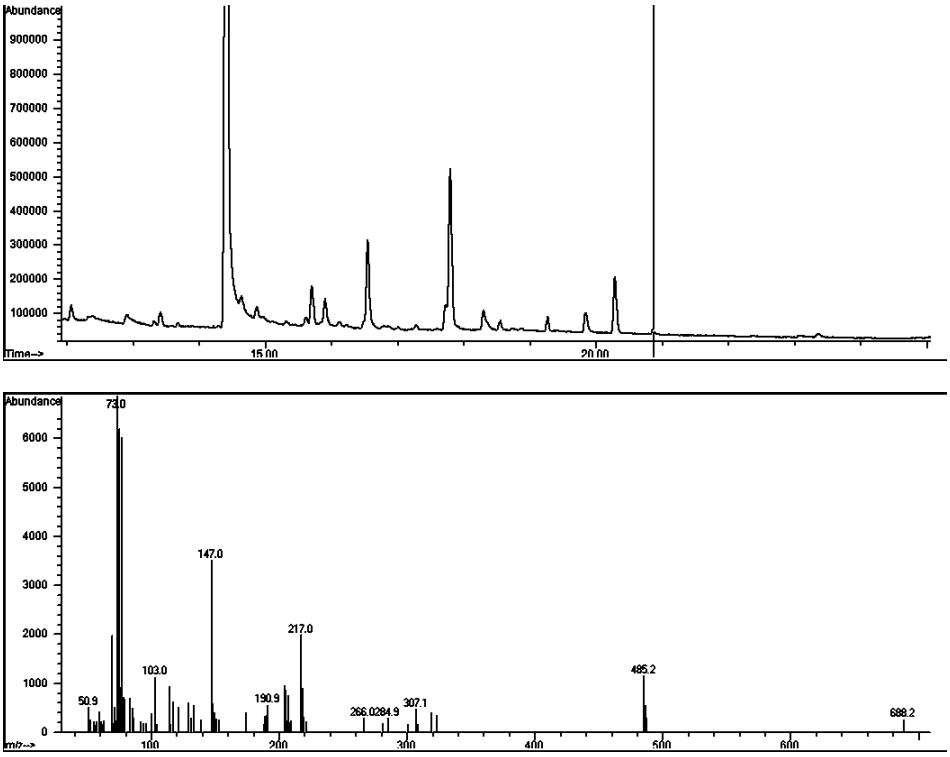

Fig A1. The chromatogram of the TMS derivatives of the dephosphorylated product of the control reaction with glucose-6-phosphate as acceptor substrate and hydroxypyruvate as donor (upper part) and the mass spectrum of the TMS derivative of the octulose candidate (lower part). The TMS derivative of the internal standard xylitol is labeled by a triangle and that of the octulose candidate is labeled by a vertical line. The reaction contains 58 mM glycylglycine (pH 7.7), 0.01% (w/v) Na-azide, 0.002% thiamine pyrophosphate, 15 mM $MgCl_2$, 5.3 mM donor and 16 mM acceptor. After 24 h of the catalyzing reaction, sugar phosphates in the product were dephosphorylated using acid phosphatase. The dephosphorylated products were purified on a column containing ion-exchanging bed resin AG 501-X8(D) (BIO-RAD). The flow-through fractions were used for GC/MS analysis.

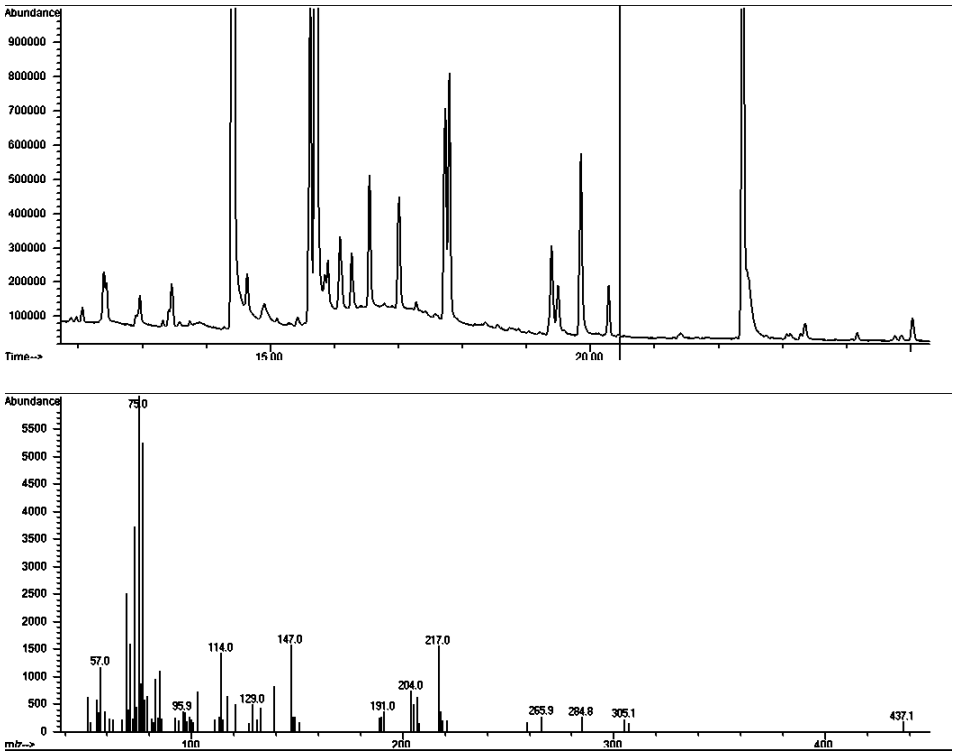

Fig. A2. The chromatogram of the TMS derivatives of the dephosphorylated reaction product with ribose-5-phosphate as acceptor substrate and fructose-6-phosphate as donor (upper part) and the mass spectrum of the TMS derivative of the sedoheptulose candidate (lower part). The TMS derivative of the internal standard xylitol is labeled by a triangle and that of sedoheptulose candidate is labeled by a vertical line. The reaction condition is the same as described in Fig. A1.

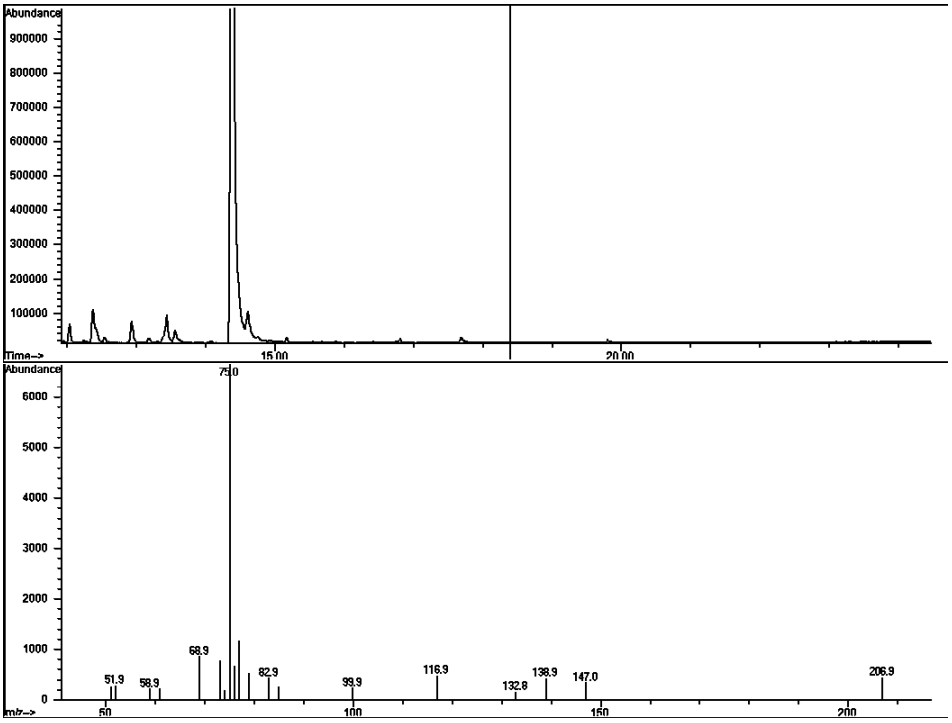

Fig. A3. The chromatogram of the TMS derivatives of the dephosphorylated product of the control reaction with glucose-6-phosphate as acceptor substrate and hydroxypyruvate as donor (upper part) and the mass spectrum of the TMS derivative of octulose candidate (lower part). The TMS derivative of the internal standard xylitol is labeled by a triangle and that of octulose candidate is labeled by a vertical line. The reaction contains 25 µg protein purified from *E. coli* cells transformed by empty vector pET28a+, 58 mM glycylglycine (pH 7.7), 0.01% (w/v) Na-azide, 0.002% thiamine pyrophosphate, 15 mM $MgCl_2$, 5.3 mM donor and 16 mM acceptor. After 24 h of the catalyzing reaction, sugar phosphates in the product were dephosphorylated using acid phosphatase. The dephosphorylated products were purified on a column containing ion-exchange bed resin AG 501-X8(D) (BIO-RAD). The flow-through fractions were used for GC/MS analysis.

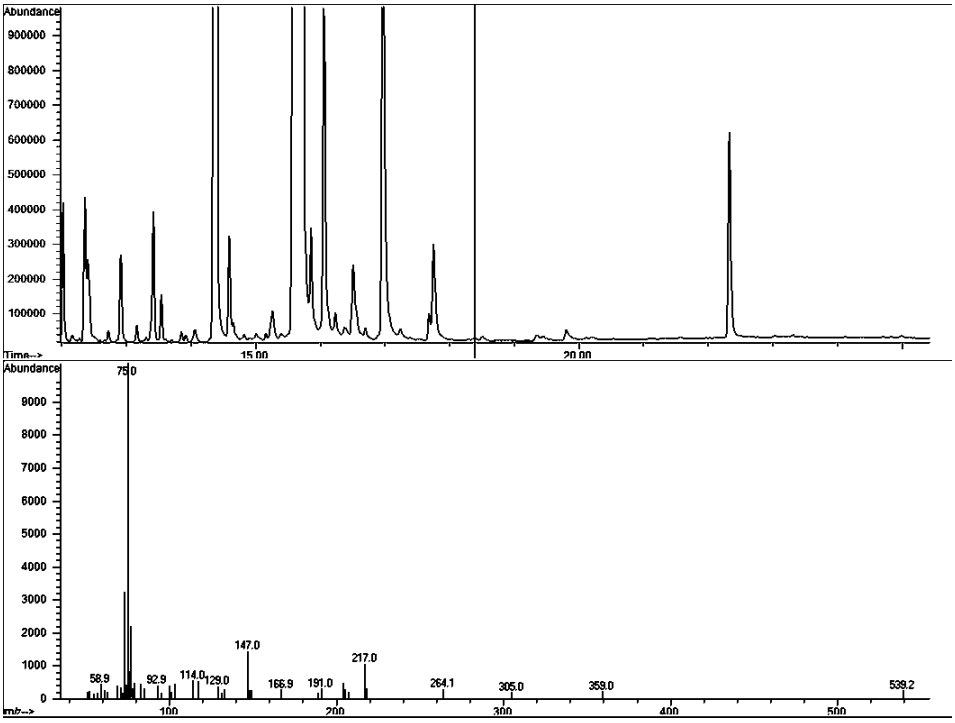

Fig. A4. The chromatogram of the TMS derivatives of the dephosphorylated reaction product with ribose-5-phosphate as acceptor substrate and fructose-6-phosphate as donor (upper part) and the mass spectrum of the TMS derivative of the sedoheptulose candidate (lower part). The TMS derivative of the internal standard xylitol is labeled by a triangle and that of the sedoheptulose candidate is labeled by a vertical line. The reaction condition is the same as described in Fig. A3.

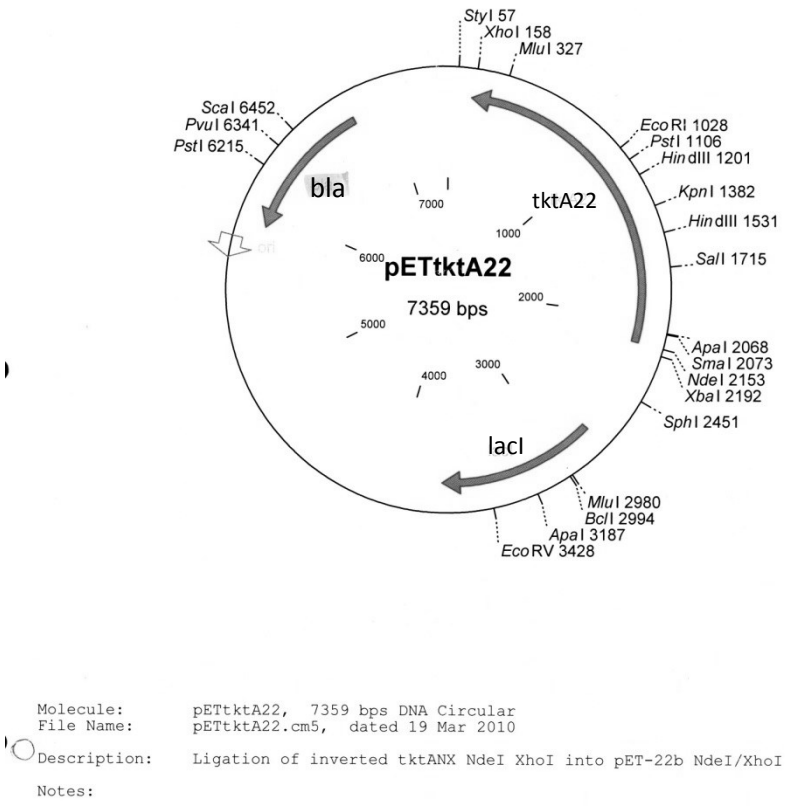

Fig. A5. The information of vector pET-22b containing *E.coli* K12 tktA insert.

Information of fragments obtained from PCR reactions using degenerate primers in the cloning of phosphatase genes

X1a sequence

GCACGAGGGTCGCCGATCACCTCCCAAATCGATCGCCGGCGCCGAACCCACCCGGGCGGCGCGTAGGATCCACGA
GCTCGAAAAGGGCTGCCTCTTAATCGCCACGGAAAAGCTAGACGGCCTCGAAGTCTTCGAACGCACCGTCGTCCTG
GTCCTATCGACGGCGCCGACGGGCCTAATCCTCAACCGTCCGTCGGCGCTGTCGATCAAGGAGGTACCAACGTGCC
CGTTCAACTCCGCCGCGGCGTTCAGGGAAATGCCGTTGTTCGACGGAGGGCCGATCGAGGACGTGCACTTTCTGA
TGAGCCCGAGGTGCAGCGGCGGAGACGGAGGAGGCGGGAAATTGGAGGAGCTGGCGAATGGATCGATGTACTA
TGGGACGAAGGAGAGCATTGGCTTCGCCGCCGATATGGTGGGTAGGGGGTTTGGCGGCGGCGAGCGACTTTAGG
TTCTTCGATGGTTACTGTGCTTGGGAAACAGGGCAGCTTAGGGATGAAATTAGGGCTGGAAAATGGATTGTAGCT
GATTGTAATCCGTGTGTTATTGGGCTTGAGGTTGTTGGGAAGAGTTGGGCTTTGGGGGGGAGGTTA

X1b sequence

GCACGAGGCATCGATGAACAAACAATCCATGGCTGCGACGAGACCTAGATGTTTTCTGGGCGTTAGCATTGGTGA
CGAACTTGAAGGTCGTATCATAGTCGAACTCTTCACCGATGTCGTGCCCAAAACTGCCGAGAACTTTAGGGCTCTTT
GCACCGGAGAGAAAGGCATTGGACCCAACACTGGCGTTCCTCTTCATTTCAAGGGATCTCGATTTCATCGGGTCAT
TAAAAGCTTCATGATACAAGGTGGTGATATCTCCGCTGGTGATGGAACTGGCGGCGAATCTATCTATGGGCTCAAA
TTTGAGGACGAAAACTTTGAGTTAAAACATGAAAGAAAGGGTATGCTGTCGATGGCAAATGCTGGACCTATACTA
ACGGCTCGCAGTTTTTCATTACCACAACTCGAACTTCTCATTTGGATGGAAAGCATGTTGTGTTTGGAAAAGTTATC
AAAGGAATGGGAGTTGTCCGTTCCATCGAGCACGTCACTACGGGCGAGAACGATCGTCCTACAGTTGATGTGGTC
ATAGCTGTTTCCTG

X1c w1-2 sequence

TGCTCGATGGAACGGACAACTCCCATTCCTTTGATAACTTTTCCAAACACAACATGCTTTCCATCCAAATGAGAAGTT
CGAGTTGTGGTAATGAAAAACTGCGAGCCGTTAGTATTAGGTCCAGCATTTGCCATCGACAGCATACCCTTTCTTTC
ATGTTTTAACTCAAAGTTTTCGTCCTCAAATTTGAGCCCATAGATAGATTCGCCGCCAGTTCCATCACCAGCGGAGA
TATCACCACCTTGTATCATGAAGCTTTTAATGACCCGATGAAATCGAGATCCCTTGAAATGAAGAGGAACGCCAGT
GTTGGGTCCAATGCCTTTCTCTCCGGTGCAAAGAGCCCTAAAGTTCTCGGCAGTTTTGGGCACGACATCGGTGAAG
AGTTCGACTATGATACGACCTTCAAGTTCGTCACCAATGCTAACGTCCAGAAAACATCTAGGTCTCGTCGCAGCCAT
GGATTGTTTGTTCATCGATGCTTCTTTCTAATAAGGAAATGATCGCCTCGTGC

X1d w1-3 sequence

GATGTCGTGCCCAAAACTGCCGAGAACTTTAGGGCTCTTTGCACCGGAGAGAAAGGCATTGGACCCAACACTGGC
GTTCCTCTTCATTTCAAGGGATCTCGATTTCATCGGGTCATTAAAAGCTTCATGATACAAGGTGGTGATATCTCCGCT
GGTGATGGAACTGGCGGCGAATCTATCTATGGGCTCAAATTTGAGGACGAAAACTTTGAGTTAAAACATGAAAGA
AAGGGTATGCTGTCGATGGCAAATGCTGGACCTAATACTAACGGCTCGCAGTTTTTCATTACCACAACTCGAACTTC
TCATTTGGATGGAAAGCATGTTGTGTTTGGAAAAGTTATCAAAGGAATGGGAGTTGTCCGTTCCATCGAGCA

X2a w2-1 sequence

TTTTTTTTTTTTTTTTTTTACTCCTAAATAGGGTAATTTTATTTCAAACGACGCATAATACAACATAACACGCAGCATA
AGACATACAAACATTATTTTTGTTATTCCATTATTTGAAATTTAGGTATAAATCAAATCCTATGGGATCTGATAGGAA
AACGCAGACACAACCACGCATAAGTAGGACACATATATCTGATCATAATAACAACAATTAAGCTCCACAGTACTCCT
TCAAAGTATCAGGAAGGTTCCCATCTTTGCTCGGTGAAGAGTTGCCGTAAAACTTGAGGAATTCGCCGTATTTAAA
AGGCTTGTATTTCAACGGATGCTCCTCGTCTACCATCTCGGGCGCAACCCTAATTTCATAATCGGGCTTAGGAGACG
AACCCACTGCAATCATATATCGATCCCTATCCACCGCCGCCACCTTATGTGCGCACGGAGGAAGCCTCCCATTCGTT
ATCGCGCTGAAGCAGTCGCCTGTCATGACTGCAAAAGAGTTCACGGACGAGGGGTCGTAGGTTATCCACTGGCCG
TCGTTTTACA

X2b w2-4 sequence

ACTCCAGCTGTATTGGAGAGACCAAGCAATACACCCGAATAACGGGGAGCAATATCTTGATGGTTCGAATACAATC
CTGACTGAGAAAAAGCGTCGGTTCCCTGACTGCATGCCATGCATAGAACTGCAGCTGCGGGTGAATCCACGTGGC
TTAACTGAGTTAGGAAGAAAGCAGGACCCAGAAACCCTATCGTCTGCATGATCTTTCTAACCATGGTGACTGATAC
ACCTTTCCTCACGAGAGTATCTGCAATCCAACCCCCAAAATTTGCAGAGACGGCCATAGTTAACCATGGAAAGACG
GAAATAAGTCCCGATTCAGAAAGATCAAACTTCAACACCTGGTGATAGTATGTTGGCATCCAAGTAAGAATGATAA
ATGTCCCCCAGTTGTGACAGAAATGTGAAACTATCAAGGCCCACACTGGTTTTTTAGACAATATCAATTTCCATGGT
ATGGACTTAACCGGTTCCTTTGATGCGCAGTGACTGAGAATCAGCTTCTTTTCTCTTGGAAGCAAGTGAGGATCGTC
TATTGGTGAGCTATATGCCTTGCTGATCCACAATGCAAACCAAACCGTGCCCAGGGAACCAAAAGAATAAAACACA
GATGGCCACCCAAATTTGTGGATCAACATTGGTGAAAATGCCAAACCAGTCACGGAACCAAGGTACATCCCACT

X2c w2-5 sequence

TTTTTTTTTTTTTTTTTTCTCACAGTGCATTTTCTAATATAGTAGAGAAAGAAAATCACAGCATAAATAAAATGTTAAA
AAAAGTAATAAGCTATACATTTATTGCAAACTCAATGATGTCCTCGTTCTCCTAGCATTGGGTGTTCCAAACAACCTC
GTAAAGCCAAACCCCCTCGCAACGAGGTACAAAATGAAGCTCACATACGCCGCCGTAAACACCGAAACCCCACAAC
TGAACAGTACGCCGCCGCGGACGATCCCTTCCGACGCAAAGAAGTCCACCAACAAATACCCATTGATCACCATCAC
AAACGCCGCCACCACCCACGATACAACCTGAAGAAAAGATCCAATCTTGAAGCAGCCCATAACCTCCTCCTTGGAA
ACCAAGCAGAGCAGAGGAATTAGGGCAAAGGGAATCTGAATCGACTGAAGAACGTTAAGCCATTCGTTCAAGAC
GTCCAAAGAATCCTCCGACGCGTCGGAGATTAGGGCGACGATCAAAGTAGGGACTATGGCCGAACCCCTAGTGAT
CAAAGCCCTGACCCATTTCCTCAGCTTAAGGTTCAAGAACCCGCCCATGATGAACTGACCCGCGTATGTCCCGGTG
ATGGTGCTGCTCTGGCCCGCCGCCAGCAAGCCCGCGGCCCATATGTAGAGTATGGGGGAAAAGCCCGCCGCCGTA
CTTTTCTTGGAGGTACTGGCCGTCGTTTTACA

Acknowledgements

Although the first impression on Bonn is still clear in my mind, the farewell is approaching. In the past three years, I have been learning how to be a scientific researcher, how to understand this multiple world and how to make balance between working and living. Being the end of my experience in Germany, this thesis is to record my study, to summary my experience in Germany and to express my gratitude.

Firstly, I thank greatly Professor Dr. Bartels for providing the valuable opportunity for me to study in the institute of plant molecular physiology and biotechnology at University of Bonn and for giving various genuine concern and disinterested help in my life. Secondly, I thank the China scholarship council (CSC) for providing fellowship to me from Sept. 2012 to Sept. 2015. Thirdly, I am grateful for Professor Dr. Lukas Schreiber and his Ph. D student Thomas Linnemann for giving the guide in sugar analysis using GC/MS and the suggestions on the analysis of experimental results and the revision of my manuscript. Especially, it is my honor that Professor Dr. Lukas Schreiber agreed to be the second supervisor for my Ph. D thesis. Finally, I would like to acknowledge Prof. Dr. Matthias Wüst and his colleagues Dr. U. Wölwer-Rieck and Mr. Andereas Wawrzun for giving help in the usage of HPLC for sugar analysis.

It is challenging to study abroad, but it is lucky for me to own kind friends in Germany in work and life. Although I will leave Germany and maybe we will not work and live together again, I will remember them forever. It is Quancan Hou that helped me solve lots of problems since my arrival at Bonn, Dinakar explained what the resurrection plants are, Valentino gave me help in searching the database of *C. plantagineum* transcriptome, Karolina helped me in the purification of recombinant proteins, Tauhid, Junyi and Xiaomin helped me collect samples for several times... I am grateful for the help from Guido, Verena and Barbara for giving a hand in finding a new flat for me. There are still some colleagues whose names are not mentioned here, I would like to acknowledge them in the same way.

I don’t know what expectation I would have for my children if I was a father, but I can image how happy my parents would be when I get the doctoral degree. I thank greatly my parents for supporting me so much. With love, I could go further in an academic career. Similarly, with the

love from Yu Cai, I reshape myself and recognize the world in a novel way. I am grateful for the encouragement, understanding and support from Yu Cai. I believe that we can enjoy the scenery of life with smiles and walk hand in hand forever.

At last I acknowledge the review committee for my Ph. D thesis that is composed of Prof. Dr. Dorothea Bartels, Prof. Dr. Lukas Schreiber, Prof. Dr. Matthias Wüst and Prof. Dr. Gunter Menz. They gave the last lesson to me before I get the degree and their suggestions are vital for improving my dissertation.